# PAPERS

# Department of Geology

## University of Queensland

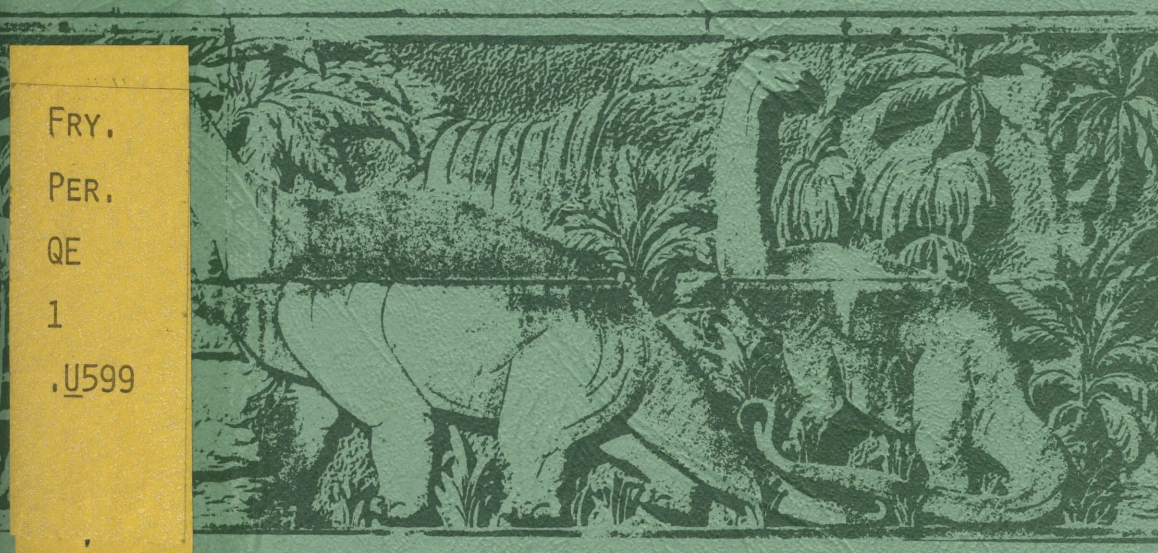

FRY.
PER.
QE
1
.U599

Volume 11 Number 4

PER
QE
1
.U599

FRYER

FRYER MEML LIBY AUST MUSEUM QLD

PAPERS

Department of Geology • University of Queensland

VOLUME 11 NUMBER 4

REG DON
1981
FRYER

# THE TWEED AND FOCAL PEAK SHIELD VOLCANOES, SOUTHEAST QUEENSLAND AND NORTHEAST NEW SOUTH WALES

*by* A. Ewart, N.C. Stevens and J.A. Ross

**ABSTRACT** .Two overlapping shield volcanoes of Late Oligocene – Early Miocene age form mountainous country in southeast Queensland and northeast New South Wales. The basaltic-rhyolitic volcanic formations and the putonic rocks (gabbros, syenites, monzonites) of the central complexes are described with regard to field relations, mineralogy, geochemistry and petrogenesis. The Tweed Shield Volcano, centred on the plutonic complex of Mount Warning, comprises the Beechmont and Hobwee Basalts, their equivalents on the southern side (the Lismore and Blue Knob Basalts), and more localized rhyolite formations, the Binna Burra and Nimbin Rhyolites. The earlier Focal Peak Shield Volcano is preserved mainly on its eastern flanks, where the Albert Basalt and Mount Gillies Volcanics underlie the Beechmont Basalt. A widespread conglomerate formation separates formations of the two shield volcanoes. Mount Warning plutonic complex comprises various gabbros, syenite and monzonite with a syenite-trachyte-basalt ring-dyke, intrusive trachyandesite and comendite dykes. The fine-grained granite of Mount Nullum and the basaltic sills of Mount Terragon are included with the complex. Each phase was fed by magma pulses from deeper chambers. Some degree of *in situ* crystal fractionation is shown by the gabbros, but the syenitic phase was already fractionated prior to emplacement. There is evidence of independent evolution of the intrusive and extrusive magma phases in the Tweed Volcano. A caldera is postulated at Focal Peak as a source for the Albert Basalt, together with other mafic vents farther east. The Focal Peak Pluton, composed of gabbro, monzonite and syenite is intrusive into vent volcanics and surrounded by a ring of microsyenite intrusions and a zone of dolerite cone sheets. The rhyolites of the Focal Peak Shield Volcano were erupted from fissure vents (Mount Gillies, Campbells Folly) and plugs. The fissure vents are thought to occur within 'closed graben' structures or polygonal calderas. The Albert Basalt shows considerable chemical variability consistent with crystal fractionation involving separation of olivine, plagioclase, augite and magnetite phases prior to eruption. The Focal Peak mafic intrusives are chemically similar to the Albert Basalt. The chemistry of the microsyenite intrusions indicates fractionation from a more mafic parental liquid. Silicification of devitrified rhyolitic lavas of the Mount Gillies Volcanics is interpreted as a weathering feature. Norms of residual glasses of the pitchstones suggest ternary minimum crystallisation. Evidence of strong crystal-liquid fractionation of feldspar in the rhyolites is presented.

## INTRODUCTION

Tertiary volcanic rocks in eastern Australia are confined mostly to the highlands and near-coastal regions. The greatest thickness and volume of lavas erupted was in southeast Queensland and northeast New South Wales during the Late Oligocene and Early Miocene Periods, forming the Tweed Shield Volcano and the lava pile of the Main Range.

Despite its age (20.5 – 23.5 Ma, Appendix 2), the Tweed Shield Volcano is still recognisable as a volcanic shield whereas erosion has removed most of the eastern side of the Main Range volcanic mass. A separate shield volcano centred on Focal Peak, between the Tweed Volcano and the Main Range, has

*Pap. Dep. Geol. Univ. Qd.*, 11(4): 1–82, January, 1987.

been proposed (Ross, 1974), including the two lowermost volcanic formations (Albert Basalt and Mount Gillies Rhyolite) previously assigned to the volcanic sequence (Lamington Group) of the Tweed Volcano.

Mount Warning, 14 km southwest of Murwillumbah N.S.W., is a prominent peak (1125 m) at the centre of the Tweed Volcano, composed of trachyandesite and surrounded by plutonic rocks. The mountain mass is isolated from the remaining parts of the volcanic shield by a deep erosion caldera, which exposes the underlying Palaeozoic and Mesozoic rocks. To the north, west and south of Mount Warning, precipitous cliffs, largely of basaltic lava flows with interlayered rhyolites, border the erosion caldera. The rim of the caldera is highest in the north, where there is a maximum thickness of about 1000 m for the lava flows.

From the caldera rim, the surface of the Tweed Shield Volcano gradually decreases in all directions away from Mount Warning at slope angles between 1 and 3 degrees. Much of the eastern part of the volcano has been removed by erosion, but basaltic remnants crop out on the coast at several places (Burleigh, Tweed Heads, Fingal Point) and are known to exist below present sea level. Basalts presumed to have been erupted from the vicinity of Mount Warning extend for distances of up to 50 km to beyond Canungra to the north and Lismore to the south (Text fig. 1).

On the western margin of the Tweed Volcano, where it overlaps the slightly older Focal Peak Shield Volcano (23.2 – 25.5 Ma), formations of the former have been largely removed, exposing those of the latter. Because of the overlapping of the lavas of the shield volcanoes, and the asymmetrical distribution of the older lavas with respect to Focal Peak, the earlier shield volcano is more difficult to visualize. As with the Mount Warning centre, no basaltic lavas are found close to Focal Peak, probably because of uplift and erosion. There are, however, agglomerates and 'vent volcanics' (Stephenson, 1956) intruded by plutonic rocks at Focal Peak. A conservative estimate of the former extent of the basaltic lavas of the Focal Peak Volcano is indicated in Text fig. 1, but the area covered may have been much greater. It has been suggested that some of the lavas of the southern part of the Main Range (Fig. 21) have emanated from the Focal Peak Shield Volcano, because of westerly dips of trachyte flows (Ewart and Grenfell, 1985). Basaltic rocks, presumed to be flows, occur at 300 m elevation about 15 km NNE. of Focal Peak, and these too could be remnants of a more extensive shield volcano.

## PREVIOUS LITERATURE

Richards (1916), in his pioneer work on the volcanic rocks of southeast Queensland, established a basalt-rhyolite-basalt sequence for the volcanics of the McPherson Range, and investigated their chemistry. No further work on the volcanics was published during the next 40 years, except for a brief summary and a name, Lamington Series, being given to them (Bryan & Jones, 1946) and the first mention of the mass of lavas centred on Mount Warning being a shield volcano (Hill, 1951).

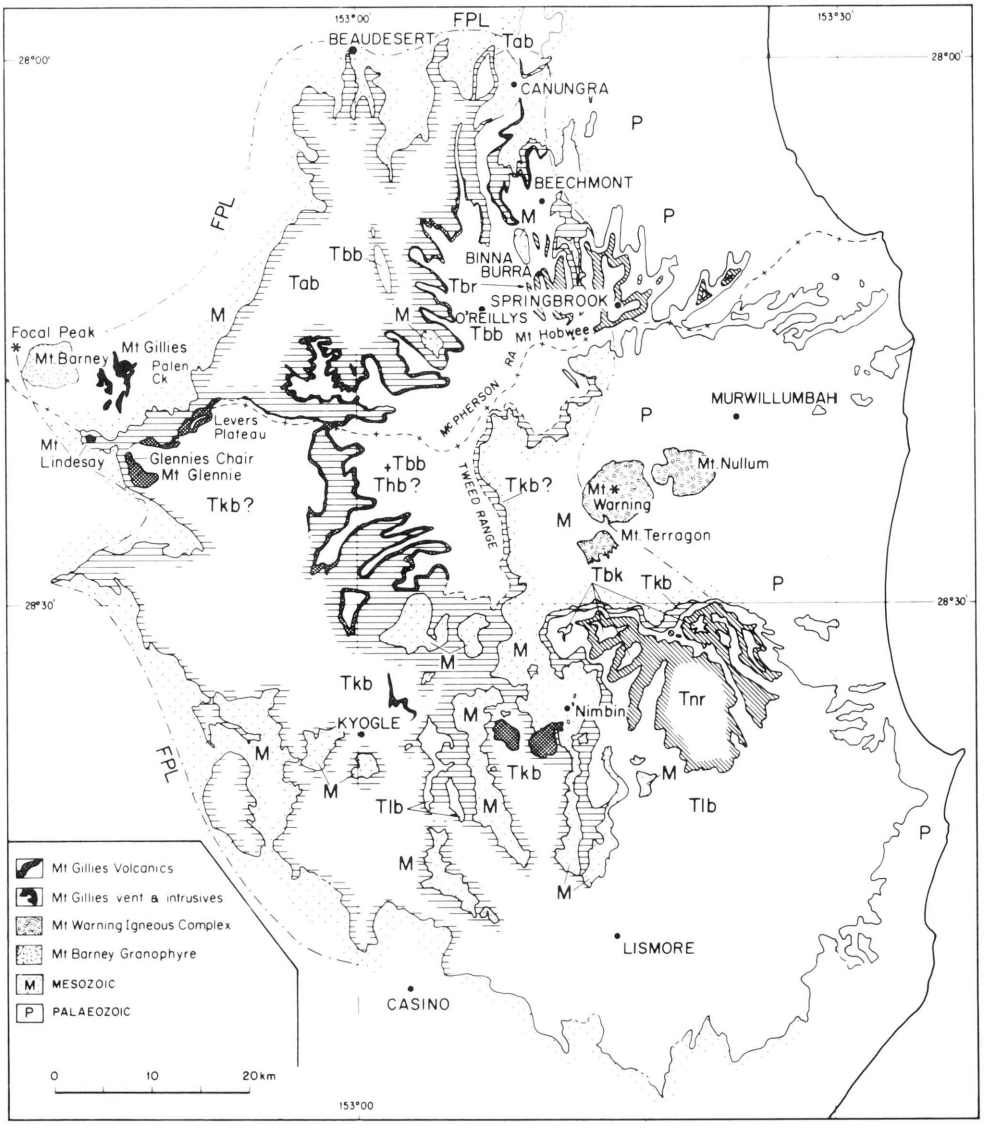


Text fig. 1. Geological map showing distribution of volcanic formations, Tweed Shield Volcano and eastern flank of the Focal Peak Shield Volcano. Tab: Albert Basalt, Tkb: Kyogle Basalt, Tbb: Beechmont Basalt, T1b: Lismore Basalt, Tbr: Binna Burra and Springbrook Rhyolites, Tnr: Nimbin Rhyolite, Thb: Hobwee basalt, Tbk = Blue Knob Basalt, M: Mesozoic, P: Palaeozoic. FPL: possible former limit of basaltic lavas of the Focal Peak Shield Volcano (Albert and Kyogle Basalts). Boundaries in the Canungra-Numinbah area based on mapping by Willmott (1983).

The first detailed mapping of any part of the volcanic area was completed by Tweedale (1950) at Binna Burra, and was followed in 1954 by Stephenson's detailed investigation of the Tertiary intrusive rocks of the Mount Barney-Mount Ballow area to the west. Later this work was extended to include Mount Gillies, with its rhyolitic vent; and the adjacent Tertiary rhyolites and basalts of Mount Lindesay (Stephenson, 1956, 1959).

South of Mount Warning, a small area of rhyolitic volcanics near Minyon Falls was described by Crook and McGarity (1956). Solomon (1959) carried out reconnaissance mapping of the central mass of Mount Warning, discovered a ring-dyke system, and made the first petrological study of the complex. Only the first part of this work, mainly on geomorphological aspects of the shield, was published (Solomon, 1964). Planezes were extrapolated to give a height of 6300 feet (1890 m) for the uneroded Mount Warning.

McTaggart (1962) made a notable contribution to the stratigraphy of the lavas in recognising two separate horizons of rhyolitic rocks, mapping their outcrop and naming and defining the formations. Names given to volcanic formations south of Mount Warning by McElroy were published in a regional survey (McElroy, 1962) in which two principal volcanic focal areas, one centred on the Mount Warning Complex and the other in the Mount Barney-Mount Ballow area, were postulated. .

On the north side of Mount Warning, the Mount Tamborine area was studied by Green (1964), who found that the lowest basaltic formation (Albert Basalt) was more alkaline than the overlying basalts, and distinguished a number of flows in the overlying Beechmont Basalt. He also found that the higher basalts were largely transitional tholeiitic in affinity (Green, 1964, 1968, 1970). This observation was reinforced and extended by Wilkinson (1968) who studied basalts from the southern and eastern parts of the shield. Stevens (1970) considered relations between lavas and eruptive centres in this and other volcanic areas to the north and presented the first chemical analyses of the Mount Warning igneous complex.

The intrusive complex of Mount Warning has been studied by Paterson (1970), Smart (1970), and Gould (1970), mostly east of the summit, and by Bruce (1978) who worked on the southern slopes. Some of the earlier work was published in an excursions handbook (Ewart, Smart, and Stevens, 1971).

Work on areas near Springbrook (Watt, 1971) and Binna Burra (Uttley, 1972) provided new details for the higher rhyolitic formations at these localities and added to the known occurrences of the tholeiitic andesite and dacitic lavas, and to data on the chemical differences within the basalts.

Ross (1974), working on the northwestern margin of the volcanics, proposed that the lower volcanic formations (Albert Basalt and Mount Gillies Rhyolite) should be considered part of a slightly older shield volcano centred on Focal Peak, west of Mount Barney, and that the lavas from Mount Warning and nearby centres overlapped these earlier volcanics, with the Chinghee Conglomerate separating lavas of the two shield volcanoes.

Mapping in the Kyogle district N.S.W. by Duggan and by Mason in 1969 was followed by a Ph.D thesis on the volcanics by Duggan (1975) and a joint

publication (Duggan and Mason, 1978). A summary of the geology, with notes on the geomorphology (Stevens, 1976) was published as part of a Border Ranges symposium.

Apart from previously mentioned papers on geochemistry of the Tertiary lavas that of Ewart, Oversby and Mateen (1977) deals specifically with the volcanics of this shield volcano, and papers by Ewart (1981, 1982) deal with the geochemistry of southeast Queensland Tertiary volcanics.

Twenty isotopic age determinations (with references) on the lavas and intrusive rocks of both Shield Volcanoes are listed in Appendix 2.

## TWEED SHIELD VOLCANO — VOLCANIC FORMATIONS

### Beechmont Basalt

This name has been given to the earliest basalts of the Tweed Shield Volcano, on the northern side. They form the Beechmont Plateau and overlie either the Chinghee Conglomerate, rhyolites and/or tuffs of the underlying rhyolite formation, the Albert Basalt or Palaeozoic metamorphic rocks. The upper limit of the formation is marked by the Binna Burra Rhyolite, but where this is absent, the Beechmont Basalt is difficult to distinguish from the overlying basalts. There are also difficulties in delineating the base of the Beechmont Basalt where it overlies Albert Basalt without sedimentary or rhyolitic intercalcations. On the west side of the erosion caldera, west of Mount Warning, there is an apparently unbroken basaltic succession over 1000 m thick. Exon (1972) maintained that the basaltic formations should not have regional names and preferred to call the whole sequence Lamington Volcanics. In view of the different source of the lower two volcanic formations, it is now debatable whether this name should be used, or if it is retained, whether the lower formations should be included in this Group.

The best described succession in the Beechmont Basalt is located along Flying Fox Creek, Canungra, and in the Mount Tamborine area to the north (Green, 1964) where 15 to 25 flows have been recognised. Of five units mapped at Mount Tamborine, two, the Eagle Heights Member near the top and the Cameron Falls Member near the base, are thick flows (24 m and 20 m respectively), distinctive physiographically as cliff-forming lavas, and mineralogically, the former because of its large plagioclase phenocrysts, and the latter for its secondary minerals. Thin sedimentary beds, largely shales and diatomite, are intercalcated in the lowermost unit of at least 10 thin flows on Mount Tamborine, and also near Beechmont.

Except at the base of the succession, where dips may be up to $25^{o}$ locally in basalt flows which filled irregular despressions, the general dip of the formation is northerly at a low angle. Green (1964) considered that there was an unconformity with the underlying Albert Basalt, as he obtained a $1^{o}$ dip to the south on the latter.

## Lismore Basalt

On the south side of the Mount Warning Shield Volcano the Lismore Basalt corresponds to the Beechmont Basalt and similarly overlies earlier Tertiary volcanics from other sources.

The following description is from Duggan and Mason (1978). The Lismore Basalt is the underlying rock of wide areas of low relief between Lismore, Ballina and Coraki. Much of the upper part of the succession in this area has been removed by erosion and remains where protected by the overlying flows. Like the Beechmont Basalt the Lismore Basalt is predominantly tholeiitic, with occasional alkaline types; flows rarely exceed 10 m in thickness. Some examples of ropy surfaces indicate pahoehoe lavas, other occurrences suggest aa types. The source of these lavas is not definitely known, but probably they came mainly from the direction of the Mount Warning Central Complex.

## Binna Burra Rhyolite

This formation, which outcrops on the northern side of the border in the Lamington National Park (Text fig. 2), consists of thick rhyolite flows with conspicuous tuffs at the base of the succession, and also at the top of the formation in some places, e.g. White (Talangai) caves area.

In the type area near Binna Burra, there are at least four or five individual rhyolite flows, each up to 100 m thick. Both upper and lower surfaces of the flows are usually glassy. The upper selvedges (2–10 m) are perlite, usually with obsidian cores. The lower selvedges consist of glassy auto-breccias or agglomerates, or pumiceous agglomerates, or perlites. Flow layers and flow folding are well developed, as are spherulitic structures near the base of flows (e.g. Koolanbilba Cave).

Bryan (1941, 1954) proposed the name 'spheruloid' for spheroidal bodies in the rhyolite, which differ from spherulites in the lack of a radial structure. He distinguished four groups of spheruloids, each group 'restricted to one particular flow':

(1) Small spheruloids, up to 2.4 cm diameter, with a smooth, glossy surface, occurring as clusters along particular fluxion planes which penetrate them,

(2) Large spheruloids, up to 30 cm, spherical, hollow, in a groundmass of perlitic glass,

(3) Mostly irregular, roughly ellipsoidal, more closely-spaced and numerous than in (2), non-cavernous, loose textured, each with a distinct crust. Growth and amalgamation of spheruloids were figured.

(4) Large spheruloids, closely packed in black glass, dense or cavernous or loose textured.

The group of rhyolite flows is underlain by tuff beds, ranging from 20 to 120 m in thickness, and forming steep, smooth, convex cliffs.

The tuffs are almost all of ash-fall type, in which graded bedding is common and is manifested by grading in basaltic fragments, ranging from boulders

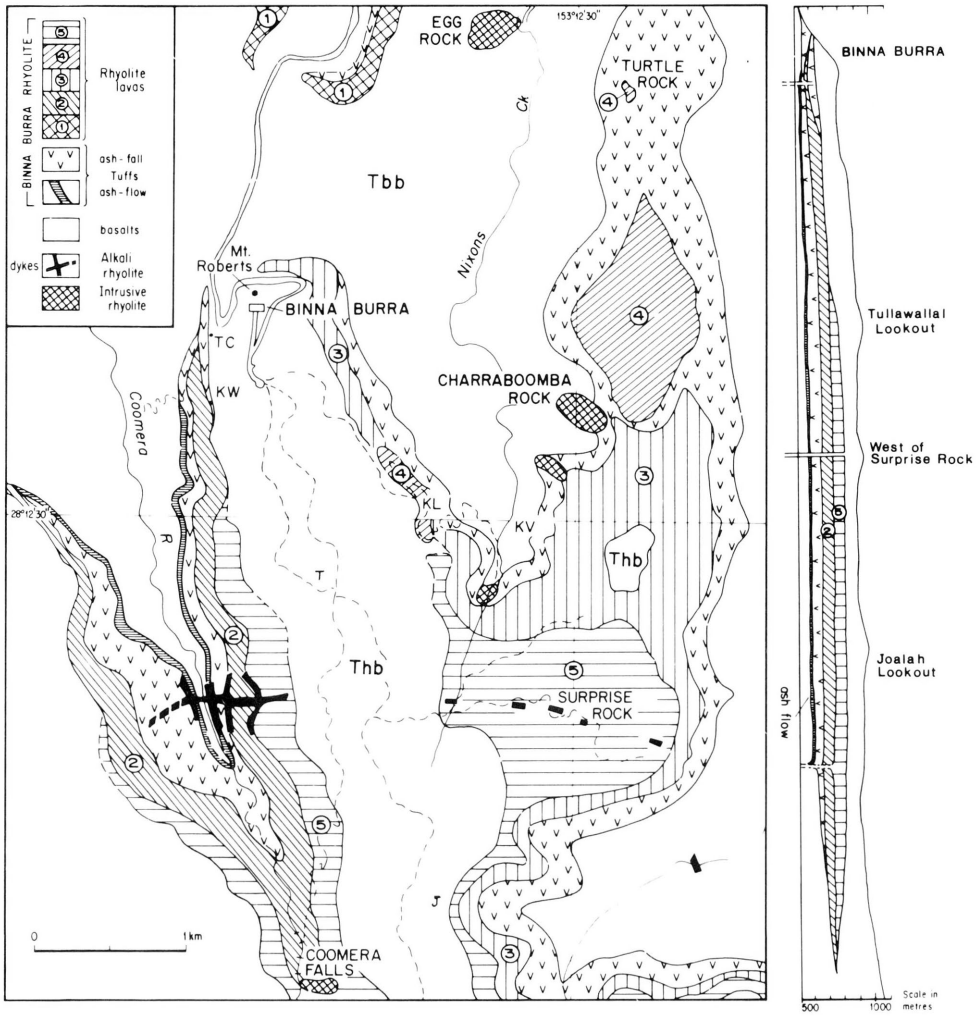


Text fig. 2. Geological map of the Binna Burra area (after Uttley, 1972) showing outcrop pattern of the Binna Burra Rhyolite. TC: Talangai Cave, KW: Kweebani Cave, KL: Koolanbilba Cave, KV: Kurrajin Valley. Tbb and Thb: Beechmont and Hobwee Basalts. The geological sketch section is from Binna Burra south towards the state border.

to lapilli. Rhyolite, rhyolite glass and sandstone boulders also occur. Marked disconformities are present in the tuffs in the Kurrajin Valley, indicating contemporaneous stream erosion (Uttley, 1972).

Tuffs on either side of the Coomera River Valley are underlain by an ash flow deposit up to 10 m thick. Carbonized tree trunks and branches occur in the lower part of the deposit. Assuming that the orientation of the logs is perpendicular to the flow direction, the latter has been determined as along the valley, in a direction slightly west of north.

The ash flow deposit is massive, vertically jointed, has uniform lithology and overlies basalt. It does not show cores of welding, devitrification or eutaxitic structures. The tuff below the upper rhyolite at Ship Stern (Binna Burra area) was welded or fused by the overlying rhyolite, resulting in darkening of pumice fragments.

On the western side of Mount Roberts, near Binna Burra, up to 70 m of tuff lies disconformably on southerly-dipping rhyolite, on agglomerate and tuff horizons and also on Beechmont Basalt. The lower rhyolite flow is thought to have terminated here against a hill of Beechmont Basalt.

The best exposures of the upper tuff are at White Caves and along the track to the Swimming Pool. It is a well bedded ash-fall tuff with thin bands of lapilli. The lower part lacks drape structures and is thought to be a lacustrine deposit; it grades upwards into beds of possible aeolian origin (Uttley, 1972). The lowest 3 m of the upper tuff contains large angular boulders of fragmented rhyolite and dark glass. It is underlain by a thin layer of dense welded ash (1 m), and this in turn is underlain by boulder agglomerate, which is thickest at Kweebani Cave. The agglomerate is here intruded by rhyolite glass, suggesting that this is a cross-section of a vent.

On the same stratigraphic level as the Binna Burra Rhyolite, but farther to the southeast, a flow of dacite, approximately 20 m thick with a glassy upper margin, is associated with a glass boulder tuff about 10 m thick. It is best exposed at Bushrangers Cave, located on the caldera wall.

On the western slope of the Springbrook Plateau, basalt is intercalated between two major rhyolitic flow units, each about 100 m in thickness. The upper rhyolite is topographically higher than the rhyolitic sequence at Binna Burra, and may be younger; because of this, and the separation from the Binna Burra Rhyolite, another name, the Springbrook Rhyolite, is necessary. The rhyolite flows usually exhibit a glassy base and top, the base consisting of obsidian at the margin ($\sim$ 3 m) with perlite above ($\sim$ 8 m). Near Horsehoe Falls, there is a lateral gradation from rhyolite to a dark-coloured dacite containing xenoliths of basalt.

### Nimbin Rhyolite

The following notes on this formation are from Duggan and Mason (1978). The Nimbin Rhyolite is the counterpart of the Binna Burra Rhyolite on the south side of Mount Warning, occupying a similar area (estimated at 400 $km^2$), and with a maximum thickness of 500 m. The flows, which are of both porphyritic and aphyric rhyolite, vary in thickness from 50 m to 150 m,

and are interstratified with rhyolite tuffs and agglomerates in beds up to 20 m thick. Although individual flows may have a considerable lateral extent with little change in thickness, there are instances of rapid thinning out. The base of most flows is composed of pitchstone without much devitrification. Pyroclastics show evidence of fluvial reworking and include blocks of rhyolite and tholeiitic volcanics with sedimentary material. Some basaltic flows are intercalated with the rhyolites. A rhyodacite 3 km ESE. of Nimbin is included in the formation.

The source of the rhyolite flows seems to be in the north, where thickening is marked and where several small intrusive plugs occur (e.g. Doughboy Mountain).

### Hobwee Basalt

The highest basaltic formation on the north side of Mount Warning, termed the Hobwee Basalt, comprises a maximum of nearly 600 m of basalt which overlies the Binna Burra Rhyolite formation. At least twenty flows can be counted in the cliffs close to Mount Hobwee indicating an average of 30 m for each flow. The flows of the lower part of the Hobwee Basalt are similar to those of the upper part of the Beechmont, in being porphyritic in plagioclase, whereas earlier flows (of the lower part of the Beechmont Basalt) are less porphyritic and later flows (of the upper part of the Hobwee Basalt) are more strongly porphyritic in plagioclase and olivine.

Basaltic rocks with large, closely-packed plagioclase phenocrysts, presumably a lava flow belonging to the Hobwee Basalt, occur on the road to O'Reillys at about 550 m, and at higher elevations on the Duck Creek Road and near O'Reilly's guest house. A similar rock has been quarried much farther east near the Antarctic Beech stand in Wiangaree National Park (south of the State border) at 920 m.

Watt (1971) has recorded basaltic pyroclasts above the Springwood Rhyolite, and Uttley (1972) has mentioned two horizons of similar rocks, presumably in the lower part of the Hobwee Basalt at 800 m and 600 m in the Beechmont and Sarabah Ranges, respectively. The latter occurrence is probably the one exposed in the circular one way cutting on the O'Reillys road.

### The Blue Knob Basalt

On the south side of Mount Warning, this basaltic formation is the highest stratigraphically, and forms cappings on many higher areas near Nimbin. Like the Hobwee Basalt, it was probably erupted long enough after the rhyolites to occupy depressions in a highly irregular land surface. The maximum thickness of about 350 m is attained at Blue Knob, where the basalt lies on petrologically similar Lismore Basalt. The above information is from Duggan and Mason (1978).

## THE MOUNT WARNING CENTRAL COMPLEX

### Introduction

This igneous complex occurs at the centre of the Tweed Shield Volcano and forms a prominent peak which is surrounded by lowlands of the erosion caldera and farther out by the cliffs of the caldera rim. It is situated on a steeply dipping unconformable junction between the folded and metamorphosed Carboniferous Neranleigh-Fernvale beds and west-dipping Triassic strata (including Chillingham Volcanics at the base) which at this point changes from almost north-south (north of Mount Warning) to NNW.-SSE. to the south of Mount Warning. The bend may, in part, be due to the upthrust of the igneous mass on the Mesozoic strata. Alternatively, the bend, and the influence of east-west basement structures (deduced from progression of ring-centres of the Mount Barney-Mount Ballow Complex), may have helped localize the site of the volcanic centre.

Mount Warning represents the eroded remains of a large magma chamber. The overall shape of the igneous complex (excluding Mount Nullum) is nearly circular with a maximum east-west diameter of nearly 8 km, and a north-south diameter of 6 km. Gabbroic rocks form a complete belt of variable width surrounding a central mass of syenite, which in turn encloses a core of trachyandesite forming the summit of Mount Warning. The gabbros extend to the outer margin of the complex, except where intruded marginally by a predominantly syenitic ring-dyke at the western margin, and a monzonite intrusion at the eastern margin. The ring-dyke has been emplaced as a prominent, although discontinuous intrusion (Text fig. 3).

The gabbros constitute the oldest exposed rocks of the complex. Two main series of gabbros are recognised in the eastern and southern portions of the complex, evidently separated by the ring dyke. The sequence of intrusion, based on currently available field data, is:
early gabbros, laminated gabbros, monzonite, central syenite, trachyandesite, tholeiitic andesite dyke-sill phase (S. area), multistage ring-dyke, and comendite dykes.

A contact metamorphic aureole is present in the Palaeozoic country rocks along the eastern margin of the complex, some 1.5 km wide. The highest grade attained is hornblende hornfels facies.

Two K/Ar dates are available, one from a laminated gabbro giving an age of 22.9–23.7 Ma (Webb, Stevens and McDougall, 1967, corrected to constants of Steiger and Jager, 1977). The second, based on a whole rock trachyandesite sample, gives an age of 23.4 Ma. (D.C. Green, pers. comm.). Both ages suggest that the Mount Warning igneous complex could be slightly older than the surrounding volcanic shield sequence (the Hobwee and Beechmont Basalt formations, and the Binna Burra and Springbrook Rhyolites) which have been dated at 20.5–23.5 Ma (Appendix 2).

As the Mount Warning complex is at the eroded geographic centre of the volcano, it has been naturally interpreted as the eruptive centre. The K/Ar dates, however, suggest that the presently exposed igneous rocks of the Mount

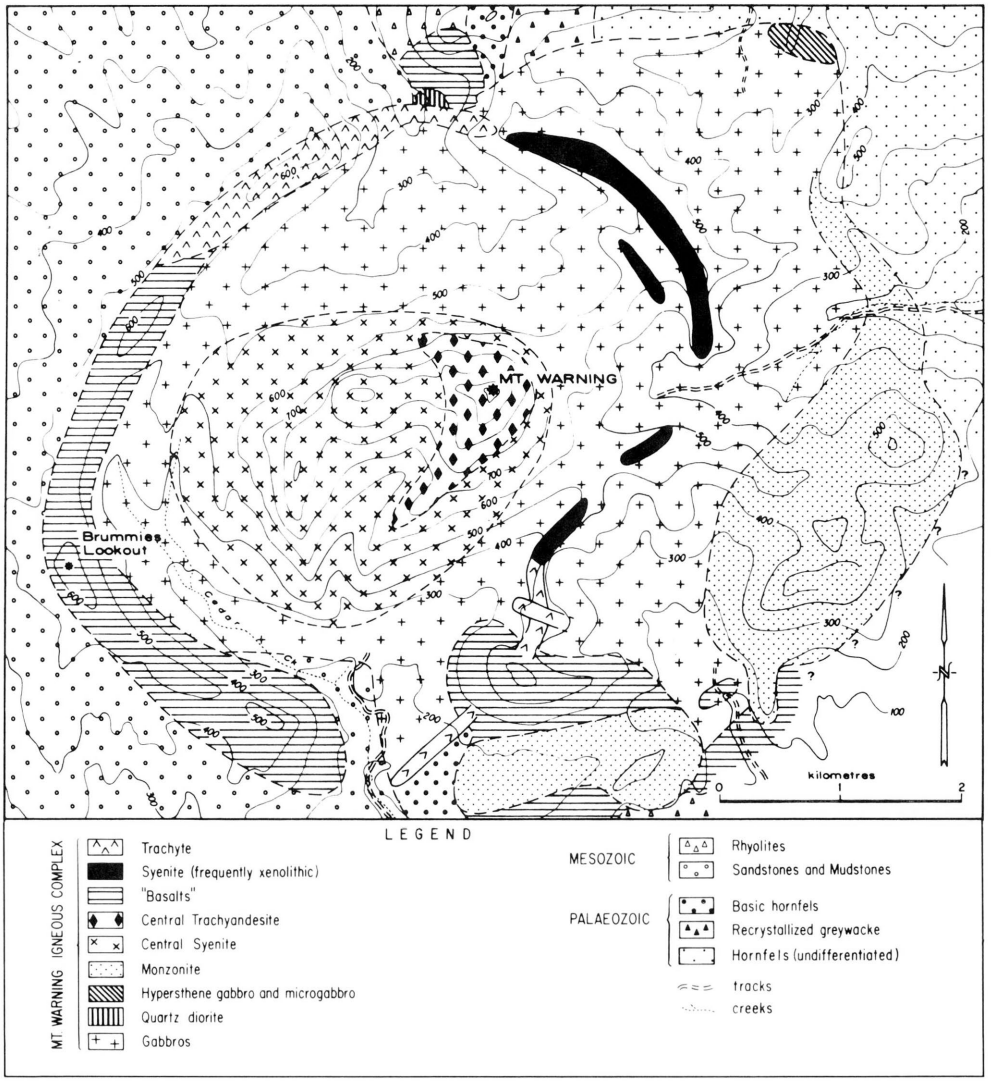


Text fig. 3. Geological map of the Mount Warning Intrusive Complex (based on maps by Bruce (1977), Paterson (1970), Smart (1970) and Solomon (1956).

Warning complex do not represent the primary magma chamber from which the lavas were erupted, a conclusion in some accord with the petrology and chemistry of the lavas (Ewart *et al.*, 1977).

To the east of Mount Warning is a second intrusive complex, the Mount Nullum Complex (Gould, 1970), comprising fine-grained granite, granite and monzonite. This intrusion is interpreted, on field evidence alone, to be Tertiary and slightly younger than the Mount Warning complex.

## The Gabbros

I Older Series. These are recognised in both the outer eastern part of the complex and the southern part, comprising a series of petrographically distinct gabbro types which do not, however, form clearly defined zones or bands in the field.

The main gabbro types recognised here are the so-called normal coarse-grained gabbros and microgabbros. These two textural varieties are intimately associated in the field, and field observations indicate that the microgabbro phase predates the coarser phase, but it is nevertheless considered that both types represent part of a single intrusive phase. There is wide variation in texture and mineral proportions within these gabbros. The mineralogy is typically andesine-labradorite, augite (with fine exsolution lamellae), inverted pigeonite, orthopyroxene, olivine, titanomagnetite, biotite, and accessory apatite and sphene, and sometimes small amounts of interstitial quartz.

Leucogabbro is recognised as a second variant, found as xenoliths in the ring-dyke, in the monzonite, and as discontinuous outcrops (presumably xenoliths) within the younger gabbro series. It is characterized by relatively coarse grain size and cumulate textures; mineralogically, it is dominated by plagioclase and augite, with accessory olivine, orthopyroxene, biotite, magnetite, potash feldspar, and quartz. This gabbro is presumed to represent the original intrusive phase.

Andesine gabbro is recognised as an additional although localized intrusive phase situated close to the margin of older and younger gabbro series, being exposed inside and immediately adjacent to the eastern segment of the ring-dyke, and could possibly represent a marginal phase of the younger gabbro core. Mineralogically, it contains andesine, augite, bronzite, olivine, magnetite, and relatively abundant biotite, with accessory apatite.

At the topographically highest parts of the outer eastern part of the complex, these older gabbros are overlain by laminated gabbros belonging to the younger gabbro series.

Within the southern (Cedar Creek) area of the complex, the normal coarse-grained gabbro constitutes the dominant type, and is exposed in a 400-500 m wide zone surrounding the central syenite; a foliation (due to alignment of feldspars) is present which dips approximately towards the centre of the Mount Warning complex at 20-30°. Syenitic veins cut the gabbro, both as linear veins and earlier irregular networks of stringers, the latter apparently injected before complete solidification of the gabbro. Petrographically, these gabbros consist of plagioclase, augite, Fe-Ti oxides, minor olivine, biotite, and uralite (interpreted to be predominantly after orthopyroxene, which is absent as an unaltered phase in these rocks).

Two additional gabbroic variants are recognised within the southern area, namely hypersthene gabbro and leucogabbro. The former are restricted to altitudes of less than 150 m, and thus evidently underlie the normal gabbros described above. Mineralogically, the hypersthene gabbros comprise plagioclase, augite, hypersthene (extensively uralitized) as essential phases, with accessory Fe-Ti oxides and biotite, and interstitial quartz. No cumulate tex-

tures are recognised. The leucogabbros occur in only a single isolated locality in the southern area, and consist of plagioclase, pyroxenes (almost completely uralitized), with Fe-Ti oxides and interstitial quartz.

II Younger Series. These outcrop at the higher elevations of the gabbro outcrops, within the ring-dyke. A wide variation of petrographic types is again found, including normal gabbro (plagioclase + augite + accessory olivine + Fe-Ti oxides), olivine gabbro (essential plagioclase + augite + olivine), ferrigabbro (essential plagioclase + augite + Fe-Ti oxides), troctolite (essential plagioclase + olivine), leucogabbro (essential plagioclase + uralite), and layered gabbros. These various types may occur in varying combinations even in the same outcrop, and are intruded by numerous dykes, including the ring-dykes, composed of syenite and rhyolites.

The younger gabbros consistently exhibit a well defined lamination, due to preferred orientation of plagioclase, pyroxene, and biotite. These laminated gabbros overlie the older gabbro series in both the eastern and southern parts of the complex. The lamination dips inwards towards the core of the complex, with dips mostly $<25^{o}$ (up to $50^{o}$ just inside the ring-dyke) in the eastern part, and up to $45^{o}$ in the southern area, thus defining an overall saucer-like structure. True layered gabbros appear to be confined to the topographically highest parts of the gabbro body; their structure again conforms to saucer-shaped, although local, small scale 'cross-bedding' and 'slump' structures are found in these layered gabbros in the eastern area. Isolated outcrops of leucogabbro occur sporadically throughout the younger gabbros, and evidently represent xenoliths of the older gabbro phases, in some cases exceeding 30 m in diameter.

The principal minerals of the younger gabbros are plagioclase, augite, olivine, Fe-Ti oxides, orthopyroxene, uralite (probably after orthopyroxene), biotite, hornblende, apatite, and interstitial potash feldspar and quartz. Cumulate textures are developed. The leucogabbros are rather coarse grained, with large randomly oriented plagioclase laths (up to 2 cm) and uralitized, poikilitic pyroxenes; felsic veins commonly cut these leucogabbros, and contain andesine, potash feldspar, biotite, green fibrous amphibole, and secondary chlorite, calcite, and epidote. Olivine occurring within the gabbros frequently exhibits marginal zones enriched in minute magnetite granules, and reaction rims of orthopyroxene are also found. Orthopyroxene also occurs, however, as discrete subhedral crystals in virtually all gabbros examined. Of particular petrographic interest in these gabbros is the persistent presence of biotite. Rare hornblende is found as reaction rims on some titanomagnetites and pyroxenes.

## Monzonite

The monzonite extends irregularly, in a lensoid form, around the eastern and southern rims of the complex, having been intruded between the gabbro and the hornfels country rocks. Its outcrops form the high peaks of Mount Uki, presumably The Sisters (not accessible during the study), through to Cedar Creek. No lineation or banding is recognised within the monzonite, and the overall grain size tends to remain almost constant. Three sets of joint patterns

are extremely well developed, one subhorizontal, and two very steeply dipping. The monzonite is cut by numerous felsic veins (potash feldspar, quartz, altered augite, and Fe-Ti oxides). Slight displacement of these veins along joints is consistent with upward movement beneath Mount Warning (Paterson, 1970). Thin veinlets of monzonite penetrate the gabbro at the contact. The numerous xenoliths in the monzonite can be divided into four groups: leucogabbros (up to 200 m long), fine grained gabbros (near the gabbro contact, up to 50 cm across), hornfelsed gabbro, and hornfelsed country rock.

Petrographically, the monzonite is rather variable in terms of its textures and mineral proportions. When fresh, it is a dark grey to blue grey, massive rock. Two dominant types can be distinguished, normal quartz monzonite, and fayalite-quartz monzonite, which cannot, however, be distinguished in the field. The fayalitic variety contains relatively higher proportions of plagioclase and total mafics, and occurs adjacent to the gabbro contact. The minerals present are plagioclase (oligoclase-andesine), potash feldspar (microperthitic, forming mantles around plagioclase as well as discrete crystals), interstitial quartz, augite, hornblende, apatite, magnetite, ilmenite, and biotite, $\pm$ fayalitic olivine, and micrographic intergrowths. Uralitization of the pyroxene is commonly developed.

**Central Syenite**

This unit forms a concentric band of variable width surrounding the trachyandesite core, the contacts between these units being steeply dipping. The central syenite is, in turn, completely surrounded by the gabbros which the syenite clearly intrudes. Within the southern part of the complex, four types of syenite are recognised:

(a) Marginal peralkaline syenite, consisting of a relatively mafic phase which intrudes and interfingers with the normal syenite, the latter becoming locally relatively coarse grained in proximity to the marginal phase. Petrographically, the peralkaline syenite contains alkali feldspar (microperthitic), sodic pyroxene (with cores of calcic compositions), sodic amphibole, quartz, aenigmatite, fayalitic olivine pseudomorphs, and Fe-Ti oxides.

(b) Normal syenite, a medium to coarse grained, somewhat porphyritic rock, which forms the main mass of the syenite intrusion. Petrographically, it contains subhedral phenocrysts of alkali feldspar and minor plagioclase (rimmed by alkali feldspar), up to 1.5 cm in length, in a coarse matrix of alkali feldspar, clinopyroxene, olivine, Fe-Ti oxides, and uralitic alteration products.

(c) and (d) Non-peralkaline and peralkaline dykes, both of which cut the normal syenite in the southern part of the syenite massif. In addition, post-syenite dykes are recognised in this same region, consisting of agglomerate, trachyandesites (resembling those of the summit region), and alkali trachyte.

In the eastern part of the complex, where the syenite is sandwiched as a relatively narrow band between the gabbros and the summit trachyandesite, only the peralkaline phase has been recognised which corresponds to the marginal phase in the southern area. Texturally, the peralkaline syenite is rather variable, and includes: microsyenites which occur as veins and dykes (emanating from the central syenite) intruding the underlying gabbros, although also

found locally within the main syenite mass; a pegmatitic phase, occurring in lenticular pods up to 15 m in length, close to the trachyandesite contact.

No lineation or foliation has been recognised in the central syenite intrusion. In the eastern part of the complex, the syenite-gabbro contact is either subhorizontal, or has a shallow inward dip, with the syenite overlying the gabbro. In the southern region, the contact is inwardly steeply dipping. The overall structure of the syenite is thus interpreted as essentially resembling an inverted cone, with steeper contacts occurring at the more deeply exposed levels.

## Central Trachyandesite

The porphyritic trachyandesite forms the highest parts of the central complex and has generally been assumed to represent the core of the volcano. In structure, it is interpreted to represent a steep sided central plug with numerous radiating dykes and other minor plugs. The intrusion appears to have a multistage injection history, with trachyandesite xenoliths occurring within the trachyandesite, and the occurrence of internal finer grained contacts.

On the well-exposed northern and eastern slopes, the contact with the syenite dips inwards sharply, but irregularly at $65-83^{\circ}$. Nevertheless, the contact relations between the trachyandesite and surrounding syenite are, overall, rather ambiguous. For example: veins of syenite occur in trachyandesite; pegmatitic syenite is found in the syenite close to the trachyandesite contact; two small syenite outcrops are recorded within the trachyandesite, although these could be intrusive or xenolithic; trachyandesite in contact with the syenite is finer grained; trachyandesite dykes intrude the central syenite; glomeroporphyritic aggregates of potash feldspar occur in fine grained trachyandesite near the contact, and are identified as xenocrysts derived from a syenite. Jointing in the trachyandesite is strongly developed, and these joints are oriented parallel to the contact in the north and east, and appear to be circumferentially arranged about the summit. The preferred interpretation is that the trachyandesite represents a composite dyke with radial dykes. According to Solomon (1959) the trachyandesite was intruded through the syenite during an early stage of the latter's cooling, whereas Smart (1970) interpreted the trachyandesite as predating the syenite. Evidence from xenoliths is indefinite but Solomon's interpretation is preferred, with resulting recrystallisation and some plastic behaviour of the syenite along the contact zones.

Petrographically, the trachyandesites are characterized by prominent phenocrysts of labradorite and alkali feldspar (microperthitic to cryptoperthitic), together with sporadic clinopyroxene, hornblende and olivine, set in a holocrystalline, often relatively coarse groundmass of alkali feldspar, clinopyroxene, olivine, titanomagnetite, ilmenite, hornblende, quartz, traces of biotite, and apatite. Of particular significance is the common corrosion of the plagioclase phenocrysts, usually enclosed by sharply defined rims of alkali feldspar.

### Syenite-Trachyte Ring-Dyke

The ring-dyke stands out as an almost complete elliptical, narrow, steep-sided ridge which encircles the present summit region. The dyke outcrop has been mapped as over 100 m in average width, but is usually less than 30 m at the ridge top. Where exposure permits examination, a steep inward-dipping inner contact is found. Solomon (1959) recorded a variation in rock type along the dyke; basalt along the southwestern sector, trachyte along the northwestern and southern sectors, and alkali syenite along the eastern parts. No compositional variation across the dyke has been found. Field and petrographic data indicate that dyke injection along the ring-fracture must have occurred in several distinct episodes. The following discrete phases are recognised in the northern and eastern sectors of the ring-dyke; fine grained syenite (earliest); porphyritic syenite; trachyte; porphyritic alkali syenite. Moreover, lateral traverses along the ring-dyke clearly show that it has been injected to varying heights, giving a step-like profile in longitudinal section. The top of the northern and eastern sectors of the ring-dyke is frequently heterogeneous due to the abundance of gabbro xenoliths up to 30 m across; some of these outcrops are best described as breccias. They afford evidence of dyke intrusion along a zone of fracture (and subsidence?), together with stoping. A number of petrographically identical radial dykes is associated with the porphyritic syenite phase.

Mineralogically, these ring-dyke syenites are characterized by phenocrysts of potash feldspar (microperthitic) and much less commonly plagioclase (as oligoclase cores in alkali feldspar phenocrysts). The coarse groundmass is holocrystalline and consists mainly of microperthite, quartz, arfvedsonite, aenigmatite, and sodic pyroxenes. In the eastern segment the ring-dyke consists of an almost aphanitic quartz trachyte at the southern end; northwards, the ring-dykes become dominated by blocks of layered gabbro, intermixed in a matrix of fine to medium grained syenite.

### Basalt-Dolerite-Tholeiitic Andesite Dyke-Sill and Ring-Dyke Phases

Numerous dykes and sills pervade much of the southern and eastern parts of the complex, with the exception of the central syenite and trachytic ring-dyke. A major 'basaltic' phase forms the western segment of the ring-dyke. The southwestern segment of this dyke northwards to, but excluding Brummies Lookout, consists of tholeiitic andesite containing common xenoliths of sandstone and conglomerate, but no gabbros. In the area of Brummies Lookout, there is a break in the elevation of the ring-dyke, from 520 m to 570 m, and this is associated with a change in rock type from tholeiitic andesite to an aphanitic vesicular basaltic rock; it represents a separate intrusive phase.

Additionally, small dykes and sills intrude weathered gabbro adjacent to the ring-dyke, and these are typically extensively recrystallised. Solomon (1959) has also noted that some of the ring-dyke 'basalts' in contact with the gabbros are recrystallised. A complex intrusive mass of porphyritic tholeiitic andesite also occurs as an E-W trending ridge east of Cedar Creek along its

northern margin, this intrusion is cut and brecciated by trachytes associated with the southeastern arm of the ring-dyke. An additional intrusive sill complex occurs at Mount Terragon, approximately 2 km south of the southern margin of the Mount Warning complex. In this locality, gently southwesterly-dipping sills of tholeiitic andesite alternate conformably with coarse sediments of the Jurassic Tabulam (= Bundamba) Group (Bruce, 1978).

As noted above, dykes and sills of tholeiitic andesite commonly intrude the gabbro, and these are petrographically indistinguishable from the sill complex of Mount Terragon. Moreover, recrystallised basaltic dykes intrude the gabbro adjacent to the ring-dyke. These relations suggest that the gabbro predates a relatively complex 'basaltic' intrusive phase, although no gabbro xenoliths have been so far recognised in the western ring-dyke largely through the Marburg Sandstone, only cutting the gabbros at a relatively shallow level. The various basaltic dykes are cut by trachytic and comenditic dykes and veins, including the southern termination of the eastern ring-dyke. It is suggested that the western segment of the ring-dyke acted as one of the major centres of eruption of the mafic lavas of the Tweed Shield Volcano.

### Late Stage Felsic Dykes

These represent the youngest recognised intrusive phase, composed of comendites and trachytes, the former being predominant. They are found intruding all rock types in the complex, including the youngest ring-dyke phase. Although the distribution of these dykes tends to be random, some show a tendency to be radially disposed about the trachyandesite core, and few are concentric. The dykes vary from 0.3 m – 10 m in width. One very prominent dyke (or plug?) occurs as the northern cliff of the summit.

### Mount Nullum Igneous Complex

This is dominated by microgranite, forming a high level intrusive mass about 3 km by 1.8 km in plan. It is interpreted as a Tertiary intrusive. Within the microgranite occurs a relict lenticular body of monzonite, some 900 m by 300 m. As xenoliths of this monzonite are locally abundant in the enclosing microgranite, it is interpreted as an earlier phase of the complex. The mineralogy of this monzonite varies across the body from augite monzonite (oligoclase-andesine, potash feldspar, augite, hornblende, Fe-Ti oxides, biotite, and minor apatite) to augite-hypersthene monzonite (less quartz, more plagioclase, and exsolution lamellae in hypersthene, and possibly inverted pigeonite).

The dominant feature of interest within the microgranite is the essentially inward change of mineralogy from an outer fayalite-augite-hornblende microgranite through augite-hornblende granite, to an inner zone of hornblende-biotite granite. This change of mineralogy and chemistry is also accompanied by an inward increase in grain size. Considerable development of secondary epidote and chlorite has occurred. Miarolitic cavities are common in the microgranite, ranging in size from 1–15 cm, and are of varying shapes. These cavities typically contain euhedral quartz, and less common feldspar.

## Intrusives on the Flanks of the Mount Warning Shield Volcano

Most of these can be considered as possible sources for some of the lavas and tuffs and some may have built up parasitic (adventive) cones, now removed partly or completely by erosion. The most obvious vents are rhyolitic, especially those intrusive into rocks less resistant to erosion, which stand out from their surroundings as conical peaks, e.g. Egg Rock and Pages Pinnacle on the northern flanks, Dinseys Rock to the east of Mount Warning, and Nimbin Rocks and Doughboy Mountain to the south.

Pages Pinnacle is a vertical linear intrusion, with columnar jointing dipping steeply, outwards from the axis. Extrusive rhyolite occurs to the southeast, with a glassy base and poorly developed columnar jointing (Watt, 1971).

Surprise Rock, south of Binna Burra, is a dyke of alkali rhyolite, of a type not represented amongst the lavas, which appears to intrude the Binna Burra Rhyolite, so that the determined age (Appendix 2) is anomalous. It stands out as a narrow ridge with vertical walls, and shows well marked horizontal columns about 1 m in diameter.

Other rhyolitic intrusions which are less obvious as vents, but which may well have been, include Charraboomba Rock and intrusives at the base of Ballanjui Falls, at Kweebani Cave near Binna Burra, and on the Beechmont-Binna Burra Road (Stevens, 1984).

## Mineralogy of Mount Warning Intrusives

The various rock types of Mount Warning exhibit, between them, an extreme range of compositional variations within the constituent minerals. Representative averaged mineral analyses are presented in Tables 1 to 3. An account of the mineralogy of the volcanic rocks from the northern flank of the Tweed Shield is provided in Ewart *et al.* 1977.

Pyroxenes and Olivines. The gabbros are characterized by coexisting augite and hypersthene (Text fig. 4), which almost always coexist with olivine ($Fa_{38-55}$). All three phases have undergone variable deuteric alteration; the significant proportion of 'uralite' shown in the modal data (Table 4) is interpreted to be predominantly, if not entirely, replacement of orthopyroxene. Compositional ranges of hypersthene and olivine within individual rock samples are typically limited to $< 5\%$ (mol.), with orthopyroxene only exceeding 5% in a leucogabbro (sample 26558), occurring as a xenolith in the monzonite. Augite compositions show similarly narrow ranges, although the trends in which inter-sample variation does occur (e.g. Ca or Fe- enrichment) are variable. These relatively narrow compositional ranges exhibited by the pyroxenes and olivines are attributed to subsolidus re-equilibration processes, and contrast markedly with the compositional variability observed within the rapidly quenched mafic lavas of the Tweed Shield Volcano (e.g. Ewart *et al.*, 1977; Ewart, Baxter and Ross, 1980).

Within the monzonite and trachyandesite intrusive phases, only a single 'equilibrium' Ca-rich pyroxene occurs, also coexisting with relatively Fe-rich olivine ($Fa_{77-91}$). The pyroxenes are significantly more Fe-rich than those in

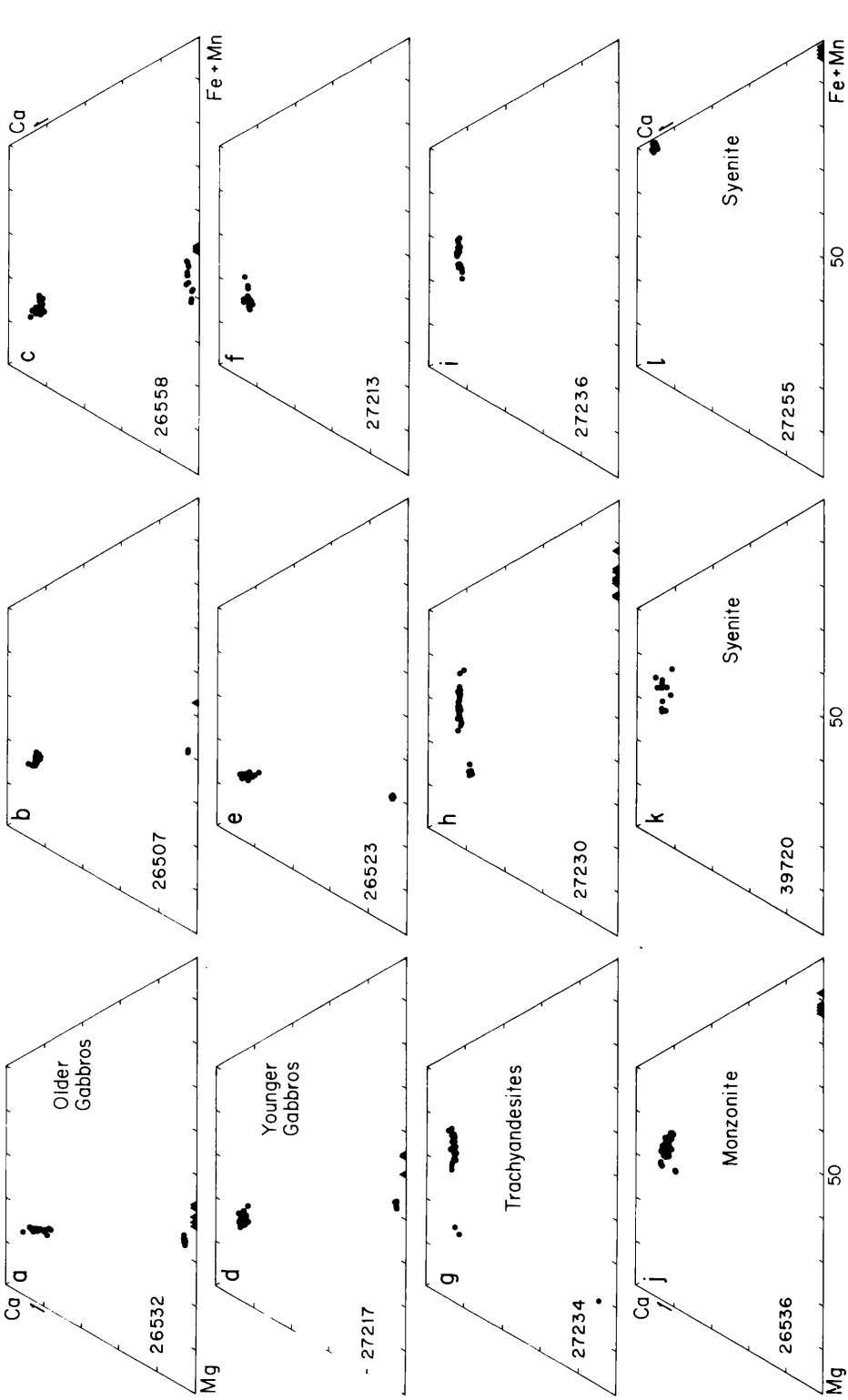


Text fig. 4. Pyroxene (solid circles) and olivine (solid triangles) compositions (atomic %) within the Mount Warning mafic to intermediate intrusives. Microprobe analyses.

the gabbros, and also compositionally more variable in the trachyandesite (presumably reflecting its more rapidly quenched nature). In addition, two trachyandesite samples (27234 and 27230) contain crystals of distinctly more Mg-rich augite, plus bronzite, which are considered to be xenocrystal as their compositions overlap those of the gabbroic pyroxenes.

The syenites, peralkaline granite, and comendite phases exhibit extremely Fe-enriched calcic pyroxenes and olivines (i.e. to hedenbergite and fayalite), extending in the comendites to extreme Na-enrichment, with the development of aegirine. Details of the stages of Na-enrichment are provided in Text fig. 5. It is clear that no Na-enrichment occurs until the calcic pyroxenes have become hedenbergitic, this occurring only within the more evolved syenites and peralkaline granite; samples of these two latter phases exhibit complete gradations between hedenbergite (usually forming cores of crystals) and aegirine (occurring as rims and interstitially). The overall compositions become progressively more sodic in the sequence, syenite to peralkaline granite to comendite. Factors controlling Na-enrichment in such pyroxenes are discussed in Ewart (1981). It is shown that for a given $a^{\text{liquid}}_{Al_2O_3}$ and T, increasing $fo_2$ favours increasing $a^{\text{pyroxene}}_{\text{acmite}}$, whereas if crystallisation follows a constant $fo_2$ buffer curve, then decreasing $a^{\text{liquid}}_{Al_2O_3}$ favours increasing aegirine-rich solid solutions.

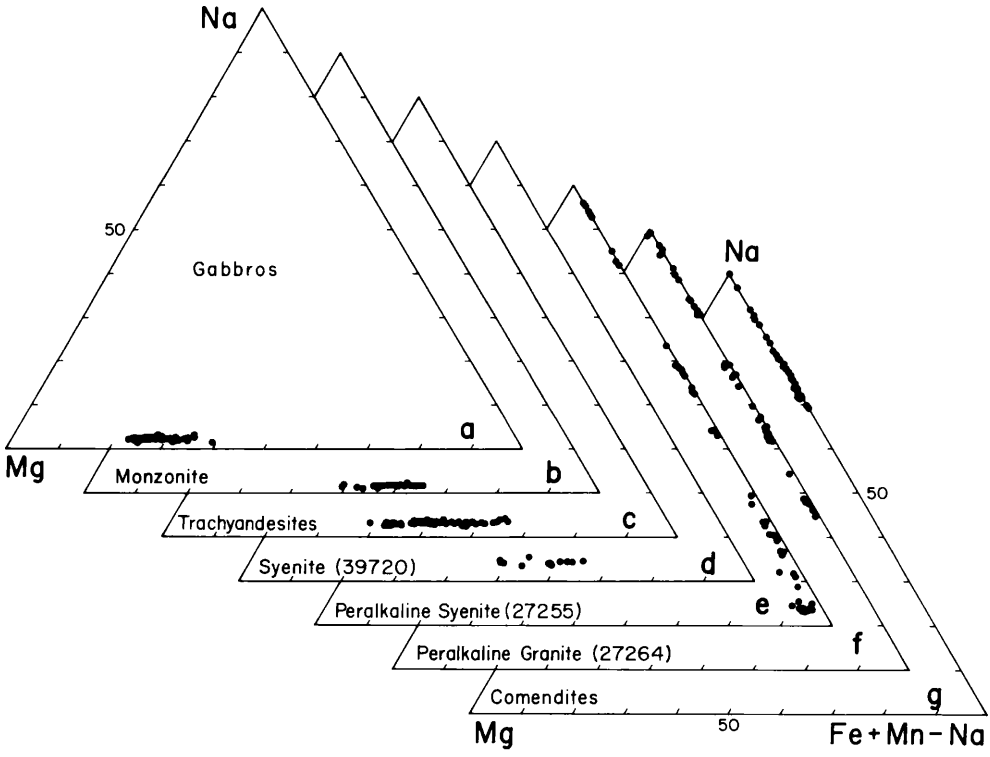


Text fig. 5. Pyroxenes from the various Mount Warning intrusive phases, plotted in terms of Mg, Na, and Fe + Mn – Na (atomic %), showing the changes in Na-enrichment that accompany the development of peralkaline chemistry. Microprobe analyses.

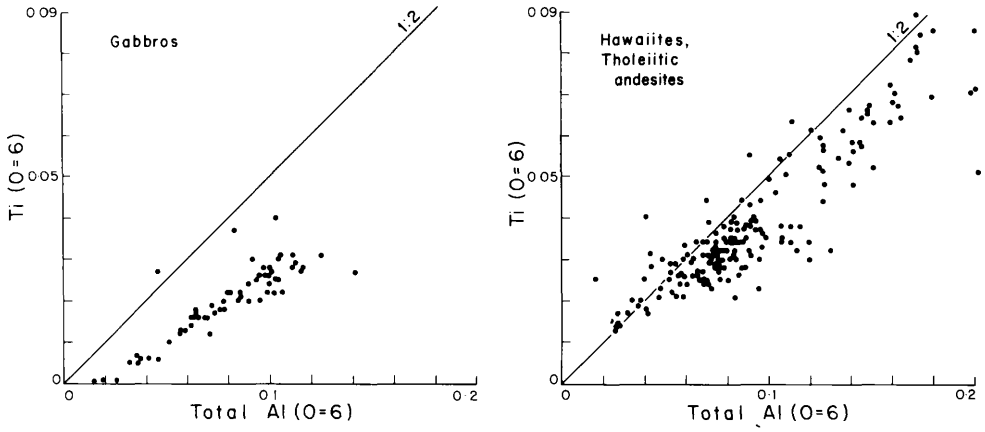


Text fig. 6. Ti-Al relations (based on 0=6) within the Mount Warning gabbroic augites, compared to the groundmass augites of the Beechmont-Hobwee mafic lavas.

The occurrence of Na-enrichment, only after extreme Fe-enrichment is attained in the Mount Warning intrusive suite, is entirely consistent with the same phenomena observed in the volcanic rocks of the southern Queensland region (Ewart, 1981), and is attributed to progressively decreasing $a^{liquid}_{Al_2O_3}$ during fractional crystallisation, combined with relatively low $fo_2$, which is likely to delay the onset of Na-enrichment for a given level of $a^{liquid}_{Al_2O_3}$, in magmas of silica-oversaturated compositions.

Ti-Al relationships within the gabbroic augites (Text fig. 6) indicate a smaller range of concentration (extending to a very low levels of solid solution, and a higher degree of correlation, when compared with augites (groundmass) from the associated mafic lavas. The explanation is again assumed to reflect slower cooling rates, and thus higher degrees of ordering, within the gabbroic augites. The latter do, however, exhibit a shift of their Ti-Al trend away from the ideal 1:2 ratio.

Amphiboles and Biotites. Primary amphibole occurs in the monzonite, syenite-peralkaline granite, and comendite intrusive phases, but not in the gabbros. In contrast, biotite is widespread in the gabbros, mostly as a minor mineral phase, and also occurs in very low modal abundance in the monzonite, trachy-andesites, and syenites.

Amphibole compositions (Text fig. 7) range from edenitic (monzonite), tending towards richterite (trachyandesites), and to riebeckite-arfvedsonite (peralkaline syenite and granite, and comendites). These gross changes in Ca-alkali-alumina chemistry are accompanied by progressively increasing Fe-enrichment, again increasing in the sequence monzonite, trachyandesite, to syenites and comendite (Text fig. 8). Two analyses of secondary amphiboles from the gabbros are edenitic, and show the expected relatively high Mg/Fe ratios (Text fig. 8).

Biotite compositions (Text fig. 9) again exhibit significant changes of Mg/Fe ratios. Within the gabbros, the compositions span a relatively wide range of intermediate Mg/Fe ratios, which tend to extend to more Fe-enriched com-

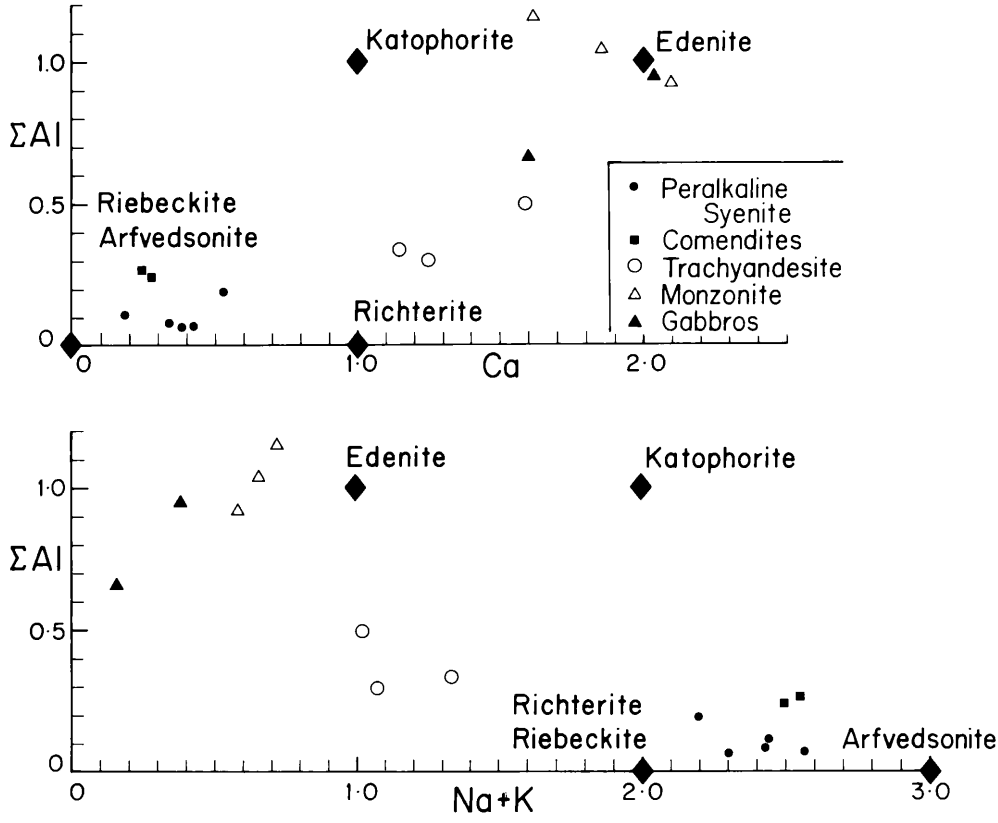


Text fig. 7. Amphibole compositions occurring within the various Mount Warning intrusive phases, expressed in terms of Al, Ca, and Na + K (atomic %; based on 0=23). The compositions of the ideal amphibole end members are shown. Microprobe data.

positions in the younger gabbros. The monzonite and trachyandesite biotites become very Fe-enriched (annites), more so than the coexisiting amphiboles. In Text fig. 9, these annite compositions are seen to be similar to, but even more ferriferous, than the phenocrystal annites occurring within certain of the Binna Burra Rhyolites.

Feldspars (Text fig. 10). The gabbros are dominated by plagioclase whose compositions are surprisingly variable within most individual samples examined, extending from labradorite through to oligoclase (see also Text fig. 25). The greatest variation occurs in the leucogabbros, in which the most sodic compositions are found, and these are interpreted to represent crystallisation from entrapped and relatively differentiated liquid, developed at the more advanced stage of gabbro solidification. This interpretation is strengthened by the additional occurrence of interstitial K-rich orthoclase in the leucogabbros.

Two quite discrete feldspars, plagioclase and alkali feldspar, are found in the trachyandesite and monzonite phases. Within the trachyandesites, the plagioclase is relatively calcic (calcic andesine to labradorite) and coexists with a heterogeneous and clearly variably unmixed alkali feldspar, the average composition of which indicates an original calcic anorthoclase ($Or_{30.8}An_{7.8}$ to

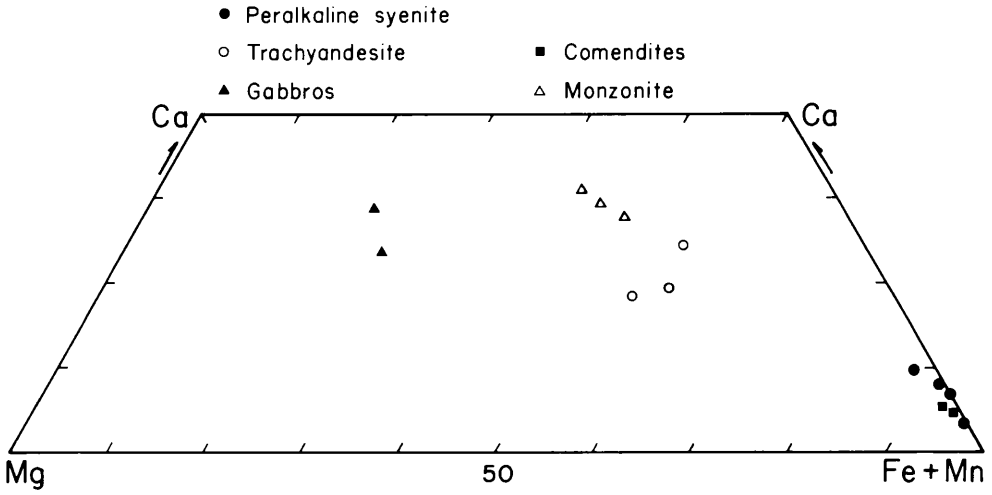


Text fig. 8. Mount Warning amphibole compositions expressed in terms of Mg, Ca, and Fe + Mn (atomic %). This plot should be compared with Fig. 7.

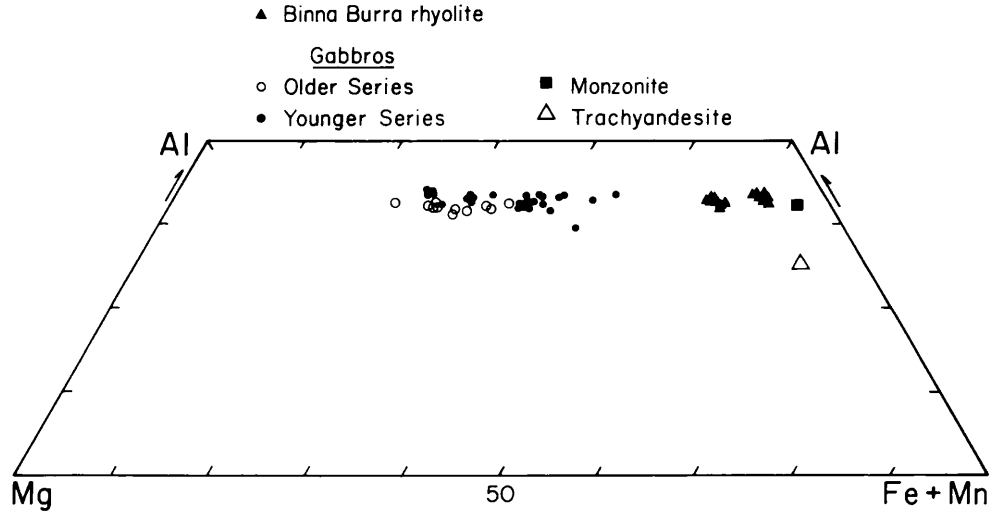


Text fig. 9. Compositions of Mount Warning biotites occurring within the various intrusive phases, expressed in terms of Mg, Fe + Mn, and Al (atomic %). The phenocrystal biotites in the Binna Burra Rhyolite are shown for comparison (after Ewart, 1981). Microprobe data.

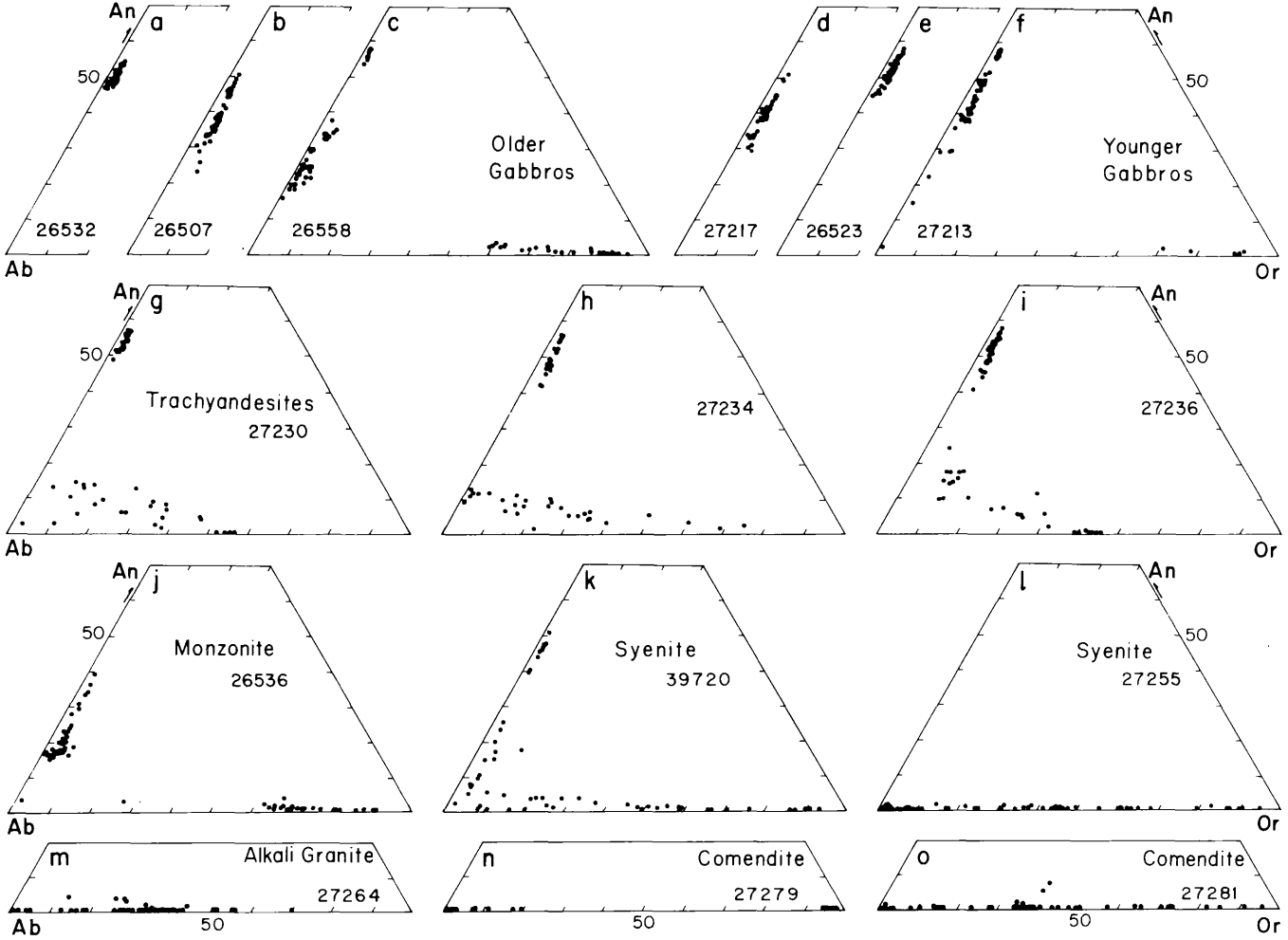


Text Fig. 10. The compositions of feldspars (mol %) occurring within the various Mount Warning intrusive phases. Microprobe data.

$Or_{34.3}An_{4.9}$). These compositions contrast markedly with those in the monzonite, which contains oligoclase-andesine coexisting with an originally potash-rich alkali feldspar ($Or_{66.8}An_{1.2}$). The mineralogy thus suggests that the trachyandesites are not simply the subvolcanic equivalent magma of the monzonite.

The monzonitic feldspar compositions are quite similar to those observed within the two-feldspar ferrohypersthene rhyolites of SE. Queensland (Ewart, 1981), whereas the trachyandesite feldspars are rather similar to those of SE. Queensland trachytes, especially in respect to the calcic anorthoclase; none of the trachytes, however, contains such calcic plagioclase compositions (Ewart, 1981). This observation suggests that some, if not all, of the plagioclase in the trachyandesites is xenocrystic, which is in accord with the occurrence of xenocrystic pyroxenes (previous discussion), together with the corroded and rimmed nature of the plagioclase (see petrography), and the occurrence of disequilibrium Fe-Ti oxide compositions (Table 3). The compositions of the trachyandesite plagioclases are similar to the more calcic compositions of the gabbroic plagioclases; it is further noted that the xenocrystic pyroxenes in the trachyandesites are also similar to those within the gabbros. It is thus concluded that the trachyandesites represent hybrid rocks.

Feldspars in the various syenite and alkali granite phases are compositionably variable, but clearly reflect the increasing fractionation towards, and within, the peralkaline magmas. The non-peralkaline quartz syenite contains bimodal plagioclase compositions, oligoclase and calcic andesine, together with a wide range of alkali feldspar compositions (representing unmixing), the average of which indicates an original sodic sanidine ($Or_{42.2}An_{1.5}$). Thus, the averaged compositions occurring within this syenite are $An_{45}$ and $An_{15}$, and $Or_{42}$; again, it seems possible that the more calcic plagioclases are inherited, supported by their occurrence as small cores enclosed especially by the alkali feldspar. This suggests that the equilibrium coexisting feldspar compositions are $An_{15}$ and $Or_{42}$.

The peralkaline syenite and granite phases contain no primary plagioclase, but are characterized by a highly exsolved alkali feldspar whose average compositions ($Or_{32.0}$ $An_{32.0}$ $Ab_{36.0}$ and $Or_{33.0}$ $An_{0.2}$ $Ab_{66.8}$) suggest initial Ca-poor anorthoclase. This feature is very similar to those of the comenditic phases, both in the Mount Warning Complex, and in other centres of southern Queensland and New South Wales (Ewart, 1981).

## Chemistry

Introduction. Available major and trace element analyses of representative samples from the main intrusive phases of the Mount Warning complex are listed in Table 4. It is of some interest to initially compare the general chemistry of gabbros with the associated mafic lavas of the Beechmont and Hobwee Basalts. Although the gabbros are unlikely to have a direct genetic link to the lavas (because of probable age differences, the very shallow level of the gabbroic magma chambers, and the eruption of the lavas from independent dyke complexes), their occurrence within the same volcanic centre suggests that some degree of geochemical affinity should be evident. A compli-

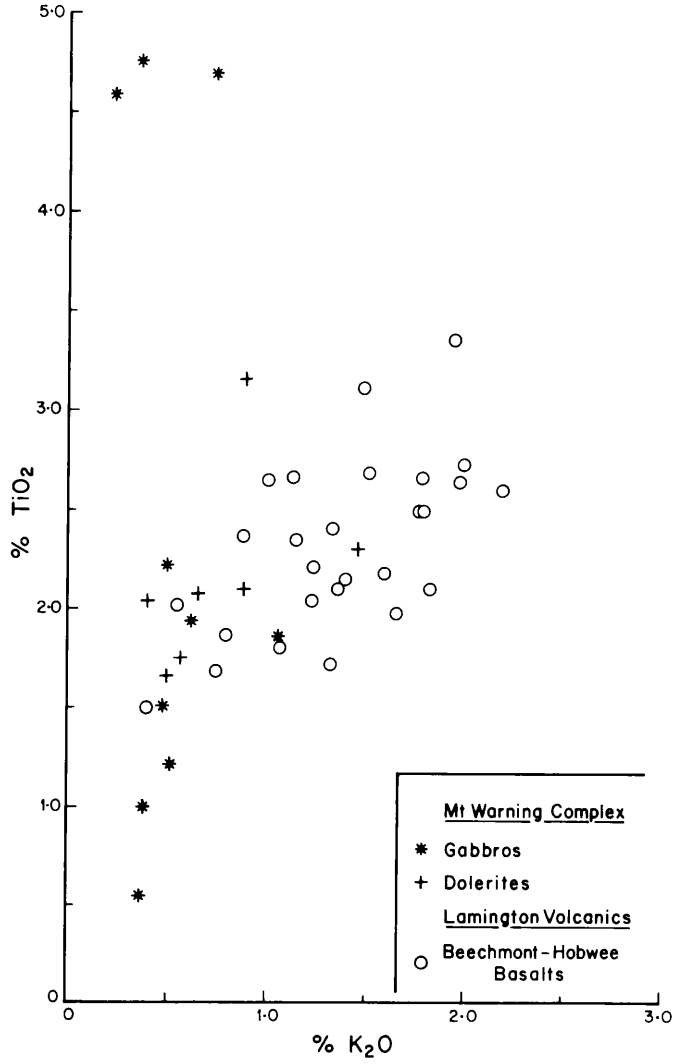


Text Fig. 11. $K_2O$ versus $TiO_2$ (wt %) within the intrusive gabbros and dolerites of Mount Warning, and the Beechmont-Hobwee mafic lavas. Data from Table 4, Ewart *et al.* (1977), Ross (1977) and Wilkinson (1968).

cating factor in such a comparison is, however, the likely partially cumulative nature of the gabbros. An account of the chemistry of the various eruptive phases of the northern flank of the Tweed Shield is provided in Ewart *et al.* (1977).

Element Abundances. Comparison of certain of the element/oxide abundances, notably $K_2O$, Zr, CaO, and Sr, does indicate significant differences between the gabbros and lavas (Text figs 11-15), the gabbros being distinctly depleted in Zr and $K_2O$, but enriched in CaO and less clearly, Sr. Such differences are interpreted to be primarily the result of cumulative processes in the gabbros with the effective loss of a residual liquid component enriched in Zr, K, and related

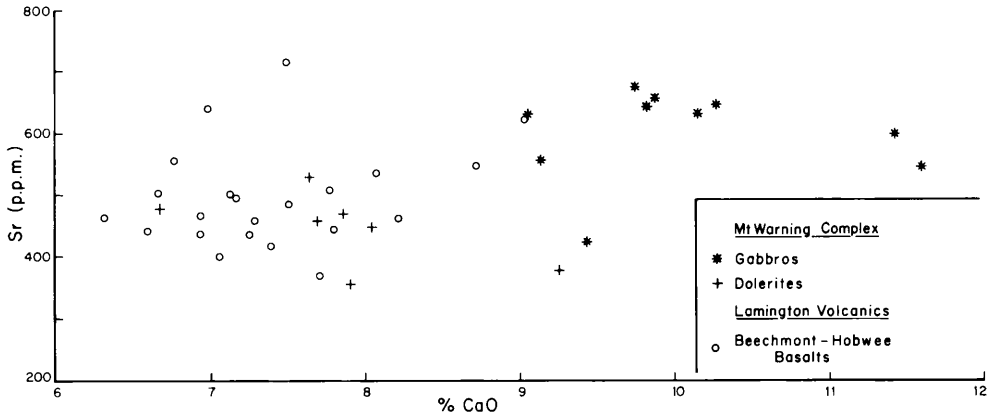


Text fig. 12. CaO (wt %) versus Sr within the Mount Warning intrusive gabbros and dolerites, and the Beechmont-Hobwee mafic lavas. Data sources from Table 4, Ewart *et al.* (1977), Ross (1977), and Wilkinson (1968).

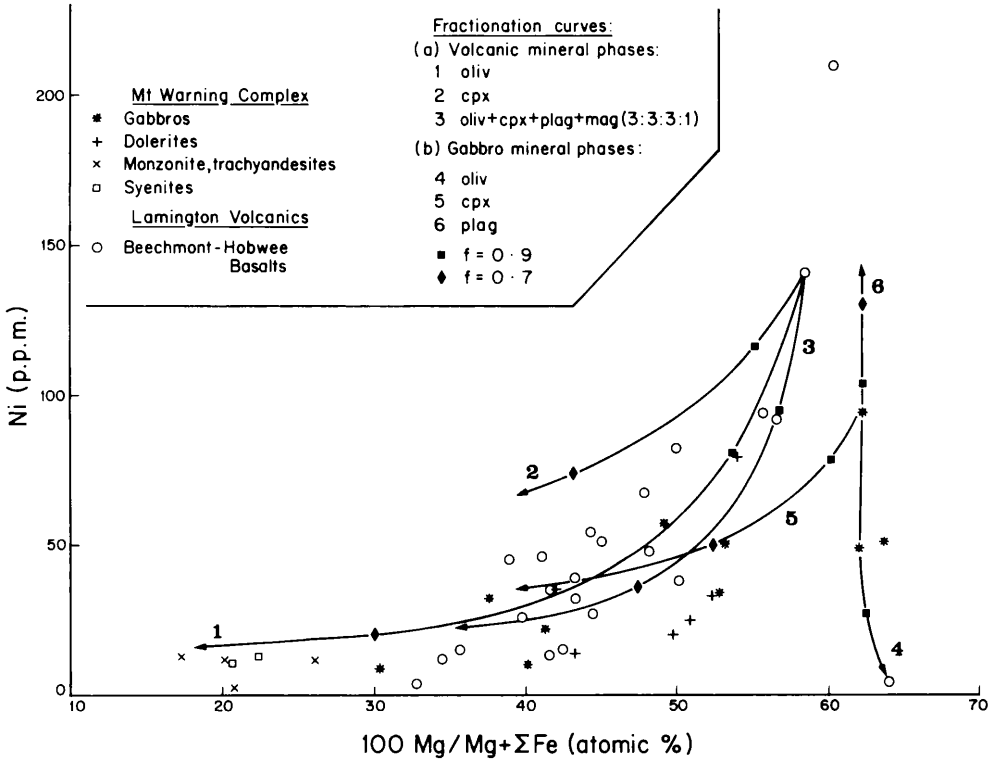


Text Fig. 13. Ni versus Mg/Mg + ΣFe in the mafic and intermediate Mount Warning intrusives, and the Beechmont-Hobwee lavas. The fractionation curves are based on Rayleigh fractionation, from representative lava and gabbro samples as starting compositions. f represents the weight fraction of liquid remaining. Basaltic partition coefficients used (see Appendix 1). Further details of calculated curves given in text. Data sources as in Fig. 12.

elements. An example is provided by the $TiO_2$–$K_2O$ plot (Text fig. 11), in which the highly variable $TiO_2$ levels of the gabbros is clear; the highest values correlate with high modal Fe-Ti oxides (Table 1), certainly a cumulative feature. The higher CaO levels in the gabbros (Text fig. 12) are similarly attributed to combined plagioclase-augite accumulation.

In contrast, the Ni and Cr abundances of the gabbros and mafic lavas (Text figs 13, 14) overlap, there being a tendency for the higher Cr values to correlate with lower Ni in the gabbros and dolerites; this is not, however, simply correlated with modal augite (see Table 4), but most probably is controlled by the combined cumulative effects of both Cr-spinels (included in olivines) and pyroxenes (both augite and orthopyroxenes). Within the gabbros and associated intrusive mafic phases, V and FeO* (=ΣFe as FeO) are closely correlated (Text fig. 15), contrasting with the much greater data scatter within the extrusive mafic lavas. The V-FeO* trend exhibited by the intrusive mafic rocks does not, however, extrapolate centrally through the compositional fields of the Beechmont-Hobwee lavas, nor near the monzonite and syenite data, the latter evidently defining a separate trend. These differences are again inter-

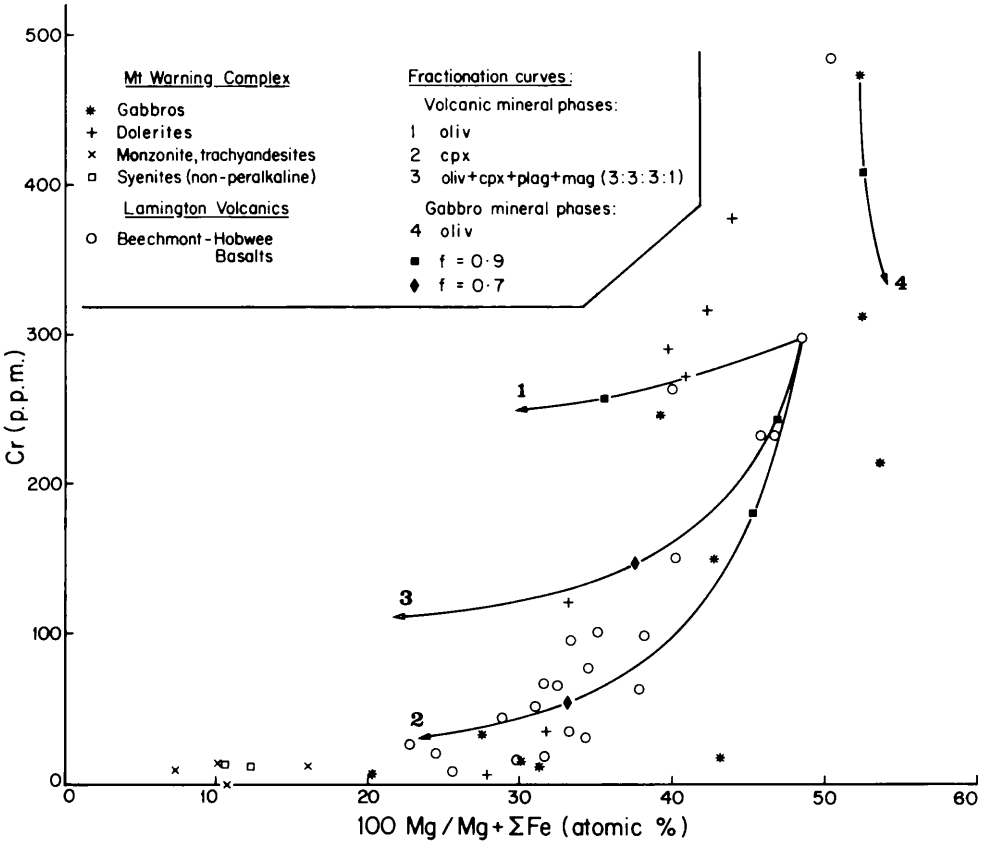


Text fig. 14. Cr versus Mg/Mg + Fe in the mafic and intermediate intrusives of Mount Warning, and the Beechmont-Hobwee lavas.

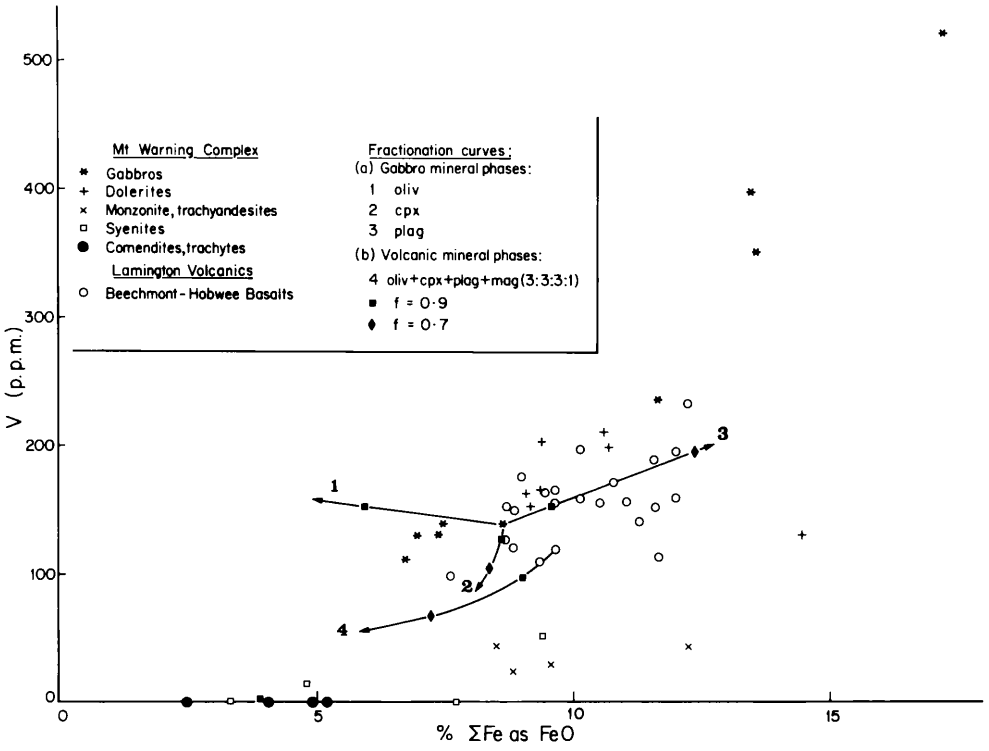


Text fig. 15. V versus FeO* in the Mount Warning intrusives, and the Beechmont-Hobwee lavas.

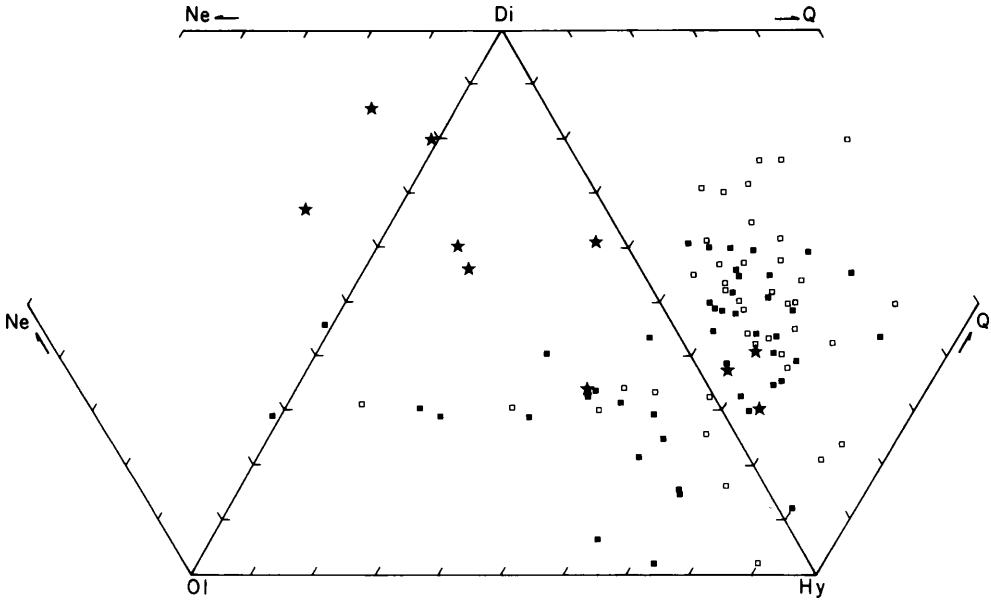


Text fig. 16. Normative (C.I.P.W.) compositions of the Mount Warning gabbros (filled stars) and Beechmont-Hobwee lavas and intrusive dolerites (squares; hollow symbols based on analysed $Fe_2O_3$ and FeO; solid symbols assume $Fe_2O_3/Fe_2O_3 + FeO = 0.2$).

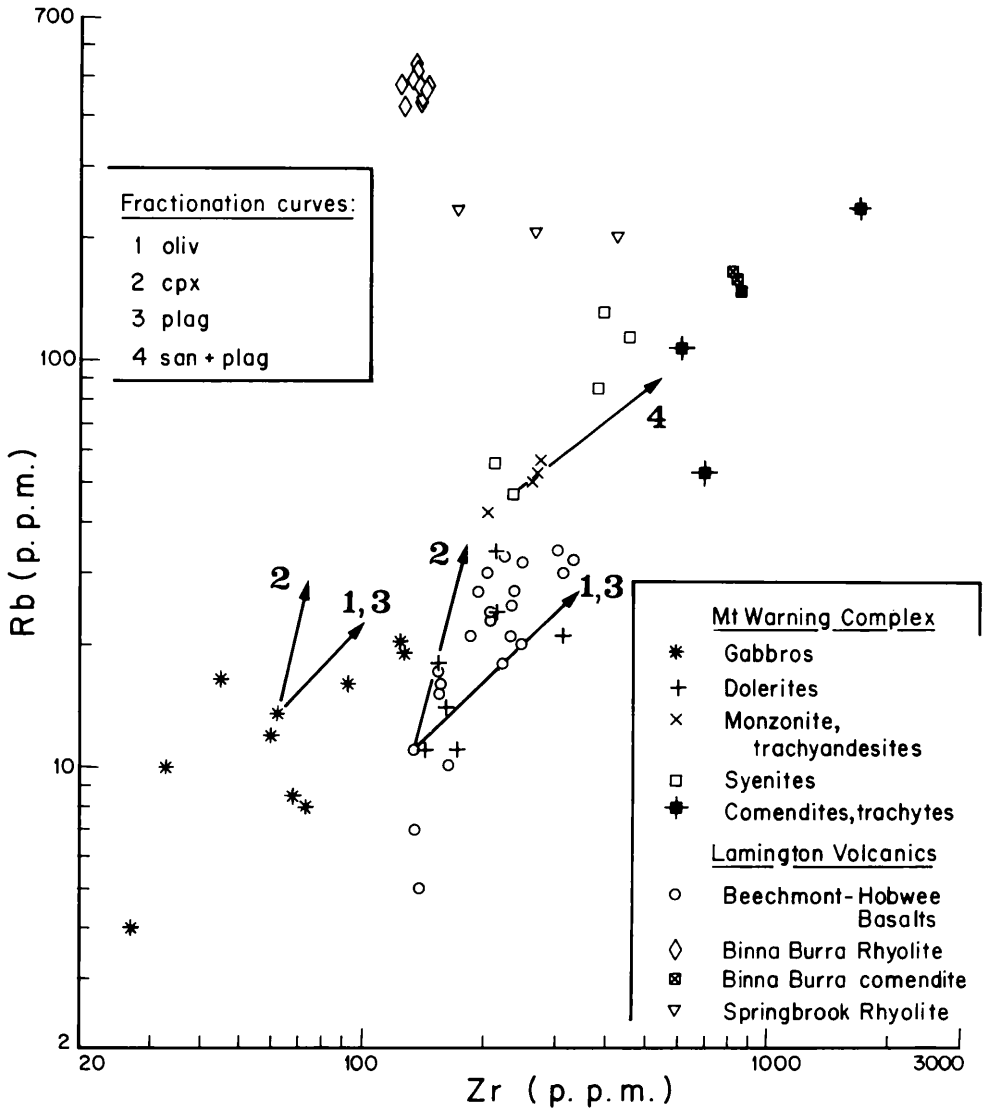


Text fig. 17. Rb versus Zr for the Lamington from the northern flank of the Tweed Shield. Basaltic partition coefficients used for curves 1 to 3, and trachytic coefficients for curve 4 (see Appendix 1).

preted in terms of cumulative processes, and within the gabbros the higher V levels are readily correlated with higher modal Fe-Ti oxide abundances.

With respect to the levels of silica saturation, the intrusive and extrusive mafic rocks are compared in Text fig. 16 in terms of normative *ne, ol, di, hy,* and Q. The Beechmont-Hobwee lavas are predominantly quartz-normative, although *ol*-normative compositions occur, whereas the gabbros extend from Q to *ne*-normative compositions, the latter group reflecting significant modal biotite occurrence.

Fractional Crystallisation. A second aspect of the chemistry of the Mount Warning intrusive complex, and the associated volcanic sequences, is the role of

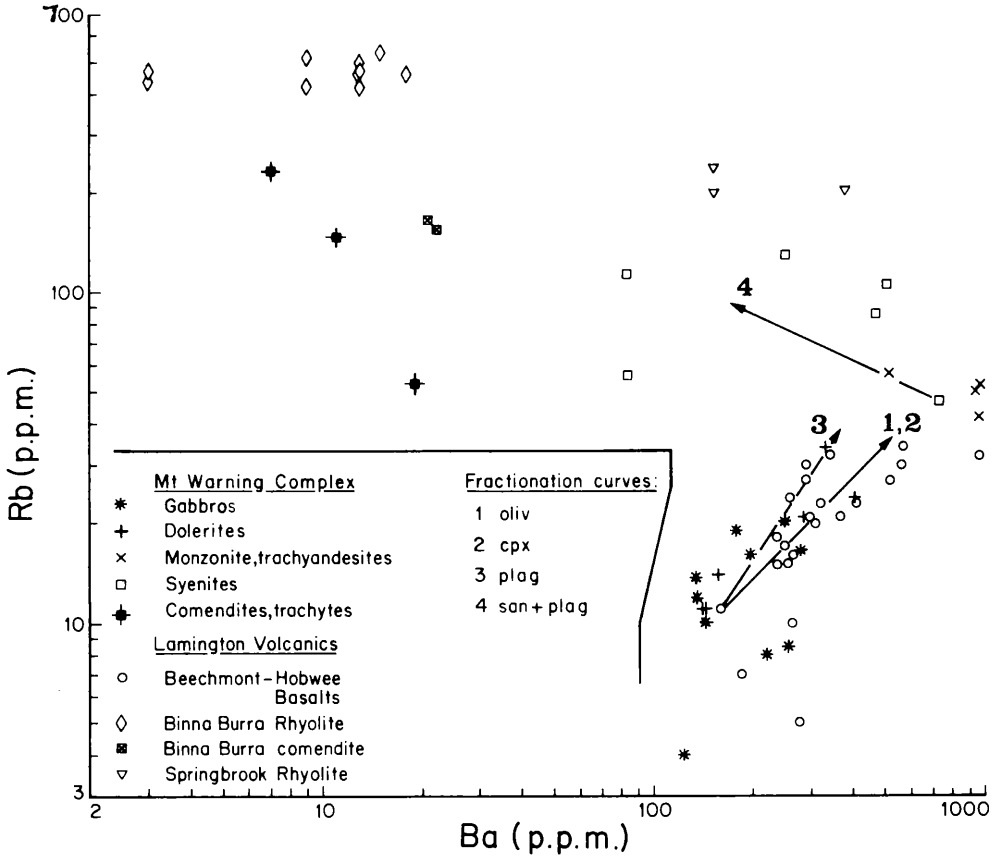


Text fig. 18. Rb versus Ba for the Mount Warning intrusives, and the Lamington Volcanics from the northern flank of the Tweed Shield. Partition coefficients as in Fig. 17.

crystal-liquid fractionation in producing the evolved magma compositions; these include the monzonite, trachyandesite, syenite, and comendites in the Mount Warning complex. Various plots of major and trace element data are presented, three of which (Text figs 17 to 19) utilise Rb as an incompatible element, based on its observed behaviour in the silicic volcanic rocks of eastern Australia (Ewart, Chappell, and Le Maitre, 1985).

The Mount Warning data exhibit a broad coherence between Rb-Zr (Text fig. 17); similar behaviour is found between Rb-Ce, Rb-Nb, and to a lesser extent, Rb-Zn (in which Zn can be modified by Fe-Ti oxide fractionation). With respect to Rb and Zr, the calculated effects of olivine, augite, and plagioclase fractionation are shown for a typical gabbro and a Beechmont/Hobwee lava; these are based on Rayleigh fractionation and basaltic partition coefficients (see Appendix 1). The effect of plagioclase + sanidine fractionation is also shown for one of the syenitic compositions. It can be seen from the calculated trajectories that a fractionating mineral assemblage in which olivine and feldspar (either together or separately) comprise the dominant phases, will explain the overall gabbro-syenite-comendite trend for the Mount Warning

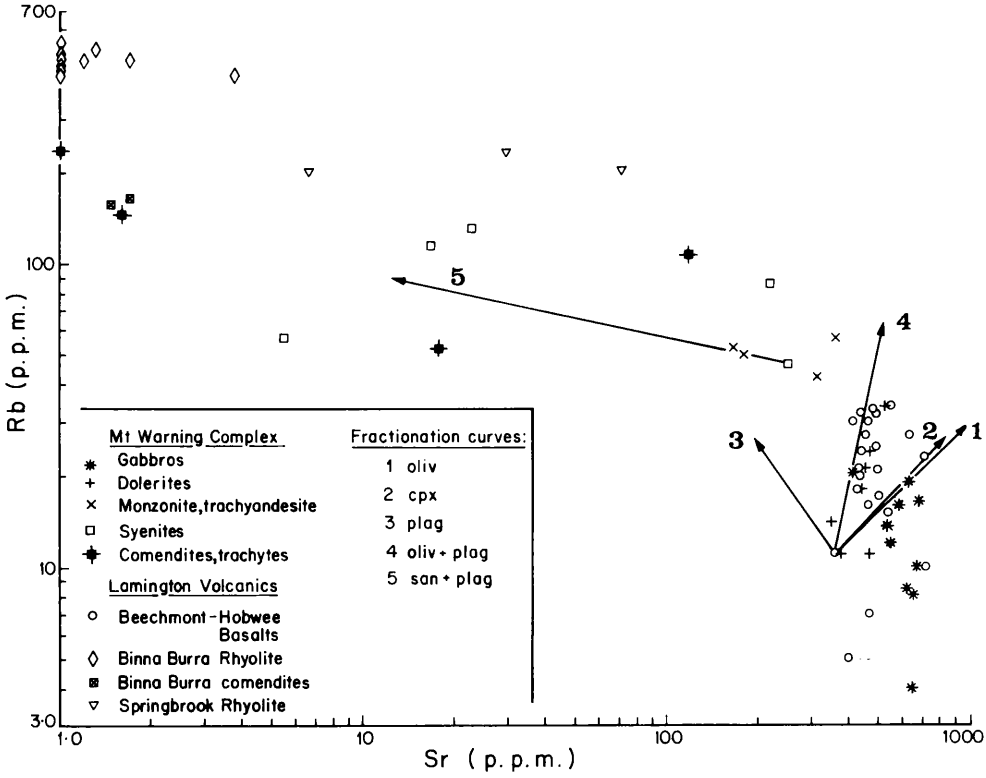


Text fig. 19. Rb versus Sr for the Mount Warning intrusives, and the Lamington Volcanics from the northern flank of the Tweed Shield. Basaltic partition coefficients used in curves 1 to 4; trachytic coefficients for curve 5 (see Appendix 1).

Complex, and is a possible explanation for much of the variation observed within the Beechmont-Hobwee lavas. Augite is clearly not a dominating fractionating phase. The Rb-Zr plot also illustrates the geochemical uniqueness of the Binna Burra and Springbrook Rhyolites, indicating that they are not a simple product of continued fractional crystallisation of a more primitive mafic parental magma. The petrogenesis of these rhyolites is discussed in more detail in Ewart (1982, 1985), in which it is concluded that the rhyolites initially develop as localized crustal anatectic magmas.

More complex behaviour is shown by the Rb-Ba and Rb-Sr plots (Text figs 18,19), in which Ba initially increases (in the gabbros and mafic extrusives), and then decreases as the magmas become more evolved, and more siliceous. Sr shows the change of behaviour more strongly than Ba. Reference to the calculated fractionation trends in Text figs 18 and 19 shows that the initial increase in Rb, Sr, and Ba is explicable in terms of a fractionating olivine + augite + plagioclase-bearing phase assemblage (the trend of the Sr variation certainly requiring the presence of a major plagioclase component); these trends are based on basaltic partition coefficients (Appendix 1). The subsequent relative decrease in Ba and Sr is, in terms of the fractional crystallisation model, only consistent with feldspar-dominated fractionation, and the appropriate sanidine + plagioclase curves shown in Text figs 18 and 19 are based on

trachytic partition coefficients (Appendix 1). It should be noted that in both plots, the extremely high Rb concentrations of the Binna Burra Rhyolite are a conspicuous feature.

Modelling of the behaviour of Ni and Cr (versus Mg/Mg + Fe) and V (versus FeO*) is graphically illustrated in Text figs 13 and 14 by means of calculated olivine, augite, and plagioclase fractionation curves, and a combination of these phases, including additional magnetite. Compositions (mol. %) of the mineral phases used are for the mafic lavas and gabbros, respectively: $Fa_{22}$ and $Fa_{38}$ (olivines); $Mg_{43.6}$ $Fe_{12.8}Ca_{43.6}$ and $Mg_{42.3}$ $Fe_{15.5}$ $Ca_{42.2}$ (augites); and $An_{53}$ (plagioclase). These compositions are based on analysed phases; these volcanic mineral compositions are further discussed and applied in a later part of this paper dealing with the Focal Peak lavas. Reference to Text figs 13 and 14 indicates that the sharp decreases of Cr and Ni abundances with decreasing Mg/Mg + $\Sigma$Fe ratios are generally consistent with olivine and augite fractionation, both for the Mount Warning gabbro to syenite intrusive phases, and as an explanation for the variation observed within the Beechmont-Hobwee lavas. As the actual curvature of the calculated fractionation curves in these plots is sensitive to changes in the Fe/Mg ration of the augite and especially the olivine phases, improved fits to the data can be obtained by suitable adjustments to mineral compositions; this would require independent, direct information concerning the compositions of fractionating minerals, not currently available.

Reference to the V behaviour (Text fig. 15) indicates that the development of V depletion, as observed in the Mount Warning syenitic and monzonitic rocks and trachyandesites, requires the presence of augite, and particularly magnetite, in a fractionating mineral assemblage. Notwithstanding this, the V-FeO* abundances of these more evolved intrusive phases do not lie on the gabbroic trend, are not immediately related, and in the trachyandesites show mixing evidence. As mixtures the trachyandesites would require a less fractionated member as one of the end members, quite unlike the gabbroic trend. It is also relevant to note the mineralogical evidence suggesting mixing within the trachyandesites.

## Comparison of the Evolved Extrusive and Intrusive Phases of the Tweed Volcano

A significant feature of the chemistry of the Mount Warning complex and the associated volcanic sequences relates to the degree of geochemical discordance between on the one hand the Binna Burra Rhyolite and comendite (and also the Nimbin Rhyolite) and on the other the evolved intrusive phases of Mount Warning. This discordance is particularly well illustrated by Rb-Zr, Rb-Ce, Rb-Nb, and to a lesser extent, the Rb-Zn relations in which the rhyolites do not simply plot on the extension of the geochemical trends defined by the Mount Warning intrusive phases. In each case, the rhyolites exhibit relative depletion of Zr, Ce, Nb and Zn when considered in terms of their highly enriched Rb abundances. These discontinuities of the rhyolite trace element patterns are, however, consistent with (i) their distinctly more radiogenic Sr and Pb isotopic compositions, and higher $\delta^{18}O$ compared to associated mafic and intermediate volcanics, suggesting an essentially distinct source from the mafic and intermediate lavas (Ewart, 1982, 1985); this source

is interpreted as localized crustal melts. (ii) The absence of equivalent intrusive phases to the Binna Burra rhyolites within the Mount Warning intrusive complex (with the possible exception of Dinseys Rock in the Tweed Valley), suggesting that the evolution and eruption of the rhyolites occurred peripherally around (and beneath) the intrusive complex, consistent with their deduced anatectic origin (Ewart, 1985). It is noteworthy, however, that the rhyolites still exhibit extreme Ba and Sr depletion, indicating the operation of feldspar-dominated crystal fractionation.

It is also relevant to compare the comendites from Binna Burra and Mount Warning; the former have similar isotopic compositions to the rhyolites (Ewart, 1982), in contrast to comendites from other volcanic centres in SE. Queensland, which are more closely allied isotopically to associated mafic and trachytic lavas. The Rb-Nb, Rb-Zn, and Rb-Ce relations suggest that the comendites from Binna Burra are intermediate between those of Mount Warning and the Binna Burra Rhyolites, although in the Rb-Zr plot (Text fig. 17), they are closer to those of Mount Warning. The trace element data are thus ambiguous, but on balance, suggest that the Mount Warning comendite magmas have developed independently from those outcropping at Binna Burra.

**Summary of Petrological Characteristics of Complex**

1. The complex consists of a sequence of discrete intrusive phases, ranging from gabbros to comendite. Each phase was evidently fed by magma pulses from deeper chambers, and the syenitic and other more evolved magmas were already considerably fractionated to their more evolved chemistries prior to emplacement. The Mount Warning complex, however, must have constituted a shallow subvolcanic magma reservoir.
2. Some degree of *in situ* crystal fractionation has occurred within the gabbroic phase of the intrusive complex, as evidenced by the lamination and layering, and by the trace element data. The syenitic phase, however, appears to represent separate pulses of non-peralkaline and peralkaline magma. It is significant to note here that least squares calculations have failed to provide acceptable solutions in linking the various syenitic and gabbroic compositions by fractional crystallisation, the residual errors being high. This is believed to be primarily due to the fact that the gabbroic chemistry is not that of the primary magmas from which the syenites are interpreted to have been derived, due certainly in part to the effects of cumulative processes during gabbro solidification. This again argues against an *in situ* derivation of the syenitic phases. It is shown, however, that the overall geochemistry of the evolved intrusive phases of the Mount Warning complex is consistent with a crystal-liquid fractionation mechanism for their evolution.
3. Although the Mount Warning complex appears to represent the core of th Tweed Shield volcano, the available K-Ar ages suggest that its solidification predates the main phase of volcanic activity. Whether older or contemporaneous, the elevation of the intrusive complex, relative to the volcanic succession, implies significant erosion and possible central uplift (Stevens, 1970). This may parallel the uplift history of the Mount Barney Central Complex.
4. The syenitic, monzonitic, and trachyandesite phases of the intrusive complex have no strictly extrusive equivalents within the Lamington volcanic

## TABLE 1. AVERAGE MICROPROBE ANALYSES OF PYROXENES OCCURRING IN THE MOUNT WARNING INTRUSIVES
(See Table 4 for additional sample data)

| | Gabbros | | | | | | | | | | | Monzonite |
|---|---|---|---|---|---|---|---|---|---|---|---|---|
| | 26532[(1)] | 26532 | 26507 | 26507 | 26558 | 26558 | 27217 | 27217 | 26523 | 26523 | 27213 | 26536 |
| $SiO_2$ | 51.31 | 52.49 | 52.14 | 52.39 | 51.19 | 51.83 | 52.01 | 51.26 | 51.85 | 52.70 | 51.36 | 50.11 |
| $TiO_2$ | 0.76 | – | 0.43 | 0.15 | 0.87 | 0.17 | 0.54 | 0.19 | 0.84 | 0.41 | 0.51 | 0.26 |
| $Al_2O_3$ | 2.14 | 1.02 | 1.10 | 0.46 | 2.24 | 0.54 | 1.36 | 0.55 | 1.96 | 1.09 | 1.82 | 0.71 |
| FeO | 10.05 | 20.65 | 11.47 | 24.82 | 10.15 | 26.04 | 11.44 | 26.09 | 9.39 | 18.81 | 11.01 | 20.37 |
| MnO | 0.27 | 0.47 | 0.29 | 0.63 | 0.24 | 0.49 | 0.30 | 0.68 | 0.24 | 0.40 | 0.29 | 0.55 |
| MgO | 14.61 | 22.42 | 13.54 | 20.18 | 14.32 | 19.43 | 13.26 | 19.37 | 14.81 | 24.16 | 13.66 | 7.79 |
| CaO | 20.05 | 1.48 | 20.62 | 1.26 | 20.20 | 1.16 | 20.42 | 1.38 | 20.54 | 1.94 | 20.54 | 19.35 |
| $Na_2O$ | 0.35 | 0.04 | 0.34 | 0.04 | 0.36 | 0.02 | 0.34 | 0.03 | 0.34 | 0.04 | 0.37 | 0.24 |
| $Cr_2O_3$ | 0.17 | n.d. | 0.02 | n.d. | n.d. | n.d. | 0.06 | n.d. | n.d. | n.d. | 0.04 | 0.04 |
| NiO | 0.10 | n.d. | 0.02 | n.d. | n.d. | n.d. | – | n.d. | n.d. | n.d. | 0.04 | 0.08 |
| $ZrO_2$ | n.d. | n.d. | n.d. | n.d. | n.d. | n.d. | n.d. | n.d. | n.d. | n.d. | n.d. | n.d. |
| Total | 99.81 | 98.57 | 99.97 | 99.93 | 99.57 | 99.68 | 99.73 | 99.55 | 99.97 | 99.55 | 99.64 | 99.50 |
| Calculated $Fe_2O_3$ and FeO assuming 0 = 6, $\Sigma$ cations = 4 | | | | | | | | | | | | |
| $Fe_2O_3$ | 1.93 | 0.44 | 1.31 | 0.49 | 1.64 | 0.68 | 0.49 | 1.93 | 1.30 | 1.73 | 2.06 | 0.71 |
| FeO | 8.31 | 20.25 | 10.29 | 24.38 | 8.67 | 25.43 | 11.00 | 24.35 | 8.22 | 17.25 | 9.16 | 19.73 |
| Total | 100.00 | 98.61 | 100.10 | 99.98 | 99.73 | 99.75 | 99.78 | 99.74 | 100.10 | 99.72 | 99.85 | 99.57 |

– = not detected
n.d. = not determined

(1) Sample numbers refer to rock collection in Dept of Geology and Mineralogy, University of Queensland.

**Table 1 (continued). AVERAGE MICROPROBE ANALYSES OF PYROXENES OCCURRING IN THE MOUNT WARNING INTRUSIVES**
**(See Table 4 for additional sample data)**

| | Trachyandesites | | | | | | Syenites, alkali granite | | | | Comendites | |
|---|---|---|---|---|---|---|---|---|---|---|---|---|
| | 27230 | 27230 | 27234 | 27234 | 27234 | 27236 | 39720 | 27255 | 27255 | 27264 | 27281 | 27279 |
| $SiO_2$ | 49.87 | 49.92 | 49.10 | 49.75 | 53.14 | 49.83 | 50.39 | 47.48 | 50.30 | 50.25 | 50.95 | 50.73 |
| $TiO_2$ | 0.62 | 1.00 | 0.72 | 1.18 | n.d. | 0.61 | 0.39 | 0.72 | 0.15 | 0.31 | 0.48 | 0.34 |
| $Al_2O_3$ | 1.05 | 3.67 | 1.02 | 5.32 | 3.33 | 1.02 | 0.56 | 0.58 | 0.52 | 0.18 | 0.19 | 0.31 |
| FeO | 18.48 | 10.85 | 19.71 | 9.38 | 12.18 | 17.25 | 19.56 | 28.61 | 29.54 | 29.46 | 29.86 | 29.65 |
| MnO | 0.68 | 0.27 | 0.76 | 0.18 | 0.24 | 0.62 | 0.69 | 0.99 | 0.65 | 0.49 | 0.52 | 0.63 |
| MgO | 8.77 | 14.70 | 7.37 | 14.31 | 27.90 | 9.62 | 7.39 | 0.64 | 0.09 | 0.12 | 0.03 | 0.09 |
| CaO | 19.62 | 18.61 | 19.75 | 19.25 | 2.22 | 19.70 | 19.85 | 19.70 | 10.32 | 8.42 | 4.52 | 5.52 |
| $Na_2O$ | 0.48 | 0.46 | 0.46 | 0.63 | 0.08 | 0.44 | 0.59 | 0.46 | 6.95 | 8.38 | 10.64 | 10.13 |
| $Cr_2O_3$ | n.d. | n.d. | n.d. | – | n.d. | n.d. | 0.03 | – | – | n.d. | – | – |
| NiO | n.d. | n.d. | n.d. | 0.04 | n.d. | n.d. | 0.05 | 0.14 | – | n.d. | – | – |
| $ZrO_2$ | n.d. | n.d. | n.d. | n.d. | n.d. | n.d. | n.d. | n.d. | 0.06 | n.d. | 0.28 | 0.27 |
| Total | 99.57 | 99.48 | 98.89 | 100.04 | 99.09 | 99.09 | 99.50 | 99.32 | 98.58 | 97.61 | 97.47 | 97.67 |
| Calculated $Fe_2O_3$ and FeO assuming 0 = 6, $\Sigma$ cations = 4 | | | | | | | | | | | | |
| $Fe_2O_3$ | 2.20 | 3.02 | 1.89 | 2.39 | 2.02 | 2.42 | 1.17 | 0.94 | 17.42 | 21.86 | 27.04 | 26.27 |
| FeO | 16.50 | 8.14 | 18.01 | 7.23 | 10.36 | 15.07 | 18.51 | 27.77 | 13.87 | 9.79 | 5.53 | 6.01 |
| Total | 99.79 | 99.78 | 99.08 | 100.28 | 99.29 | 99.33 | 99.62 | 99.41 | 100.33 | 99.80 | 100.18 | 100.30 |

– = not detected
n.d. = not determined

(1) Sample numbers refer to rock collection in Dept of Geology and Mineralogy, University of Queensland.

Table 2. AVERAGED MICROPROBE DATA FOR AMPHIBOLES AND BIOTITES OCCURRING IN THE MOUNT WARNING INTRUSIVE COMPLEX

| | Amphiboles | | | | | | | | | Biotites | | | | | | |
|---|---|---|---|---|---|---|---|---|---|---|---|---|---|---|---|---|
| | Gabbro | Monzonite | Trachyandesites | | | Syenites | | Comendites | | Gabbros | | | | | Monzonite | Trachyandesite |
| | 26523 | 26536 | 27230 | 27234 | 27236 | 27255 | 27264 | 27281 | 27279 | 26532 | 26507 | 27217 | 26523 | 27213 | 26536 | 27234 |
| $SiO_2$ | 52.07 | 46.93 | 48.29 | 47.12 | 48.36 | 49.89 | 49.12 | 48.59 | 49.23 | 36.41 | 36.75 | 35.59 | 36.41 | 35.76 | 33.19 | 39.52 |
| $TiO_2$ | 0.15 | 1.21 | 1.16 | 1.01 | 1.34 | 0.54 | 0.88 | 1.11 | 1.24 | 5.26 | 5.92 | 5.72 | 6.61 | 6.00 | 3.29 | 0.43 |
| $Al_2O_3$ | 3.81 | 5.70 | 1.58 | 2.64 | 1.79 | 0.43 | 1.00 | 1.36 | 1.26 | 13.53 | 13.13 | 13.71 | 14.12 | 13.20 | 12.55 | 9.18 |
| FeO* | 14.57 | 22.46 | 27.66 | 27.67 | 25.95 | 35.99 | 33.59 | 33.23 | 33.65 | 15.88 | 18.55 | 19.60 | 15.36 | 20.46 | 35.67 | 34.67 |
| MnO | 0.30 | 0.36 | 0.42 | 0.54 | 0.46 | 0.96 | 0.97 | 1.10 | 1.34 | 0.11 | 0.07 | 0.12 | 0.05 | 0.07 | 0.19 | 0.42 |
| MgO | 15.51 | 6.73 | 5.98 | 4.99 | 7.03 | 0.04 | 0.43 | 0.11 | 0.27 | 13.91 | 11.66 | 11.29 | 13.30 | 10.67 | 1.11 | 1.95 |
| CaO | 10.28 | 11.22 | 7.32 | 9.33 | 6.78 | 1.88 | 3.01 | 1.38 | 1.57 | 0.02 | – | – | 0.03 | – | – | 0.29 |
| $Na_2O$ | 0.55 | 1.87 | 2.99 | 2.77 | 3.96 | 6.93 | 6.16 | 7.15 | 7.22 | 0.34 | 0.38 | 0.45 | 0.38 | 0.20 | 0.04 | 0.90 |
| $K_2O$ | 0.04 | 0.51 | 0.73 | 0.87 | 0.84 | 1.24 | 1.21 | 1.24 | 1.08 | 9.77 | 9.67 | 9.58 | 9.40 | 9.99 | 9.28 | 6.69 |
| $Cr_2O_3$ | – | – | – | – | – | – | – | – | – | 0.13 | – | – | – | – | – | – |
| NiO | – | – | – | – | – | – | – | – | – | 0.03 | – | – | – | – | – | – |
| $ZrO_2$ | n.d. | n.d. | n.d. | n.d. | n.d. | 0.05 | 0.07 | 0.08 | 0.08 | – | n.d. | n.d. | n.d. | n.d. | n.d. | n.d. |
| F | – | n.d. | 0.76 | n.d. | 1.05 | 0.79 | 0.89 | 1.30 | 1.12 | n.d. | 0.20 | 0.19 | 0.08 | 0.20 | n.d. | n.d. |
| Total | 97.28 | 96.99 | 96.89 | 96.94 | 97.56 | 98.74 | 97.33 | 96.65 | 98.06 | 95.39 | 96.33 | 96.25 | 95.74 | 96.55 | 95.32 | 94.05 |
| Less O for F | – | – | 96.57 | – | 97.12 | 98.41 | 96.96 | 96.10 | 97.59 | – | 96.25 | 96.17 | 95.71 | 96.47 | – | – |

* Total Fe expressed as FeO

– = not detected; n.d. = not determined

## TABLE 3. AVERAGED MICROPROBE ANALYSES OF AENIGMATITES AND Fe-Ti OXIDES OCCURRING IN THE TRACHYANDESITES AND PERALKALINE INTRUSIVE PHASES, MOUNT WARNING

| | AENIGMATITES | | Fe-Ti OXIDES | | | | | | | |
|---|---|---|---|---|---|---|---|---|---|---|
| | Syenites | | Trachyandesites | | | | Comendites | | | |
| | 27255 | 27264 | 27234 | 27234 | 27234 | 27234 | 27281 | 27281 | 27279 | 27279 |
| $SiO_2$ | 40.39 | 40.62 | 0.08 | – | 0.03 | – | 0.03 | 0.07 | | 0.08 |
| $TiO_2$ | 8.29 | 8.73 | 49.18 | 51.39 | 21.50 | 6.38 | 51.68 | 8.21 | 51.13 | 7.58 |
| $Al_2O_3$ | 0.37 | 0.53 | 1.53 | 0.04 | 0.45 | 1.38 | 0.03 | 0.03 | 0.03 | 0.05 |
| FeO* | 42.15 | 40.63 | 46.02 | 44.98 | 73.77 | 83.92 | 41.36 | 85.43 | 44.36 | 85.47 |
| MnO | 0.76 | 1.03 | 1.98 | 2.69 | 1.20 | 0.57 | 4.91 | 0.74 | 1.85 | 0.51 |
| MgO | 0.02 | 0.03 | – | – | - | – | – | – | – | – |
| CaO | 0.29 | 0.36 | 0.09 | 0.08 | 0.06 | – | – | – | – | – |
| $Na_2O$ | 7.65 | 7.00 | n.d. | n.d. | n.d. | n.d. | n.d. | n.d. | n.d. | n.d. |
| $K_2O$ | n.d. | n.d. | n.d. | n.d. | n.d. | n.d. | n.d. | n.d. | n.d. | n.d. |
| $Cr_2O_3$ | n.d. | n.d. | 0.03 | 0.04 | 0.06 | 0.03 | – | 0.01 | – | 0.04 |
| NiO | n.d. | n.d. | 0.06 | 0.04 | 0.08 | 0.12 | – | – | – | – |
| ZnO | – | – | – | – | – | – | 0.14 | 0.41 | 1.06 | 0.41 |
| Total | 99.92 | 98.93 | 98.97 | 99.26 | 97.15 | 92.4 | 98.15 | 94.90 | 98.43 | 94.14 |
| Calculated $Fe_2O_3$ and FeO assuming ulvöspinel and ilmenite basis for the spinel and rhombohedral phases respectively. | | | | | | | | | | |
| $Fe_2O_3$ | – | – | 4.31 | 1.81 | 26.70 | 53.44 | – | 53.02 | 1.32 | 53.68 |
| FeO | – | – | 42.14 | 43.35 | 49.74 | 35.83 | 41.36 | 37.72 | 43.17 | 37.17 |
| Total | – | – | 99.40 | 99.44 | 99.82 | 97.74 | 98.15 | 100.21 | 98.56 | 99.52 |
| Mol.% Ulvöspinel | – | – | – | – | 61.1[(1)] | 18.7 | – | 23.8 | – | 22.2 |
| Mol.% $R_2O_3$ | – | – | 6.4[(1)] | 1.8 | – | – | 0 | – | 1.3 | – |

* Total Fe expressed as FeO

– = not detected  n.d. = not determined

(1) Using these values only, T = 945°C, log $fo_2$ = -11.95

## TABLE 4. CHEMICAL AND MODAL DATA FOR REPRESENTATIVE SAMPLES OF THE MOUNT WARNING INTRUSIVE COMPLEX

| | CENTRAL GABBROS | | | | | | SOUTHERN GABBROS | | | |
|---|---|---|---|---|---|---|---|---|---|---|
| | Normal ol-gabbro | Andesine gabbro | Leucogabbro xenolith in monzonite | Laminated gabbro | Laminated gabbro | Leucogabbro | Normal gabbro | Laminated gabbro | Hypersthene gabbro | Leucogabbro |
| | 26532[1] | 26507 | 26558 | 27217 | 26523 | 27213 | 39697 | 39698 | 39700 | 39703 |
| $SiO_2$ | 51.15 | 41.52 | 51.31 | 47.60 | 50.36 | 51.60 | 45.81 | 45.64 | 53.41 | 52.50 |
| $TiO_2$ | 0.55 | 4.70 | 1.52 | 2.22 | 1.21 | 1.86 | 4.76 | 4.59 | 1.00 | 1.94 |
| $Al_2O_3$ | 20.52 | 13.88 | 20.84 | 15.92 | 15.20 | 20.64 | 14.53 | 15.83 | 18.26 | 18.78 |
| $Fe_2O_3$ | 1.12 | 5.48 | 1.62 | 3.58 | 2.79 | 1.70 | 4.38 | 4.12 | 0.68 | 1.28 |
| FeO | 5.33 | 12.27 | 5.23 | 8.44 | 6.04 | 5.86 | 9.63 | 9.81 | 6.32 | 6.31 |
| MnO | 0.11 | 0.21 | 0.09 | 0.17 | 0.13 | 0.07 | 0.15 | 0.14 | 0.11 | 0.12 |
| MgO | 5.84 | 5.82 | 4.27 | 6.34 | 7.96 | 1.81 | 5.10 | 5.33 | 6.84 | 4.68 |
| CaO | 10.28 | 9.43 | 9.75 | 10.15 | 11.60 | 9.83 | 11.43 | 9.88 | 9.14 | 9.06 |
| $Na_2O$ | 3.42 | 3.50 | 3.56 | 3.23 | 2.69 | 4.76 | 3.48 | 3.52 | 3.23 | 3.54 |
| $K_2O$ | 0.36 | 0.74 | 0.48 | 0.50 | 0.53 | 1.06 | 0.36 | 0.23 | 0.37 | 0.62 |
| $P_2O_5$ | 0.15 | 0.63 | 0.06 | 0.28 | 0.09 | < 0.05 | 0.82 | 0.48 | 0.20 | 0.25 |
| $H_2O+$ | 0.78 | 1.30 | 0.43 | 0.96 | 0.62 | 0.45 | 0.52 | 0.77 | 0.56 | 1.13 |
| $H_2O-$ | 0.28 | 0.34 | 0.38 | 0.18 | 0.34 | 0.30 | 0.08 | 0.10 | 0.09 | 0.10 |
| Total | 99.89 | 99.82 | 99.54 | 99.57 | 99.56 | 99.94 | 101.05 | 100.44 | 100.21 | 100.31 |
| FeO* | 6.34 | 17.20 | 6.69 | 11.66 | 8.55 | 7.39 | 13.57 | 13.52 | 6.93 | 7.46 |
| Trace Elements (p.p.m. - x-ray fluorescence, except U) | | | | | | | | | | |
| Rb | 4.0 | 20.3 | 10 | 8.5 | 13.8 | 16.5 | 16 | 8.1 | 12 | 19 |
| Ba | 121 | 250 | 143 | 253 | 123 | 280 | 197 | 221 | 134 | 177 |
| Sr | 643 | 419 | 673 | 628 | 543 | 690 | 595 | 657 | 554 | 627 |
| Pb | 4 | 5.5 | 6 | 9 | 4 | 11.5 | n.d. | n.d. | n.d. | n.d. |
| Zn | 65 | 155 | 68 | 128 | 91 | 53 | 87 | 81 | 73 | 87 |
| Cu | 32 | 66 | 36 | 35 | 63 | 28 | 78 | 52 | 12 | 14 |
| Zr | 27 | 125 | 33 | 68 | 62 | 46 | 93 | 73 | 59 | 127 |
| Nb | 0.6 | 17 | 4.4 | 7.0 | 4.5 | 5.1 | 12 | 11 | 5 | 10 |
| La | 5.4 | 9.6 | 5.8 | 9.0 | 3.0 | 3.9 | n.d. | n.d. | n.d. | n.d. |
| Ce | 14 | 29 | 14 | 27 | 10.8 | 10 | 27 | 19 | 17 | 25 |
| Nd | 7.4 | 2.1 | 7.3 | 15 | 6.1 | 5.4 | 15 | 11 | 9.4 | 13 |
| Y | 10 | 22 | 10 | 18 | 12 | 9.3 | 20 | 14 | 16 | 18 |
| Ni | 49 | 32 | 50 | 57 | 94 | 9 | 10 | 22 | 51 | 34 |
| Cr | 312 | 32.5 | 18 | 247 | 473 | 6.5 | 15 | 12 | 214 | 149 |
| V | 93 | 520 | 112 | 235 | 138 | 130 | 350 | 397 | 129 | 138 |
| Th | 0.35 | 1.6 | 0.80 | 0.79 | 0.90 | 1.5 | n.d. | n.d. | n.d. | n.d. |
| U | 0.15 | 0.51 | 0.31 | 0.24 | 0.43 | 0.65 | n.d. | n.d. | n.d. | n.d. |

TABLE 4 (continued). CHEMICAL AND MODAL DATA FOR REPRESENTATIVE SAMPLES OF THE MOUNT WARNING INTRUSIVE COMPLEX

| | CENTRAL GABBROS | | | | | | SOUTHERN GABBROS | | | |
|---|---|---|---|---|---|---|---|---|---|---|
| | Normal ol-gabbro | Andesine gabbro | Leucogabbro xenolith in monzonite | Laminated gabbro | Laminated gabbro | Leucogabbro | Normal gabbro | Laminated gabbro | Hypersthene gabbro | Leucogabbro |
| | 26532[1] | 26507 | 26558 | 27217 | 26523 | 27213 | 39697 | 39698 | 39700 | 39703 |
| *Modal Data* (volume %) | | | | | | | | | | |
| Plagioclase | 65.7 | 45.3 | 76.8 | 57.5 | 62.5 | 85.9 | 51.7 | 58.4 | 64.9 | 71.1 |
| Alkali feldspar | – | – | 3.8 | – | – | 1.7 | – | – | – | 6.3 |
| Quartz | – | – | 0.4 | – | – | – | – | – | 0.2 | 0.3 |
| Clinopyroxene | 13.5 | 26.2 | 7.7 | 27.4 | 22.1 | 5.5 | 22.7 | 13.9 | 10.9 | 2.6 |
| Orthopyroxene | 7.4 | 2.8 | 1.6 | 2.6 | 0.7 | 1.5 | – | – | 7.5 | – |
| Amphibole-primary | – | – | – | – | – | – | – | – | – | – |
| Amphibole/uralite-secondary | 1.0 | 7.4 | 5.3 | 2.3 | 6.9 | 2.1 | 3.3 | 9.8 | 11.3 | 14.2 |
| Olivine | 9.0 | 0.5 | 0.9 | 2.9 | 0.5 | – | – | 1.3 | – | – |
| Olivine (altered) | 1.3 | 3.2 | – | 0.7 | 3.9 | 0.2 | 1.4 | 3.7 | – | 0.2(?) |
| Biotite | 0.6 | 4.7 | 0.2 | 1.7 | 1.7 | 0.9 | 4.0 | 3.2 | 1.1 | – |
| Fe-Ti oxides | 1.5 | 8.7 | 3.2 | 4.5 | 1.7 | 2.1 | 14.9 | 8.0 | 3.5 | 3.9 |
| Apatite | – | 1.1 | 0.1 | 0.4 | – | – | 2.0 | 1.7 | 0.6 | 0.9 |
| Sphene | – | – | – | – | – | 0.1 | – | – | – | – |
| Aenigmatite | – | – | – | – | – | – | – | – | – | – |
| Groundmass | – | – | – | – | – | – | – | – | – | – |

TABLE 4 (continued). CHEMICAL AND MODAL DATA FOR REPRESENTATIVE SAMPLES OF THE MOUNT WARNING INTRUSIVE COMPLEX

| | Intrusive dolerites (southern part of complex) | | | | | | | Monzonite | Trachyandesites | | |
|---|---|---|---|---|---|---|---|---|---|---|---|
| | 39707 | 39708 | 39709 | 39713 | 39710 | 39714 | 39711 | 26536 | 27230 | 27234 | 27236 |
| $SiO_2$ | 53.58 | 55.09 | 53.71 | 50.88 | 53.94 | 44.88 | 53.23 | 55.52 | 56.35 | 58.50 | 55.75 |
| $TiO_2$ | 2.08 | 2.10 | 1.66 | 2.03 | 1.75 | 3.16 | 2.31 | 1.89 | 1.37 | 1.15 | 1.37 |
| $Al_2O_3$ | 14.84 | 14.37 | 15.16 | 16.79 | 16.54 | 15.92 | 17.01 | 13.53 | 15.45 | 15.79 | 16.84 |
| $Fe_2O_3$ | 2.10 | 2.32 | 2.15 | 0.90 | 1.63 | 4.27 | 2.84 | 1.99 | 3.63 | 2.50 | 2.55 |
| FeO | 7.50 | 7.38 | 7.23 | 9.88 | 7.59 | 10.62 | 6.79 | 10.45 | 6.32 | 6.58 | 6.18 |
| MnO | 0.15 | 0.19 | 0.14 | 0.15 | 0.15 | 0.20 | 0.15 | 0.22 | 0.21 | 0.22 | 0.27 |
| MgO | 5.20 | 4.04 | 5.33 | 7.04 | 5.57 | 4.95 | 3.76 | 1.79 | 1.35 | 1.04 | 1.68 |
| CaO | 7.86 | 6.68 | 7.91 | 9.26 | 8.05 | 7.69 | 7.64 | 6.76 | 4.89 | 3.58 | 5.80 |
| $Na_2O$ | 3.50 | 4.66 | 3.26 | 3.26 | 3.40 | 3.08 | 3.62 | 4.28 | 4.81 | 5.13 | 4.72 |
| $K_2O$ | 0.66 | 0.89 | 0.51 | 0.40 | 0.47 | 0.90 | 1.47 | 2.11 | 4.18 | 4.27 | 3.41 |
| $P_2O_5$ | 0.37 | 0.44 | 0.26 | 0.31 | 0.31 | 1.62 | 0.47 | 0.67 | 0.36 | 0.33 | 0.50 |
| $H_2O+$ | 2.63 | 2.46 | 2.31 | 0.44 | 1.61 | 3.25 | 0.73 | 0.80 | 0.40 | 0.58 | 0.40 |
| $H_2O-$ | 0.16 | 0.15 | 0.18 | 0.05 | 0.08 | 0.27 | 0.23 | 0.34 | 0.50 | 0.40 | 0.34 |
| Total | 100.63 | 100.77 | 99.81 | 101.39 | 101.09 | 100.81 | 100.25 | 100.35 | 99.82 | 100.07 | 99.81 |
| FeO* | 9.39 | 10.60 | 9.16 | 10.69 | 9.06 | 14.46 | 9.35 | 12.24 | 9.59 | 8.83 | 8.48 |
| Trace Elements (p.p.m.) | | | | | | | | | | | |
| Rb | 11 | 24 | 14 | 11 | 18 | 21 | 34 | 57.2 | 50.7 | 53 | 42.5 |
| Ba | 144 | 405 | 159 | 143 | 188 | 284 | 332 | 521 | 954 | 988 | 977 |
| Sr | 468 | 476 | 353 | 375 | 447 | 458 | 526 | 365 | 181 | 168 | 317 |
| Pb | n.d. | n.d. | n.d. | n.d. | n.d. | n.d. | n.d. | 11 | 7 | 9 | 6 |
| Zn | 116 | 135 | 108 | 99 | 111 | 187 | 130 | 219 | 153 | 160 | 144 |
| Cu | 25 | 15 | 22 | 26 | 18 | 32 | 30 | 18 | 16 | 15 | 20 |
| Zr | 171 | 219 | 161 | 144 | 153 | 312 | 213 | 274 | 266 | 273 | 207 |
| Nb | 16 | 23 | 12 | 21 | 12 | 37 | 17 | 38 | 24 | 25 | 22 |
| La | n.d. | 6.7 | n.d. | n.d. | n.d. | 24 | 6 | 34 | 23 | 27 | 29 |
| Ce | 29 | 45 | 28 | 36 | 28 | 79 | 38 | 87 | 65 | 67 | 61 |
| Nd | 20 | 21 | 13 | 17 | 14 | 46 | 23 | 50 | 34 | 33 | 30 |
| Y | 25 | 29 | 25 | 25 | 23 | 53 | 23 | 56 | 30 | 30 | 29 |
| Ni | 20 | 14 | 25 | 79 | 33 | 33 | 35 | 3 | 12 | 13 | 12 |
| Cr | 290 | 120 | 272 | 377 | 316 | 6 | 35 | 0.3 | 14.5 | 9.7 | 12 |
| V | 202 | 210 | 152 | 198 | 162 | 130 | 165 | 44 | 30 | 24 | 44 |
| Th | n.d. | n.d. | n.d. | n.d. | n.d. | n.d. | n.d. | 2.7 | 2.4 | 2.0 | 1.8 |
| U | n.d. | n.d. | n.d. | n.d. | n.d. | n.d. | n.d. | 1.3 | 1.1 | 0.92 | 0.83 |

**TABLE 4 (continued). CHEMICAL AND MODAL DATA FOR REPRESENTATIVE SAMPLES OF THE MOUNT WARNING INSTRUSIVE COMPLEX**

| | Intrusive dolerites (southern part of complex) | | | | | | | Monzonite | Trachyandesites | | |
|---|---|---|---|---|---|---|---|---|---|---|---|
| | 39707 | 39708 | 39709 | 39713 | 39710 | 39714 | 39711 | 26536 | 27230 | 27234 | 27236 |
| *Modal Data* (volume %) | | | | | | | | | | | |
| Plagioclase | 0.3 | 1.0 | 1.3 | –[4] | 7.9 | – | 32.7 | 51.7 | 14.3 | 2.9 | 15.0 |
| Alkali feldspar | – | – | – | – | – | – | – | 17.2 | 15.6 | 5.9 | 17.8 |
| Quartz | – | – | – | – | – | – | – | 6.1 | – | – | – |
| Clinopyroxene | – | 0.3 | – | – | – | – | 0.1 | 10.4 | 8.5[8] | 12.8[8] | 5.0[8] |
| Orthopyroxene | – | – | – | – | – | – | – | – | – | – | – |
| Amphibole (primary) | – | – | – | – | – | – | – | 3.8 | 1.6[8] | 2.3[8] | 0.8[8] |
| Amphibole/uralite (secondary) – ($\pm$ secondary biotite $\pm$ Fe-Ti oxides) | – | – | – | – | 3.0 | – | – | – | – | – | – |
| Olivine | – | 0.1 | – | – | – | – | – | 8.1 | 2.9 | 0.4 | 1.2 |
| Olivine (altered) | 0.1 | – | – | – | – | – | – | – | – | – | – |
| Biotite | – | – | – | – | – | – | – | 0.2 | tr | 0.3 | – |
| Fe-Ti oxides | – | – | – | – | – | – | – | 2.5 | – | 0.4 | 1.3 |
| Apatite | – | – | – | – | – | – | – | < 0.05 | 0.5 | 0.3 | 0.2 |
| Sphene | – | – | – | – | – | – | – | – | – | – | – |
| Aenigmatite | – | – | – | – | – | – | – | – | – | – | – |
| Groundmass | 99.6[2] | 98.6[2] | 98.7[2] | | 89.1[2] | 100[2,3] | 67.2[2] | – | 56.6 | 74.7 | 58.7 |

TABLE 4 (continued). CHEMICAL AND MODAL DATA FOR REPRESENTATIVE SAMPLES OF THE MOUNT WARNING INTRUSIVE COMPLEX

| | SYENITES | | | | | | | | |
|---|---|---|---|---|---|---|---|---|---|
| | Qtz Syenite | Normal Syenites | | Peralkaline | | Trachyte | Comendites | | |
| | 39717(5) | 39719 | 39720 | 27255(5) | 27264(5) | 39723 | 27281(5) | 27279(5) | 39725(5) |
| $SiO_2$ | 66.68 | 61.72 | 57.66 | 62.10 | 69.63 | 68.80 | 70.85 | 71.95 | 77.52 |
| $TiO_2$ | 0.41 | 0.73 | 1.34 | 0.64 | 0.46 | 0.55 | 0.38 | 0.39 | 0.22 |
| $Al_2O_3$ | 16.03 | 16.77 | 15.28 | 14.85 | 12.50 | 14.14 | 12.23 | 12.36 | 11.10 |
| $Fe_2O_3$ | 1.55 | 1.26 | 3.05 | 3.25 | 2.46 | 5.01 | 3.97 | 3.10 | 2.50 |
| FeO | 1.91 | 3.66 | 6.64 | 4.79 | 2.67 | 0.68 | 1.33 | 1.25 | 0.23 |
| MnO | 0.04 | 0.10 | 0.23 | 0.25 | 0.11 | 0.05 | 0.06 | 0.06 | 0.02 |
| MgO | 0.01 | 0.70 | 1.51 | 0.10 | 0.04 | n.d. | 0.04 | 0.02 | n.d. |
| CaO | 0.25 | 2.16 | 4.19 | 2.41 | 0.54 | 0.43 | 0.33 | 0.17 | n.d. |
| $Na_2O$ | 6.10 | 5.79 | 5.15 | 5.17 | 5.39 | 5.12 | 5.10 | 4.29 | 5.16 |
| $K_2O$ | 5.52 | 4.59 | 3.62 | 5.23 | 4.97 | 4.11 | 4.89 | 5.20 | 2.83 |
| $P_2O_5$ | 0.04 | 0.11 | 0.37 | 0.07 | 0.03 | 0.02 | 0.01 | 0.01 | n.d. |
| $H_2O+$ | 0.34 | 0.70 | 0.38 | 0.76 | 0.86 | 0.57 | 0.42 | 0.56 | 0.11 |
| $H_2O-$ | 0.17 | 0.32 | 0.21 | 0.88 | 0.32 | 0.18 | 0.32 | 0.26 | 0.09 |
| Total | 99.05 | 98.61 | 99.63 | 100.50 | 99.98 | 99.66 | 99.93 | 99.62 | 99.78 |
| FeO* | 3.31 | 4.79 | 9.39 | 7.72 | 4.88 | 5.19 | 4.90 | 4.04 | 2.48 |
| Trace Elements (p.p.m.) | | | | | | | | | |
| Rb | 115 | 86 | 47 | 56.8 | 131 | 107 | 148 | 237 | 53 |
| Ba | 83 | 472 | 740 | 84 | 252 | 509 | 11 | 7 | 19 |
| Sr | 17 | 223 | 254 | 5.5 | 23 | 120 | 1.6 | 0.8 | 18 |
| Pb | n.d. | n.d. | n.d. | 9 | 13 | n.d. | 17 | 21 | n.d. |
| Zn | 96 | 112 | 119 | 117 | 151 | 153 | 195 | 230 | 105 |
| Cu | 9 | 13 | 18 | 17 | 15 | 7 | 8 | n.d. | 11 |
| Zr | 453 | 381 | 235 | 212 | 390 | 613 | 850 | 1680 | 802 |
| Nb | 61 | 41 | 29 | 24 | 34 | 47 | 67 | 145 | 57 |
| La | 54 | 33 | 19 | 26 | 39 | 106 | 64 | 48 | 82 |
| Ce | 78 | 58 | 52 | 63 | 95 | 93 | 159 | 125 | 117 |
| Nd | 38 | 28 | 32 | 33 | 37 | 65 | 76 | 57 | 68 |
| Y | 31 | 30 | 29 | 27 | 44 | 145 | 77 | 72 | 71 |
| Ni | 1 | 11 | 13 | 4 | 4 | 7 | – | – | 2 |
| Cr | – | 13 | 12 | – | – | – | – | 1.5 | – |
| V | – | 15 | 52 | n.d. | 1.5 | 1.3 | < 1 | < 1 | < 1 |
| Th | n.d. | n.d. | n.d. | 2.2 | 3.4 | n.d. | 25 | 27 | n.d. |
| U | n.d. | n.d. | n.d. | 0.82 | 1.2 | n.d. | 5.2 | 5.4 | n.d. |

**TABLE 4 (continued). CHEMICAL AND MODAL DATA FOR REPRESENTATIVE SAMPLES OF THE MOUNT WARNING INTRUSIVE COMPLEX**

| | SYENITES | | | | | | | | |
|---|---|---|---|---|---|---|---|---|---|
| | Qtz Syenite | Normal Syenites | | Peralkaline | | Trachyte | Comendites | | |
| | 39717[5] | 39719 | 39720 | 27255[5] | 27264[5] | 39723 | 27281 | 27279 | 39725[5] |
| *Modal Data* (volume %) | | | | | | | | | |
| Plagioclase | – | 1.2 | 4.4 | – | 0.3 | 0.4 | – | – | – |
| Alkali feldspar | 83.8 | 80.0 | 68.6 | 79.8 | 71.5 | 0.2 | 8.0 | 20.2 | 1.5 |
| Quartz | 9.7 | 2.5 | 2.1 | 4.3 | 16.3 | – | – | – | – |
| Clinopyroxene | – | 1.4 | 13.4 | 6.0 | 6.0 | 0.6(?)[6] | 0.3 | 0.6 | – |
| Orthopyroxene | – | – | – | – | – | – | – | – | – |
| Amphibole (primary) | 5.4 | 0.8 | – | 2.7 | 3.3 | – | 0.1 | 0.1 | – |
| Amphibole/uralite (secondary) – (± secondary biotite ± Fe-Ti oxides) | – | 11.9 | 3.4 | – | – | – | – | – | – |
| Olivine | – | – | – | – | – | – | – | – | – |
| Olivine (altered) | – | – | 1.7 | 6.4 | – | – | – | – | – |
| Biotite | – | – | – | 0.3 | – | – | – | – | – |
| Fe-Ti oxides | 0.9 | 1.8 | 5.6 | 0.4 | 0.3 | – | 0.1 | 0.1 | 1.9[7] |
| Apatite | – | 0.4 | 0.8 | 0.1 | – | – | – | – | – |
| Sphene | – | – | – | – | – | – | – | – | – |
| Aenigmatite | 0.2 | – | – | < 0.1 | 2.3 | – | – | – | – |
| Groundmass | – | – | – | – | – | 98.8 | 91.5 | 79.0 | 96.6 |

n.d.= not determined; – = not detected; U determined by delayed neutron counting (A. Mateen); FeO* = Fe as FeO

(1) See Table 1[1]

(2) Fine grained; modes refer to phenocrysts only.

(3) Vesicular – chlorophaeite + actinolite present.

(4) Recrystallised.

(5) Sodic amphiboles present.

(6) Completely altered.

(7) Probably secondary.

(8) Includes all augite, ranging from phenocrysts to coarse groundmass grains.

succession. Similarly, the rhyolites of Binna Burra, Nimbin, and Springbrook have no intrusive equivalents in the complex. Thus, there is a clear indication of independent evolution of the major intrusive and extrusive magma phases within the Tweed Volcano. The trachyandesite intrusive forming the core of Mount Warning is shown to represent a hybrid magma.

## THE FOCAL PEAK SHIELD VOLCANO

### Introduction

On the eastern flank of the Focal Peak Shield Volcano (Text fig. 1), the eruptive sequence comprises the Albert Basalt and the overlying Mount Gillies Volcanics*. The Chinghee Conglomerate in part overlies the latter, or in places is interbedded with it. In the area between Levers Plateau and Richmond Gap, all formations dip on the average about 1 to 3 degrees easterly, though higher dips up to 10 degrees occur near Mount Lindesay and Mount Glennie (Stephenson, 1956).

### Albert Basalt

This formation of alkaline to subalkaline basalts is widespread on the northern side of the state border between Mount Lindesay (west) and Canungra and Numinbah Valley (northeast and east); in this area it is separated from the Beechmont Basalt and higher formations of the Lamington Group by a narrow band (Text fig. 1) of Mount Gillies Volcanics* and/or Chinghee Conglomerate.

In the Mount Lindesay-Levers Plateau area, close to the inferred sources for the basalt, the formation consists of numerous thin flows averaging about 10 m thick with a maximum thickness of 440 m (Ross, 1977). The lavas are mostly alkaline with hawaiites predominating over alkali olivine basalts, mugearites, basanites, olivine tholeiites and tholeiitic andesites. Commonly microphenocrystic in olivine and/or plagioclase, the lavas have sparse amygdules containing calcite or chalcedony, with rare zeolites. A few of the lavas contain phenocrystic plagioclase. Megacrysts of clinopyroxene and orthopyroxene and lherzolite nodules are rare.

One occurrence of an autobrecciated trachyte is known, south of Mount Gillies. Some interbedded sandstones with a carbonaceous intercalation have been noted near Hillview (where they are 20 m thick) and a thin bed of white sand occurs 1 km north of Glennies Chair. A graded rhyolitic ash-fall tuff 5 m thick is present in the top 50 m of the formation west of Levers Plateau.

The Albert Basalt thins to the northeast where it has been recognized beneath the Beechmont Basalt and equivalents of the Mount Gillies Volcanics and Chinghee Conglomerate in the Canungra-Beechmont district. West of Canungra the basalt rests on Tertiary sands which have been converted to silcrete; in the Numinbah Valley the lowest basalts rest on shales and mudstones containing dicotyledonous leaf impressions. In Flying Fox Creek, north of Beechmont, nine flows with clearly-defined vesicular tops have been counted in a thickness of 87 m (Green, 1964).

* Previously Mount Gillies Rhyolite (of Ross, 1974).

## Kyogle Basalt

The Albert Basalt has been correlated (in part) with the Kyogle Basalt (Duggan and Mason, 1978) of the Kyogle-Nimbin district, and it is likely that the Kyogle Basalt forms most of the basalt country between Kyogle and Mount Lindesay, and underlies the Lismore Basalt east of Nimbin.

The total area originally covered by the Albert and Kyogle Basalts was thus very large (Text fig. 1), and may have been larger than that covered by the Beechmont and Lismore Basalts from the Mount Warning Centre. The formation has a maximum thickness of 330 m (Duggan and Mason, 1978); it thins to the east and southeast, and presumably thickens to the northwest (where no detailed studies have been made). The main vents appear to be those of the Albert Basalt and perhaps another to the southwest of Dome Mountain, SE. of Woodenbong.

Between Kyogle and Nimbin, the Kyogle Basalt contains two non-basaltic members near the top, the Homeleigh Agglomerate and the overlying Georgica Rhyolite.

## Mount Gillies Volcanics

The name Hillview Rhyolite was used by McTaggart (1962) for 'a band of agglomeratic tuffs and brecciated rhyolite' that is well exposed in the Hillview area and in the valley walls of Christmas and Chinghee Creeks, and has been mapped northeast to the Canungra district.

Ross (1974) showed that the Mount Lindesay Rhyolite of McTaggart (1962) was equivalent to the Hillview Rhyolite and suggested that the name Mount Gillies Rhyolite be used for the Hillview Rhyolite and Mount Lindesay Rhyolite because of Stephenson's (1959) prior use of Mount Gillies Volcanics for rhyolites and minor basalts of the Mount Gillies vent, source of the Hillview Rhyolite and Mount Lindesay Rhyolite.

Although rhyolitic lava (including pitchstone) is dominant close to the Mount Gillies vent (on Mount Lindesay and Mount Glennie) and present in the Mount Chinghee area, those parts of the formation more distant from the vent are mostly of rhyolitic pyroclastic rocks e.g. ash-fall tuffs, agglomerates and boulder deposits. In such places 'Rhyolite' is inappropriate as part of the name, though many of the clasts are rhyolitic. It is suggested here that the original name Mount Gillies Volcanics be used in place of Mount Gillies Rhyolite.

In the Hillview area McTaggart (1962) described the basal part of the formation as 'up to 50 feet of acid agglomeratic tuff containing boulders of rhyolite up to one foot in diameter'. He noted the abundance of 'accessory boulders' comprising 'Palaeozoic sediments, granophyre and basalt' especially around the head of Christmas Creek, and reported well bedded tuff containing pebbles of rhyolite and basalt around Canungra Creek and in the Coomera Valley. One of the most easterly occurrences, on the Beechmont Canungra Road, exposes a sandy silt with boulders of basalt, rhyolite and pitchstone, some up to 50 cm in diameter, interpreted as a lahar deposit (Stevens, 1984). Orientation of fossil wood fragments suggests that it came from the west.

The greatest thickness of rhyolite flows occurs at Mount Lindesay where two flows, making up 180 m of rhyolite, overlie 60 m of rhyolitic agglomerate

and fine-grained, light-coloured, banded rhyolitic tuff. McTaggart (1962) called these, and the higher rhyolites on Mount Glennie, the Mount Lindesay Rhyolite, and showed in his map and sections a lower rhyolite, correlated with with the Hillview Rhyolite. On Mount Glennie's lower slopes (at 500 m), this appears to be a dyke.

The rhyolitic lavas are of many different types, and in the Hillview and Mount Lindesay areas they are commonly auto-brecciated and associated with pitchstones, especially at their margins or contacts. Similar pitchstones occur in the Homeleigh Agglomerate northeast of Kyogle; this formation is described as consisting of a volcanic agglomerate containing blocks up to 1 m diameter in a pyroclastic matrix of rounded pumice, acid and altered basic volcanic rocks and crystal fragments (Duggan and Mason, 1978). It is classed as a member unit of the Kyogle Basalt and is overlain by the Georgica Rhyolite Member (and alkaline basaltic flows of the Kyogle Basalt). The Georgica Rhyolite is considered to be of local origin, probably from the rhyolite plugs of the Nimbin Rocks (Duggan and Mason, 1978). Basalt flows have also been recorded near the top of the Mount Gillies Volcanics and in the overlying Chinghee Conglomerate near Chinghee Creek. The sequence in the Kyogle district is thus similar to that of the Mount Lindesay-Hillview area, except for the presence of the Chinghee Conglomerate and less abundant alkaline basaltic flows above the rhyolite in the latter area.

### Chinghee Conglomerate

This formation stratigraphically overlies the Mount Gillies Volcanics (or, in places, the Albert Basalt) in the type area along the Chinghee Creek road, 3.5 km east of Mount Chinghee (Text fig. 20), and overlaps it to the southeast, occurring in the Tweed Range without the underlying acid volcanics, according to McTaggart's (1962) map. Exon (1972) stated that the two formations are interbedded outside the type area – the boulder deposits (which occur in both) are difficult to assign to one or the other formation if outcrop is poor.

The thickness in the type area is about 30 m, comprising 17 m of conglomerate, 8 m of sandstone, and 4 m of basalt near the top (Exon, 1972). The occurrence was first described by Walkom (1916), who formed bryozoan fossils in some of the clasts, presumably from the Carboniferous Mount Barney beds close to Mount Barney. Ross (1977) has reported a thickness of up to 130 m for the formation in the Chinghee Creek area, where it fills pre-existing valleys (Text fig. 20), including a gorge eroded through the underlying rhyolite into the Albert Basalt.

The formation consists mainly of conglomerate and coarse, feldspathic, cross-bedded sandstones which are uncemented or poorly cemented but become more strongly cemented to the east. Boulders in the conglomerate, up to one metre in diameter, are of rhyolite (probably Mount Gillies Volcanics), granophyre from the Mount Barney intrusion, Mesozoic and Carboniferous sedimentary rocks, basalt and fluidal riebeckite-bearing comendite clasts at the base (Stephenson, 1956).

The well rounded boulders and cobbles in the conglomerate and cross bedding of the sandstones suggest that it is a fluvial deposit, at least in the type area. The headwaters of the streams which deposited these sediments were

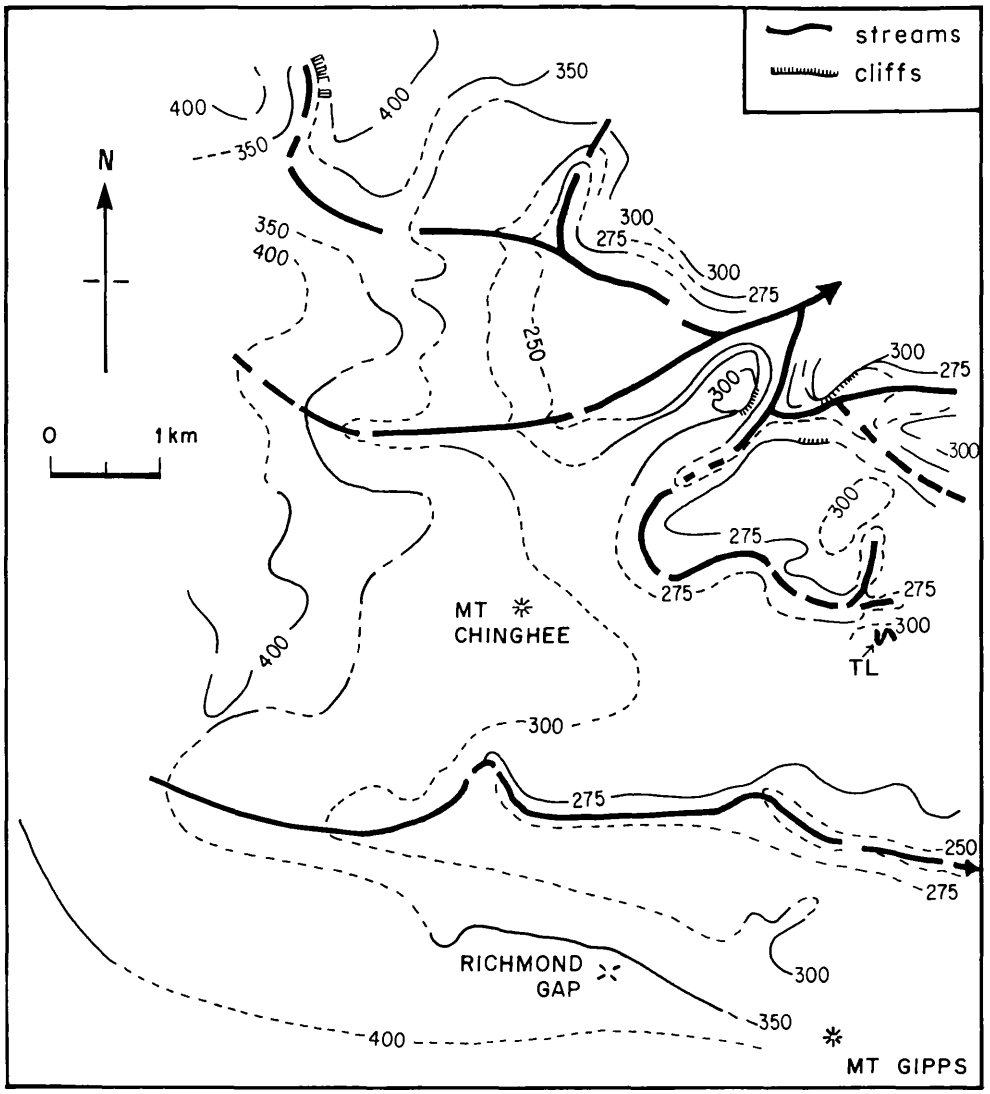


Text fig. 20. Topography existing just before deposition of the Chinghee Conglomerate (after Ross, 1977). Postulated streams are in heavy black. Dashed contours and streams are inferred. TL = Type locality (on road bends) of Chinghee Conglomerate (9441-2, 992690).

probably in the Mount Barney area, where rapid erosion would be expected because of major updoming and upfaulting around the granophyre boss. In the Chinghee Creek area, the width of outcrop of the formation (in the north-south direction) is over 10 km. Base levels indicate the presence of several former shallow valleys and deeper gorges up to about 150 m deep in which the Chinghee Conglomerate was deposited (Text fig. 20). The width of the formation and the overlapping of intervening ridges (if such occurs) are arguments against a simple fluvial deposit.

Further study of the sediments is necessary to determine whether some of the formation was a lahar.

## INITIAL DIP OF ERUPTIVES OR POST-VOLCANIC DIFFERENTIAL UPLIFT?

McTaggart suggested that all the basalts of the Lamington Group (including Albert Basalt) came from the Mount Warning centre, and that there were no large basic eruptive centres to the west to support an initial dip of the lowest basalts towards the east. However, a western source (Mount Gillies) was suggested for the Hillview Rhyolite (Mount Gillies Volcanics).

The easterly dips of the Albert Basalt were interpreted as a result of post-volcanic tectonic warping by McTaggart (1962), who postulated uplift 'possibly over 1000 feet (300 m) in the Lamington Plateau area', and 'of the order of 2000 feet (600 m) in the Mount Lindesay area'. Evidence for uplift was based largely on the occurrence in the Chinghee Conglomerate of 'boulders of metamorphic rocks (of Brisbane Schist lithology)', presumed to have been derived from the Palaeozoic mass of the Southport-Murwillumbah area to the east, since there was no western source. According to McTaggart (1962), the eastern source area was not high enough to contribute to the western part of the Chinghee Conglomerate unless the latter was much lower at that time, and was subsequently raised to its present position by differential uplift.

However, subsequent investigators have not confirmed the presence of metamorphic clasts. It is unlikely that boulders of metamorphic rocks came from the east, since the thickest and coarsest sediments of the Chinghee Conglomerate are near its western margin.

It has also been pointed out that with the scale of uplift suggested by McTaggart, some of the Albert Basalt would have been deposited below sea level, which is not in accord with evidence of its subaerial origin.

Ross (1974) at first thought that the relatively high altitudes of the lavas on Mount Lindesay and Glennie were largely dependent on uplift caused by the Mount Barney Central Complex and by a near-surface laccolith, rather than by regional arching. Later Ross (1977) put forward a second model, in which lavas from the Focal Peak Volcano were discharged upon a dissected horst (flanked on the east by a fault along the South Moreton Anticline) and flowed into a broad area of low relief drained by north and south-flowing streams (Text fig. 21). This would explain relatively steep gradients in basaltic and rhyolitic base levels along and near this fault (which was an escarpment at that time), and changes in thickness of the Albert Basalt between Mount Lindesay (320–440 m thick), Mount Glennie (about 200 m), and the Back Creek-Levers Plateau area (400 m). Northerly dips of about $10^{o}$ for the Albert Basalt on Mount Glennie, previously explained by doming, would result from flow into valleys, perhaps incised into a fault escarpment.

The second model of Ross implies no significant post-volcanic differential movement, either regional or local, at least for the area covered by the Albert Basalt on the Queensland side of the McPherson Range. Stephenson (1985, *in litt.*) has pointed out that opposing $10^{o}$ dips for the basalts on Mounts Lindesay and Glennie are severe difficulties for this model. Ross considers that these dips could be a result of faulting, doming of the Central Complex or sub-basaltic topography, or some combination of these.

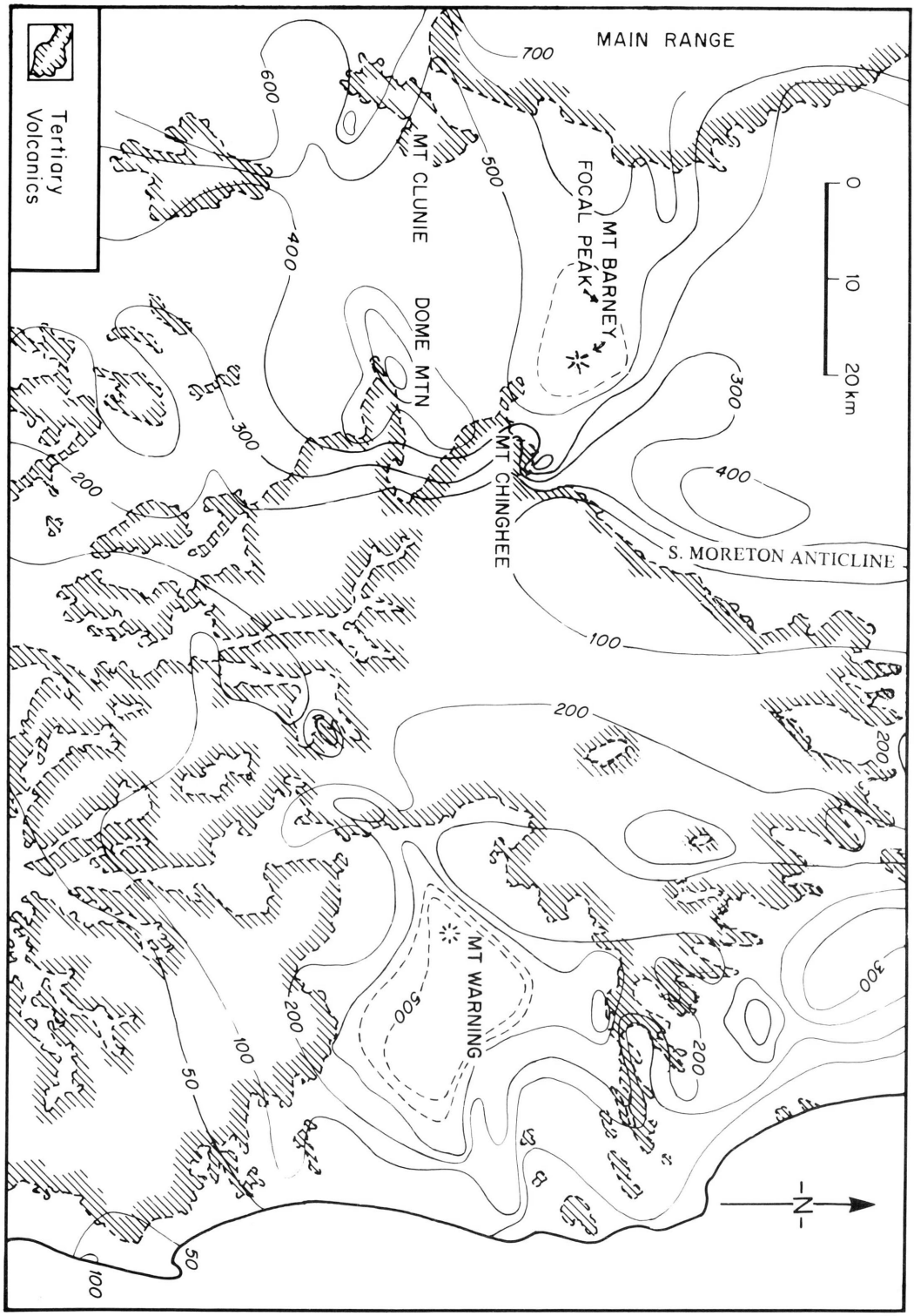


Text fig. 21. Tertiary sub-basalt topography of the Mount Barney-Mount Warning district (after Ross, 1977). Near Mount Barney and Mount Warning, the contours are schematic and probably reflect post-basaltic uplift. (Unpublished maps based on later geological mapping differ mainly in detail of the palaeovalley north of Mount Warning and do not alter the position of the ancestral Logan River adjacent to the South Moreton Anticline).

# THE MOUNT BARNEY CENTRAL COMPLEX

## Introduction

The Mount Barney Central Complex (Stephenson, 1956, 1959) consists of a variety of igneous rocks, mainly intrusive, forming a mountainous region 20 km x 15 km.

Several centres of intrusion have been recognised along an east-west line, including Focal Peak, the centre and possibly the major vent of the shield volcano of the same name, which lies both to the west of the Mount Barney granophyre boss and the centre of the Complex (Text fig. 22). Focal Peak consists of vent volcanics surrounded and intruded by plutonic rocks varying from gabbro to monzonite (Ross, 1977). The spatial and compositional relations between the rocks of these two centres (Focal Peak and Mount Barney) are similar to those between the Mount Warning core of gabbro, syenite, monzonite and trachyandesite and the more easterly micrographic rhyolite and the granitic mass of Mount Nullum.

Significant doming and upfaulting along ring-faults have taken place in the Mount Barney Central Complex, with the formation of the Barney Dome, tilting to near-vertical dips of the Carboniferous Mount Barney beds within a fault block, and the exposure of the Mount Barney Granophyre. The margin (ring-flexure zone) of the Barney Dome in most places is the junction between moderately dipping Mesozoic strata with dips of about 30 degrees and flat-lying Mesozoic strata (Jurassic Marburg Formation and Walloon Coal Measures) outside the Dome. Successively older formations, including Triassic Portal Creek Volcanics and Yamahra Conglomerate, occur towards the centre.

## Mt Barney and Barrier Granophyres and the Barney Ring-Fault

The Mount Barney Granophyre is intrusive on its eastern side into steeply dipping Carboniferous strata, the Mount Barney beds. The granophyre and Carboniferous and Mesozoic strata to the east are surrounded by the oval-shaped Barney Ring-Fault (Text fig. 22), asymmetrically placed to the east of the centre of the dome. The Barrier Granophyre, an incomplete and faulted ring-dyke, has intruded Mesozoic strata east of Mount Barney, and has been displaced by the Barney Ring-Fault.

On the basis of offsetting of the Barrier Granophyre Ring-Dyke by the ring-fault, and assuming a dip as low as 60 degrees for the fault, Stephenson (1956) estimated upfaulting to be at least 2400 m, and possibly as much as 4500 m. The only radiometric age on the Mount Barney Granophyre is 24.0 Ma, on a sample from Rocky Creek, on the eastern margin. Elevation and erosion of this granophyre must have been rapid for this rock to occur in a conglomerate underlying lavas of age 22.3 Ma (Webb *et al.*, 1967; Stevens, 1970).

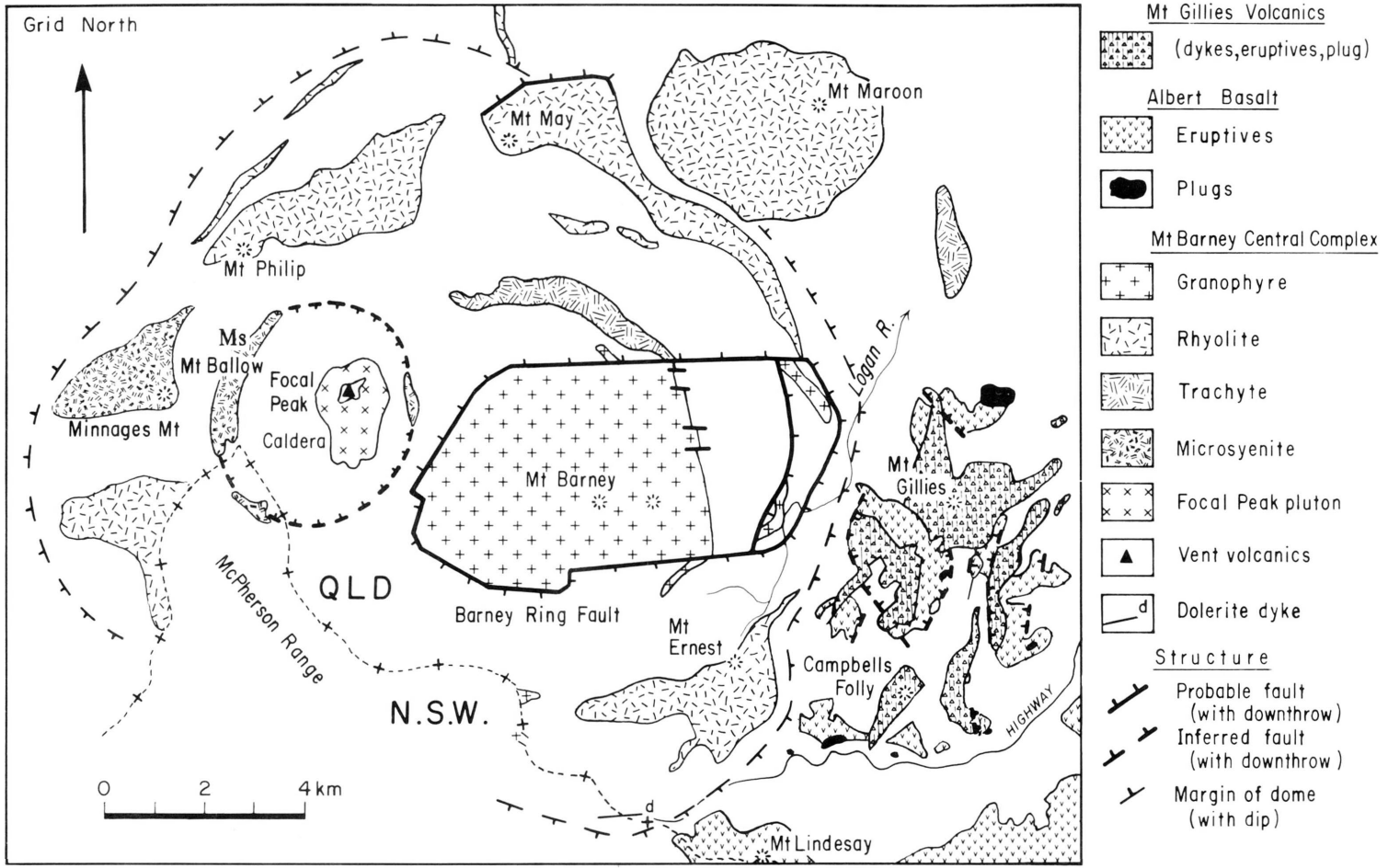


Text fig. 22. Geological sketch map of the Mount Barney Central Complex, showing intrusive rocks and structural elements (based largely on Stephenson, 1956, 1959), with minor changes by Ross (1977). Ms: Montserrat microsyenite.

### Focal Peak Pluton, Vent Volcanics, Ballow Cone Sheets and Montserrat Granophyre

Stephenson (1956) described 'a complex of varying dioritic rocks' surrounding Focal Peak as the Focal Diorite Complex, consisting of both uniformly textured diorites and 'patchy' diorites, the latter being mottled and streaked with light coloured areas.

Ross (1977) named these rocks 'gabbro, monzonite and minor syenite' and noted that they graded from one type to the other. The intrusion is referred to here as the Focal Peak Pluton.

Trachytic agglomerates occurring on the summit of Focal Peak and andesitic and basaltic volcanics to the northeast belong to Stephenson's 'Central Volcanics' or 'vent volcanics'. The basaltic rocks show evidence of thermal metamorphism at their margin, presumably by the plutonic rocks beneath.

A zone of inward-dipping doleritic cone sheets (Ballow Cone Sheets) surrounds the central volcanics and the plutonic rocks in a zone about 6.5 km in diameter. Within this zone the Montserrat Granophyre (or microsyenite according to Ross, 1977) forms a discontinuous ring of intrusions about 4 km in diameter. Within the postulated caldera Mesozoic and Carboniferous sedimentary rocks dip radially inwards, giving rise to a basin structure, attributed to central subsidence along a circular fracture (Stephenson, 1956). The central area may have been a caldera, similar to summit calderas of Hawaiin shield volcanoes.

### Peripheral Rhyolitic, Granophyric and Trachytic Sills or Laccoliths

The outer zone of the Central Complex includes a number of sill-like or laccolithic intusions e.g. the rhyolite of Mount Ernest (300–500 m thick), the intrusive rhyolitic masses of Mounts May, Philip and Maroon and the Minnages Mountain Granophyre (or microsyenite), which dips at $25^{o}$ to $35^{o}$ to the northwest. A number of minor trachytic intrusives also occurs.

### Mafic Vents

Excluding the postulated caldera at Focal Peak, eight or nine possible adventive mafic feeders for the Albert Basalt have been identified in the Mount Gillies-Campbells Folly area by Ross (1977). These feeders consist of common scoriaceous agglomerates and uncommon dolerite and basalt. One possible feeder near Palen Creek 2 km southeast of Campbells Folly contains lherzolite nodules and orthopyroxene megacrysts. Mafic dykes and a sill have also been found; some of these dykes could be feeders additional to those discussed above.

### Mount Gillies and other Rhyolitic Vents

To the east of Mount Barney and on the margin of the Mount Barney Central Complex are Mount Gillies and Campbells Folly which are largely composed of intrusive and eruptive rhyolites, rhyolitic tuffs and agglomerates. Ross (1977, 1985) has also postulated that tuff-lavas, in part, the pyroclastic dykes of Stephenson (1956), occur rarely in this area.

Stephenson (1956, 1959) regarded these rhyolitic intrusives and extrusives as part of the Mount Barney Complex, although he considered them to be much younger than the main plutonic intrusions.

Ross (1977) distinguished two types of rhyolitic volcano in the Mount Gillies, Campbells Folly, Mount Glennie and Levers Plateau area: fissure vents, which occur close to the eastern part of the flexure zone, and include Mount Gillies and Campbells Folly, and less common rhyolitic plugs, e.g. Glennies Chair, which can occur well away from the ring-flexure zone of the Central Complex.

Fissure vents comprise a great number of rhyolitic dykes, many of which are intrusive into pre-existing rhyolites interpreted to be subaerial flows. Ross estimated between 700 and 2800 thin dykes in the Mount Gillies area are composed of both conduit lava and pyroclastics. These show a great diversity in texture, compared with rhyolites of the few definite plugs recognised in the area. Most fissure vents are thought to occur within 'closed graben' structures, which are essentially polygonal calderas, in which subsidence of up to about 650 m has taken place. The rhyolitic dykes greatly predominate over eruptives and have acted as feeders for the rhyolites of the Mount Gillies Volcanics.

Much of the subsidence is interpreted (Ross, 1977) to post-date most of the rhyolitic eruptive activity because of the lack of thick rhyolitic lavas which could result from ponding within deep craters. The subsidence appears to have been non-uniform for different grabens and may have been caused by emptying or partial emptying of a near-surface magma chamber (or chambers). It was probably controlled by pre-existing faults bounding the rhyolitic vents.

To the south of Mount Gillies, the mountain known as Campbells Folly (Text fig. 22) is another example of a vent comprising a swarm of rhyolitic dykes, intrusive into flow-banded rhyolitic lavas and agglomerates. In this vent, however, the lavas strike about $15^{o}$ and dip easterly and westerly, mostly at angles between $30^{o}$ and $45^{o}$. In cases such as this, it is difficult to prove that the mountain is bounded by faults, as its margins are mostly covered by debris.

**Sequence in the Mount Barney Central Complex**

Stephenson (1956, 1959) regarded the intrusion of the Mount Barney Granophyre as the earliest event, causing the Barney Dome. The Barrier Granophyre and the rhyolite sills were also ascribed to this 'Centre'. Centre 2 activity was the intrusion of the Minnages Mountain Granophyre; Centre 3 comprised the Central Volcanics, Montserrat Granophyre, Focal Diorite Complex and Ballow Cone Sheets; Centre 4, the Mount Gillies Volcanics, and lastly came the Barney Ring Fault.

Ross (1977) modified this sequence in accord with the concept of a shield volcano centred on Focal Peak and the stages recognised by Smith and Bailey (1968) in a typical resurgent cauldron. He referred to the margin of the updomed Mt Barney Central Complex as an early ring-fault (RFI), the ring-fault around Mount Barney (the Barney Ring-Fault) as RF2, and the caldera margin fault around Focal Peak as RF3 (Text fig. 20).

The modified history differs mainly in the relative timing of intrusion of the Mount Barney Granophyre which is placed after the Ballow Cone Sheets

and Montserrat microsyenite. The younger date is based on the similar age dates for Mount Gillies and Mount Barney intrusive rocks (Webb, *et al.*, 1967), but it is possible that the Mount Barney Granophyre date represents a minimum age due to slight hydrothermal alteration. However, the similar geochemical compositions of the Mount Barney Granophyre and the pitchstones of the Mount Gillies Volcanics, calculated on the basis of zero loss on ignition (see later section), indicate that they are likely to have been co-magmatic at some stage in their petrogenesis, and thus both should have similar ages.

The postulated sequence is:

1. Doming and generation of dome flexure along RF1 (RF here can indicate ring-flexure).
2. Caldera formation at Focal Peak with basaltic eruption and caldera collapse along RF3.
3. Intrusion of the Focal Peak Diorite Complex, the Minnages Mountain microsyenite and the Montserrat microsyenite, the latter intruded along RF3.
4. Intrusion of the Ballow Cone Sheets.
5. Resurgent (?) doming during intrusion of the Mount Barney Granophyre followed by up-faulting along RF2, intrusion of rhyolitic laccoliths, sills and dykes along and inside RF1, and extrusion of rhyolites of the Mount Gillies Volcanics and minor mafic eruptives. Deposition of the Chinghee Conglomerate began, overlapping with the extrusion of the rhyolites.
6. Rapid erosion and exposure of the Mount Barney Granophyre and deposition of Chinghee Conglomerate, with minor basaltic eruption and intrusion of basaltic and trachytic dyke swarms marking the last stage of igneous activity.

Eruption of the Albert Basalt probably occurred from stage 2 through to stage 6 with most of the eruptions occurring before stage 5. The sources of the mafic eruptives are probably the caldera at Focal Peak and adventive vents.

## PETROLOGY OF THE FOCAL PEAK — MOUNT BARNEY INTRUSIVE AND ASSOCIATED EXTRUSIVE PHASES

### Introduction

Intrusive phases include a wide range of compositions extending from gabbros, through monzonite, syenites and microsyenites, to granophyre. In contrast, the extrusives comprise dominantly mafic lavas (basalts, hawaiites) and rhyolites, with minor trachytes. This is illustrated in histogram form in Text fig. 23 in which the $SiO_2$ contents of all analysed rocks are included. The strongly bimodal characteristics of the extrusives are clearly apparent, in contrast to the intrusive phases. A similar pattern of compositions exists for the Mount Warning intrusives compared to the Tweed Shield extrusives, which are also compared in Text fig. 23. Although cumulate compositions will account for some of the greater diversity of $SiO_2$ within the mafic intrusive rocks, the major differences are due to the occurrences of monzonite-syenite compositions within both intrusive complexes, which have few extrusive equivalents.

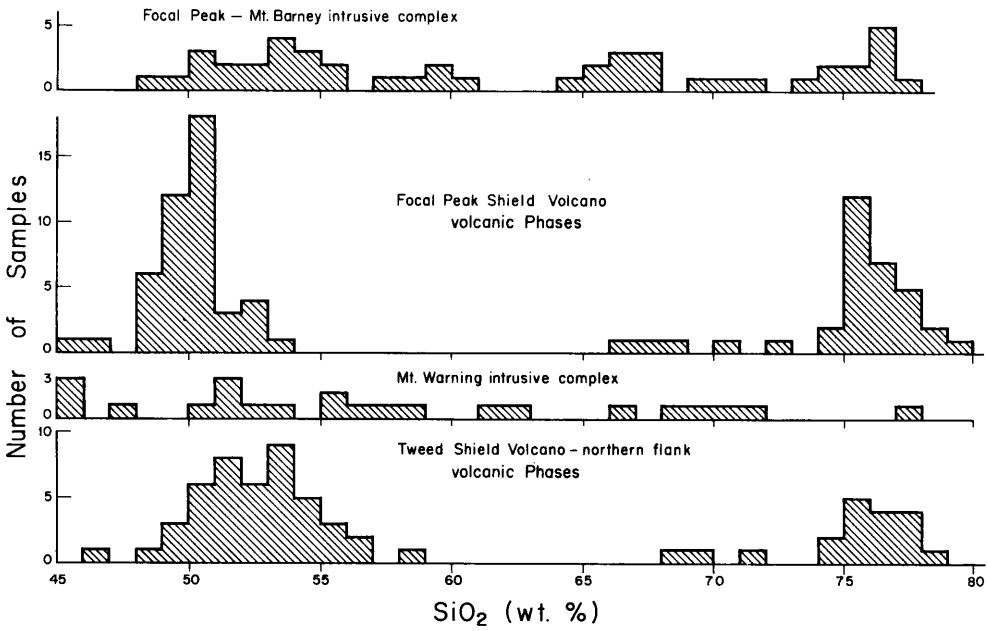


Text fig. 23. Histograms comparing the $SiO_2$ distributions of the intrusive and extrusive phases of the Focal Peak and Tweed Shield volcanoes, based on all analysed samples. The $SiO_2$ contents of the extrusives are recalculated to an anhydrous basis.

## Mineralogy

Focal Peak Pluton. Rocks include gabbros, monzonite, and minor syenite. Averaged chemical and modal analyses are presented in Table 5. The minerals comprise plagioclase ($An_{6-65}$, $Or_{0-2.4}$), augite ($Mg_{27-46}$, $Fe_{13-47}$, see Text fig. 24 (a)), ilmenite, and altered titanomagnetite. Olivine has not been observed, but uralite pseudomorphs are generally present, and possibly represent altered orthopyroxene. In Text fig. 25, the spread of the Focal Peak plagioclase compositions is compared with phenocrysts in the extrusive basalts and hawaiites of the Albert Basalt. As found for the Mount Warning gabbros, the plagioclase in the intrusives tends to exhibit a much more pronounced 'tail' towards the more sodic compositions. This is considered to result from both the extended crystallisation (particularly interstitially) of plagioclase in the intrusive rocks, together with superimposed re-equilibration during cooling.
Minnages Mountain and Montserrat microsyenites. The Minnages Mountain rock contains plagioclase ($An_{17-44}$), alkali feldspar, microperthite, quartz, hornblende, augite, biotite, ilmenite, apatite and sphene. The plagioclase is mantled by microperthitic alkali feldspar, and interstitial graphic intergrowths are commonly developed. The Montserrat microsyenites are generally similar, being distinctly porphyritic. Phenocrysts comprise plagioclase (overall range $An_{18-49}$, $Or_{0.3-0.5}$, although two distinct compositional groups appear to be present) and chloritized hornblende, set in a matrix of fine graphic intergrowths of quartz and alkali-feldspar, with additional accessory phases including biotite, ilmenite, apatite, zircon, and sphene.

Mount Barney Granophyre. All specimens examined are texturally very similar. The rocks contain prominent phenocrysts of sanidine cryptoperthite ($Or_{47-66}$, $An_{0-2.6}$; see Text fig. 27), up to 5 mm diameter, plus corroded quartz phenocrysts, which are set in a medium-grained matrix exhibiting abundant excellently developed granophyric intergrowths. Additional phases that have been identified in the matrix are minor aegirine and calcite, and relatively common opaque Fe-oxides and Fe-Ti oxides. These oxides are in part pseudomorphs after original Fe-silicates, although the exact identity of these cannot be established with any certainty. As will be subsequently shown, the Mount Barney Granophyre is interpreted as the intrusive equivalent of the Mount Gillies rhyolites, and thus the comparison of the mineralogy and textures between the two groups of rocks is of some interest.

## Ballow Cone Sheets and other Dolerites from Mount Barney Central Complex

These dolerites are typically non-porphyritic, consisting of plagioclase ($An_{6-57}$), augite to titanaugite, titanomagnetite, ilmenite, and interstitial chlorite and altered alkali feldspar. Fresh olivine has not been observed in the Ballow Cone Sheets, and is very rare in the other dolerites, only a single grain being analysed ($Fa_{64}$). The pyroxene and plagioclase compositions are plotted in Figs 24 and 26, respectively. The plagioclases, particularly the more sodic compositions, exhibit little ternary solid solution, and must have undergone subsolidus re-equilibration modification of chemistry. The pyroxenes of the Ballow Cone Sheets are more calcic, and also more aluminous and titaniferous than those of the other dolerites of the Mount Barney Complex, due to the generally more silica-undersaturated chemistry of the Ballow intrusives.

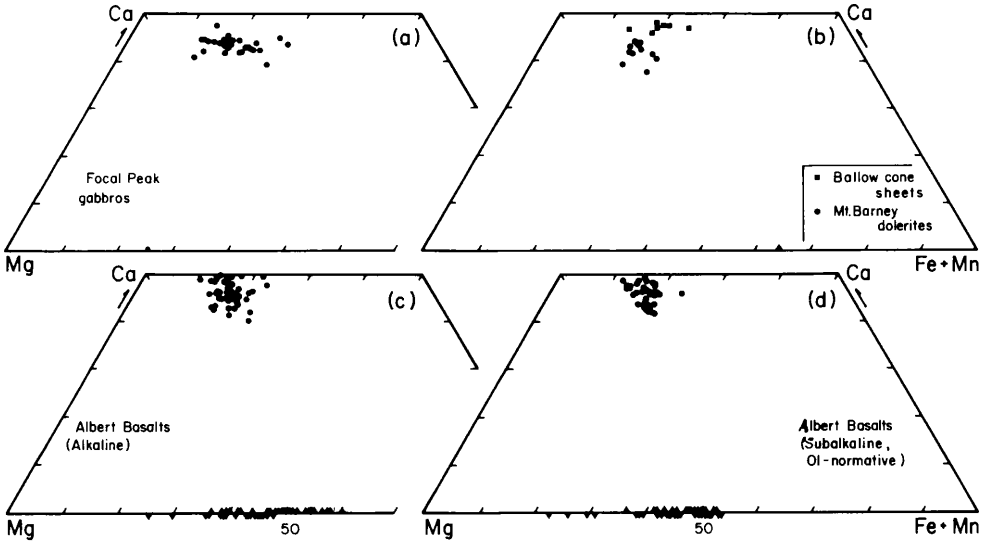


Text fig. 24. Pyroxene (filled circles and squares) and olivine (filled triangles) compositions (atomic %) of the Focal Peak gabbros, two intrusive dolerite groups, and the Albert Basalt. Only groundmass pyroxenes are plotted in (b) to (d). Groundmass olivines are represented by upward-pointing triangles; phenocryst olivines by inverted triangles. The Albert Basalt data are subdivided according to whole rock normative chemistry, the alkaline-subalkaline division based on Chayes (1966). Microprobe data. Data from Ross (1977).

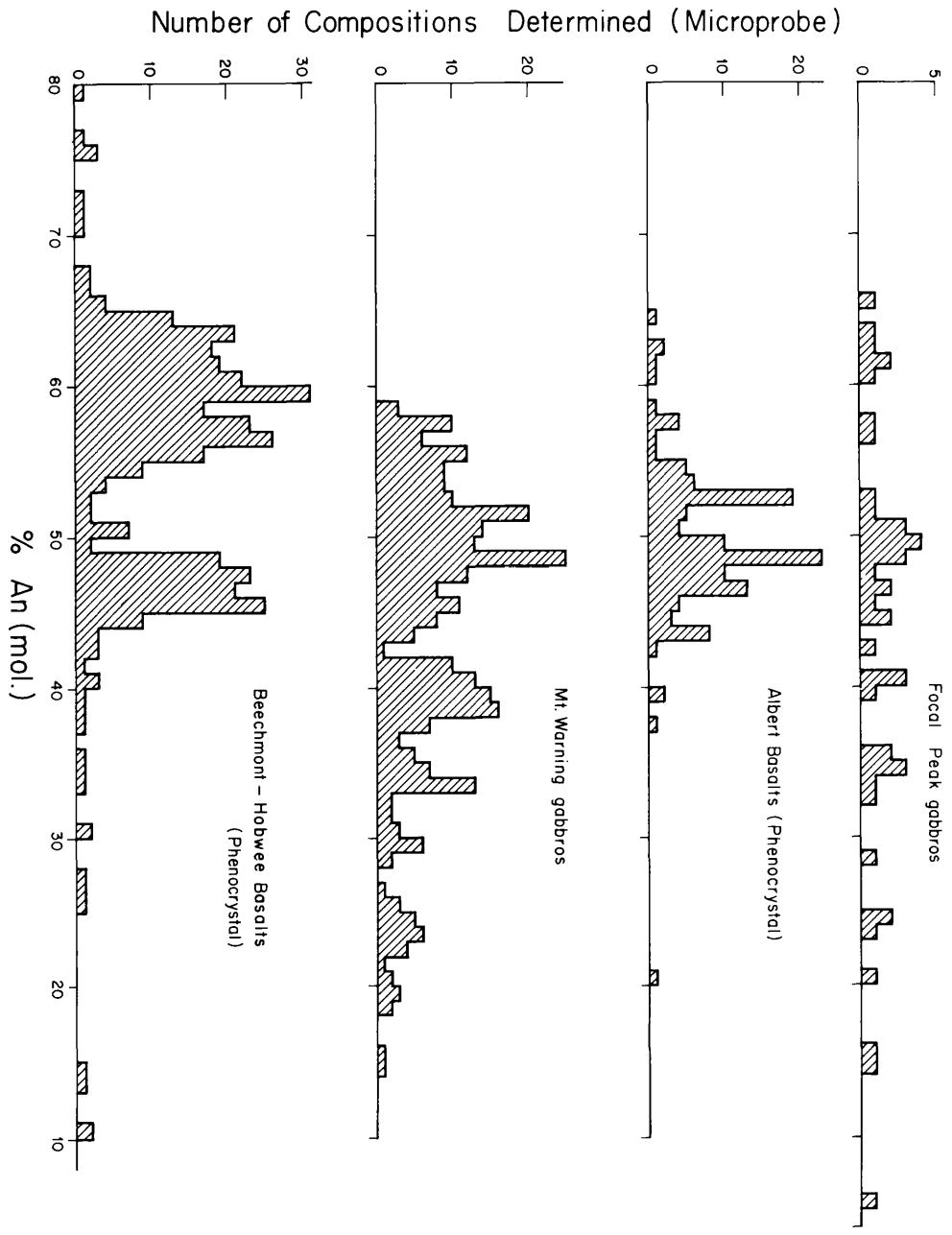


Text fig. 25. Histograms comparing the plagioclase compositional ranges found within the intrusive and extrusive mafic rocks of the Focal Peak and Tweed Shield volcanoes.

Albert Basalt. The extrusives vary chemically from alkaline to subalkaline, as subsequently discussed, and are mostly andesine-normative, thus being here classified as hawaiites rather than true basalts. The rocks are not strongly porphyritic, the average total modal phenocrystal content being approximately 3.5%, and in all samples ⟨ 10%. The main phenocrystal (and microphenocrystal) phases are plagioclase (⟨ 5% modal, averaging 1.0%; $An_{21\text{-}65}$ $Or_{0\text{-}6.7}$) and olivine (⟨ 10% modal, averaging 2.35%; $Fa_{22\text{-}51}$); augite phenocrysts are rare, being approximately $Mg_{37}$ $Fe_{15}$ $Ca_{48}$ where found. Groundmass mineralogy comprises plagioclase (varying from $An_{64}$ continously through to sanidine compositions, $Or_{50}$), augite ($Mg_{29\text{-}42}$ $Fe_{15\text{-}22}$ $Ca_{40\text{-}50}$), olivine ($Fa_{36\text{-}61}$), titanomagnetite (49-81% ulvospinel), ilmenite (1.6 to 8.5% $R_2O_3$), apatite. No subcalcic or Ca-poor pyroxenes have been found.

All groundmass plagioclase and augite compositions, and all olivine compositions, are presented in Text figs. 24 and 26. Phenocrystal plagioclase compositional ranges are illustrated in comparative histogram plots in Text fig. 25; the latter are generally less calcic than those occurring in the Beechmont and Hobwee Basalts, which are commonly more plagioclase-phyric, and also entirely subalkaline, extending to tholeiitic andesites.

The Albert Basalt groundmass compositional data (Text figs. 24, 26) have been subdivided into alkaline and subalkaline groupings, based on whole rock chemistry, the data being obtained from microprobe data on 8 alkaline and 8 subalkaline samples. Surprisingly little difference exists between the general compositional ranges within the two groupings, with respect to the pyroxenes or olivines. The extent of ternary solid solution in the groundmass feldspars is clearly shown (Text fig. 26), but again is similar in overall extent in both whole rock groupings, no doubt due to the very variable but overlapping alkali abundances throughout the Albert Basalt magmas (see later discussion).

Xenoliths and Megacrysts. The only *in situ* lherzolite nodule locality known is close to Palen Creek Prison Farm. At this locality (grid reference 771671 on sheet 9441-2), megacrysts of bronzite $Mg_{81.6\text{-}79.8}$ $Fe_{14.5\text{-}16.1}$ $Ca_{3.9\text{-}4.3}$) occur. The nodule minerals comprise olivine ($Fa_{11.0\text{-}11.3}$), bronzite ($Mg_{87.9\text{-}88.1}$ $Fe_{10.3\text{-}10.7}$ $Ca_{1.1\text{-}1.8}$), augite ($Mg_{44.0}$ $Fe_{11.7}$ $Ca_{44.3}$), and minor brown spinel (57.9% $Al_2O_3$, 9.3% $Cr_2O_3$, Mg/Mg + ΣFe (atomic) = 0.777-0.780). Coronas commonly surround both pyroxenes and olivine. Minerals within the coronas around olivine include olivine ($Fa_{24\text{-}46}$), augite ($Mg_{40}$ $Fe_{19}$ $Ca_{41}$) and plagioclase ($An_{28}$). Coronas rimming orthopyroxene consist of olivine ($Fa_{21\text{-}35}$), augite ($Mg_{43\text{-}53}$ $Fe_{12\text{-}14}$ $Ca_{33\text{-}44}$), plagioclase ($An_{16}$), and alkali feldspar ($Or_{22}$). A similar megacryst/xenolith assemblage occurs in the Kyogle Basalt (Wilkinson & Binns, 1969).

Approximately 1 km north of Richmond Gap (grid reference 0441/973666) megacrysts of bronzite ($Mg_{68.7\text{-}70.0}$ $Fe_{26.0\text{-}27.3}$ $Ca_{3.7\text{-}4.1}$) and sub-calcic augite ($Mg_{44.8\text{-}47.9}$ $Fe_{17.8\text{-}19.0}$ $Ca_{34.3\text{-}37.1}$) have been located within an Albert Basalt lava, which also contains rare gabbroic xenoliths.

Mount Gillies Volcanics. The eruptive and intrusive rhyolites of this formation consist of both pitchstones and non-glassy (devitrified) lithologies. Only within the pitchstones is the primary mineralogy well preserved. The primary phenocryst-microphenocryst assemblage typically found is: sanidine + quartz + ferrohedenbergite + fayalite + ilmenite + zircon + chevkinite + partially

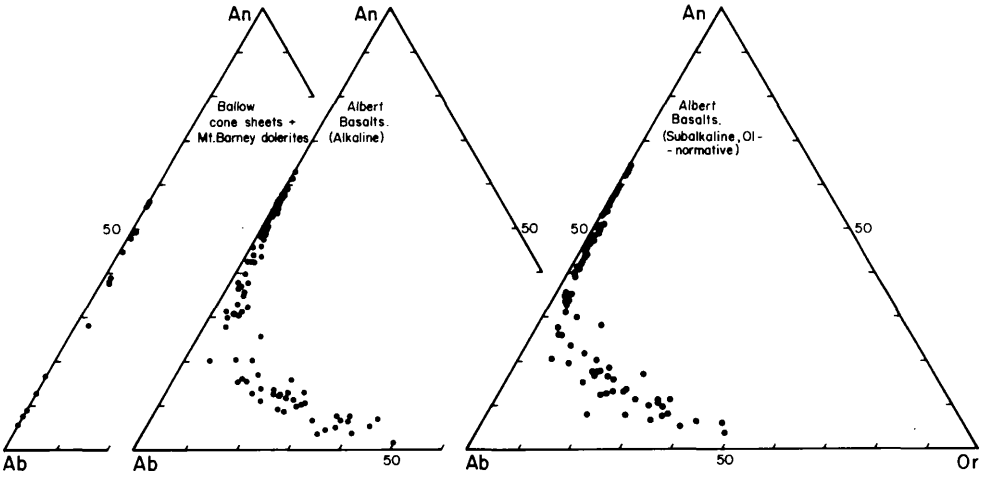


Text fig. 26. Compositions (mol. %) of groundmass feldspars occurring in the intrusive dolerites and the Albert Basalt, the latter subdivided according to the normative whole rock composition (see Text fig. 24). Microprobe data. (Ross 1977).

resorbed plagioclase, in approximate order of decreasing abundance. Of particular interest are the highly Fe-enriched compositions of the mafic phenocrysts. In addition, ferrohypersthene and ferropigeonite are found in some samples. The compositions of the feldspars are shown in Text fig. 27, and the pyroxenes and olivines in Text fig. 28. Microprobe analyses reveal the following compositional ranges:

| | |
|---|---|
| Sanidine | $Or_{36\text{-}54}\ Ab_{43\text{-}61}\ An_{2\text{-}5}$ |
| Ferrohedenbergite | $Mg_{0\text{-}1.8}\ Fe_{56\text{-}58}\ Ca_{41\text{-}46}$ |
| Fayalite | $Fe_{98.0\text{-}99.4}$ |
| Ilmenite | 1.0-1.8% $R_2O_3$ |
| Plagioclase | $An_{17\text{-}48}\ Or_{1\text{-}6}$ |

These phenocrystal phases occur in uncommon glomeroporphyritic aggregates, in which quartz is absent except as rare granophyrically textured grains. Within the devitrified rhyolites, the Fe-Mg silicates are nearly always completely altered. The sporadic occurrences of rather Mg-rich pyroxenes are considered to represent xenocrysts, although these are not uncommon in rhyolites of the SE. Queensland region (Ewart, 1985). The occurrence of traces of microphenocrystal chevkinite is noteworthy; analyses of this phase are presented in Ewart (1981). In the southeast Queensland region, it has so far been found only in fayalite-hedenbergite rhyolites, from the Mount Gillies and the Mount Alford centres.

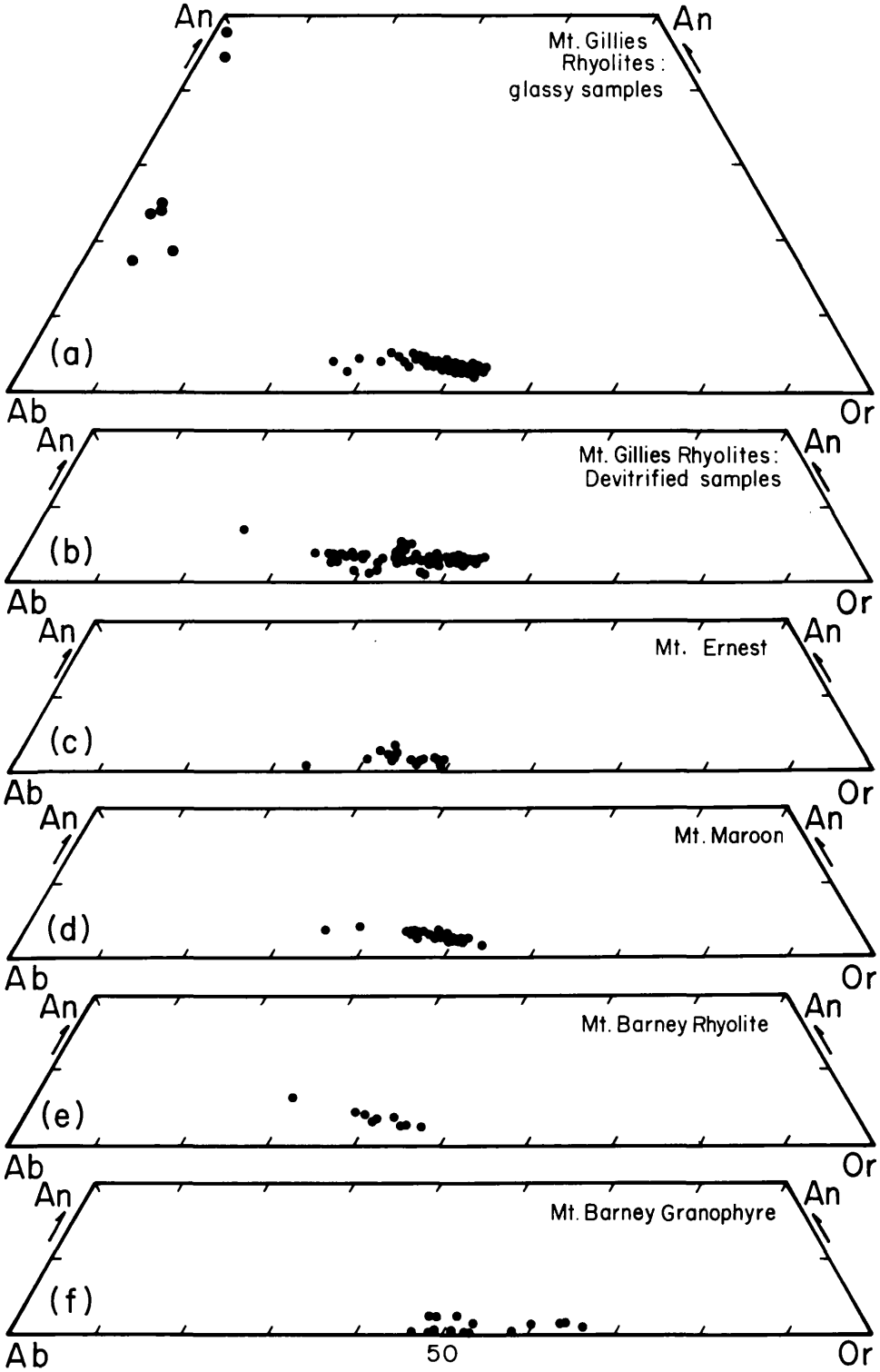


Text fig. 27. Compositions (mol. %) of the phenocrystal feldspars occurring in the rhyolites of the Mount Gillies Volcanics, Mounts Ernest, Maroon, and Barney, and the Mount Barney Granophyre. Microprobe data. Data from Ross (1977).

Averaged modal data are presented in Table 6, the pitchstone and devitrified rhyolite data being presented separately. Total phenocryst contents vary from extremes of 6.3 to 26.1% and 7.2 to 31.0% respectively. The averages and standard deviations of the mineral modes in Table 6 are, nevertheless, remarkably similar for the two data groups. No systematic variations of quartz-sanidine abundances have been found through the various occurrences of the Mount Gillies rhyolites. The observed modal variations are thus regarded as essentially random variations, the rhyolites have average crystal contents of 16–18%, somewhat higher than most other rhyolites of the region.

In Text fig. 27, the phenocrystal sanidine compositions occurring in the pitchstones and devitrified rhyolites are compared. The overall compositional ranges are similar, but there is evidently a relatively larger proportion exhibiting more sodic compositions within the devitrified samples. This is again considered to be simply a sampling effect, or a statistical effect arising from pitchstones being less common than devitrified rhyolites, but the possibility does exist that some additional growth occurred on phenocrysts during devitrification.

The matrices of the devitrified rocks consist predominantly of quartz and alkali feldspar. Wedge-shaped pseudomorphs of quartz after tridymite are common, and spherulitic development is widespread, individual spherulites usually having nucleated on phenocrysts.

Additional Rhyolites. These are intrusives associated with the Mount Barney Central Complex. They are typically devitrified types, occurring, for example, on Mounts Ernest, Maroon, and Philip. Modes of the rhyolites from Mounts Ernest and Maroon are given in Table 6. Sanidine-potassic anorthoclase comprises the dominate phenocryst (Text fig. 27), ranging between $Or_{34\text{-}50}$ $An_{6\ 0.9\text{-}5.9}$ (Mount Ernest), and $Or_{34\text{-}54}$ $An_{1.7\text{-}4.1}$ (Mount Maroon). Quartz is a conspicuous phenocryst phase, while minor ilmenite, zircon, and altered Fe-silicates are present; the latter are interpreted to have originally been ferrohedenbergite and fayalite.

Pitchstones from the Mount Barney Complex are rare. Float of a green pitchstone (33030, see also Table 6 and Figs 27 and 28) has been found in creeks to the south of Mount Ernest. It contains phenocrystal sanidine-sodic anorthoclase ($Or_{30\text{-}46}$ $An_{2.3\text{-}6.1}$), ferroaugite-ferrohedenbergite ($Mg_{7\text{-}21}$ $Fe_{39\text{-}50}$ $Ca_{40\text{-}43}$), Fe-olivine ($Fa_{86.9\text{-}93.1}$), and traces of ferrohypersthene, ilmenite, titanomagnetite, zircon, and chevkinite. The coexisting Fe-Ti oxides give 841°C at log $fO_2$ = −14.7 using data from Stormer, 1983). This rhyolite contains somewhat less Fe-enriched phenocryst compositions than is characteristic of the rhyolites of Mount Gillies, also consistent with the absence of phenocryst quartz.

Trachytes. Rare occurrences of extrusive trachytes are known. One such occurrence is 2 km south of Mount Gillies (grid reference 9441-2,756694; see sample 33148 in Table 5 and Text fig. 28(a), occurring as an autobreccia intercalated in the Albert Basalt sequence. This is a one-feldspar trachyte, containing phenocrystal anorthoclase ($Or_{31\text{-}35}$ $An_{0\text{-}4}$), ferroaugite ($Mg_{19\text{-}28}$ $Fe_{30\text{-}39}$ $Ca_{41\text{-}44}$), and titanomagnetite. This is again of interest in view of the less Fe-enriched pyroxene compositions. Groundmass phases are anorthoclase,

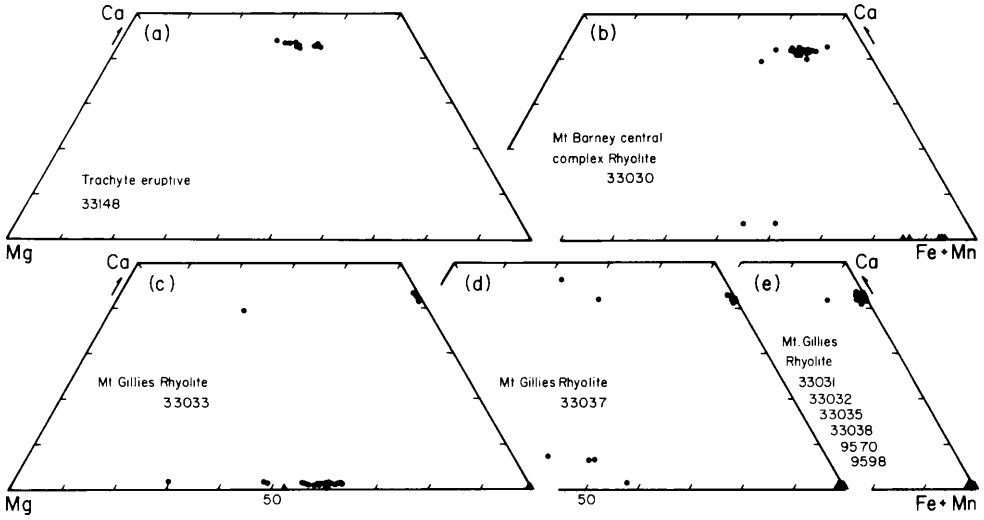


Text fig. 28. Compositions (atomic %) of the phenocrystal pyroxenes (filled circles) and olivines (filled triangles) occurring in a trachyte and rhyolites of the Focal Peak Shield and the Mount Gillies Volcanics (Rhyolite). Microprobe data. Sample numbers refer to the rock collection of the Department of Geology and Mineralogy, University of Queensland. Data from Ross (1977).

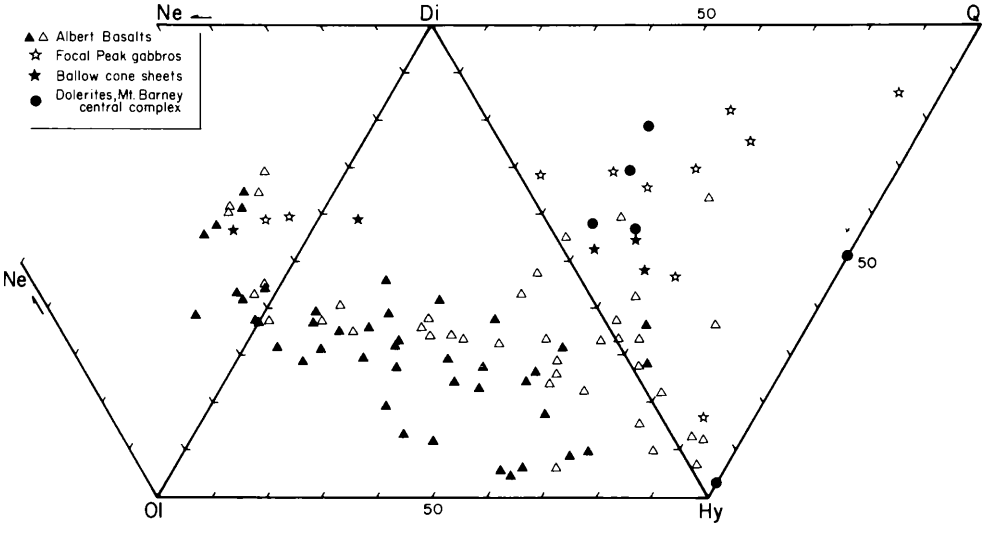


Text fig. 29. Normative (C.I.P.W.) compositions of the intrusive and extrusive mafic phases of the Focal Peak Shield volcano. The Albert Basalt data are divided according to two ferric-ferrous ratios, one based on the analysed $Fe_2O_3$ and FeO (hollow triangles), and the second on an assumed $Fe_2O_3/Fe_2O_3 + FeO = 0.2$ (filled triangles).

ferroaugite, titanomagnetite, aenigmatite, and riebeckite, the two latter minerals indicating the late stage development of a peralkaline magma chemistry during phenocryst precipitation.

## Chemistry

Albert Basalt. Forty-five analyses of samples from this formation are available (Ross 1977), and it is clear that the lavas are extremely variable chemically, as shown by other central volcanic complexes within SE. Queensland. This can be illustrated in a number of plots. For example, Text fig. 29 illustrates all data plotted in terms of normative ne-ol-di-hy-Q, in which the levels of silica saturation are clearly shown. The Albert Basalt varies continuously from ne- to Q-normative, although it is clearly dominated by ol-normative compositions. This is emphasized further by the points based on the assumed Fe oxidation ratio ($Fe_2O_3/Fe_2O_3 + FeO = 0.2$), which is considered to be a more realistic approximation to pre-eruptive oxidation states. The Albert Basalt is thus distinctly more silica undersaturated than the Beechmont and Hobwee Basalts when considered overall, and this is reflected in the lower modal $SiO_2$ distribution within the Albert Basalt as against the Beechmont-Hobwee lavas, as shown in the histograms of Text fig. 23.

The variability of the Albert lavas is further shown by most other chemical parameters, and Text fig. 30 illustrates a plot of $K_2O$ versus $TiO_2$, in which again the extensive data scatter is clear; $K_2O$ varies between 0.46-2.63% and $TiO_2$ between 1.48–3.18%. No clear correlation exists between Ti and K, although a maximum in $TiO_2$ distribution does exist. In terms of other normative parameters, the lavas are dominantly andesine-normative (total range being 23.7 to 52.9%); it is on this basis that most of these rocks are considered as hawaiites (see Ewart *et al.*, 1980). 100 Mg/Mg + ΣFe (atomic) ranges between 23 and 59.6%. The wide range of chemical parameters is thus suggestive of fractional crystallisation (or convective fractionation) processes in controlling at least some of the observed chemical variability. The possible effects of such crystal-liquid fractionation processes are best illustrated in plots incorporating trace element data. Text figs 31 to 36 illustrate, respectively, Ni and Cr versus Mg/Mg + ΣFe, V versus ΣFe (as FeO), Zn versus Nb, Ba and Sr versus Rb (in which Rb is interpreted as an incompatible element). A number of these plots also incorporates data from the intermediate to acid volcanic and intrusive phases.

The Ni and Cr versus Mg/Mg + ΣFe plots (Text figs 31, 32) illustrate broad correlations between these sets of parameters, the most magnesian lavas being most Ni and Cr enriched; the data are, however, quite scattered. On these plots are superimposed fractionation control curves using the following phases, and phase assemblages, based on observed phenocryst compositions within the lavas:

(a) Olivine ($Fa_{22.4}$, based on the most magnesian phenocrysts observed in the lavas of the Albert Basalt).
(b) Augite ($Mg_{43.6}\ Fe_{12.8}\ Ca_{43.6}$).
(c) Combinations of olivine + plagioclase (1:1), olivine + augite + plagioclase + magnetite (0.3:0.3:0.3:0.1). The plagioclase is $An_{52.7}$.

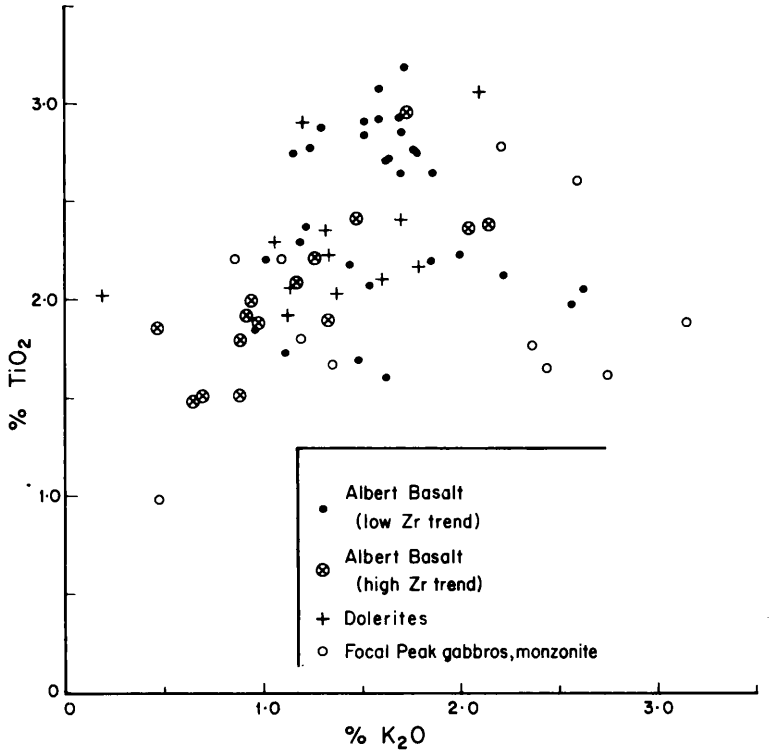


Text fig. 30. $TiO_2$ versus $K_2O$ (wt. %) within the intrusive and extrusive mafic phases of the Focal Peak Shield Volcano. High and low Zr trends, Albert Basalt, refer to Fig. 34.

It is clear that the observed Ni-Mg/Mg + ΣFe behaviour (Text fig. 31) can be reasonably modelled by a phase assemblage in which olivine is a major phase, and due to the high partitioning of Ni into Mg-olivines, the presence of either plagioclase or augite with olivine makes little difference to the overall depletion pattern of Ni during fractionation (although the presence of these additional phases does vary the rate, as measured in terms of f, at which the depletion of Mg and Ni occurs). The Cr behaviour (Text fig. 32), in contrast, requires an important augite $\pm$ magnetite component to model the observed depletion, and is also very sensitive to the actual value of the partition coefficient used for augite, which is both relatively high and rather variable (reported basaltic values varying between 1.9 to 13.0, an average value of 5.8 being used in the calculations; see Appendix 1). Notwithstanding this, the olivine + augite + plagioclase + magnetite assemblage does produce a strongly depleted Cr distribution pattern, and is broadly consistent with the observed behaviour.

V behaviour (Text fig. 33) within the Albert Basalts is very scattered, some samples exhibiting a tendency towards V (and Fe) depletion. This tendency is also well shown by the microsyenites and the gabbros and monzonites of Focal Peak. Reference to the calculated fractionation curves of the silicates indicates that none of these, alone, will produce correlated V and Fe

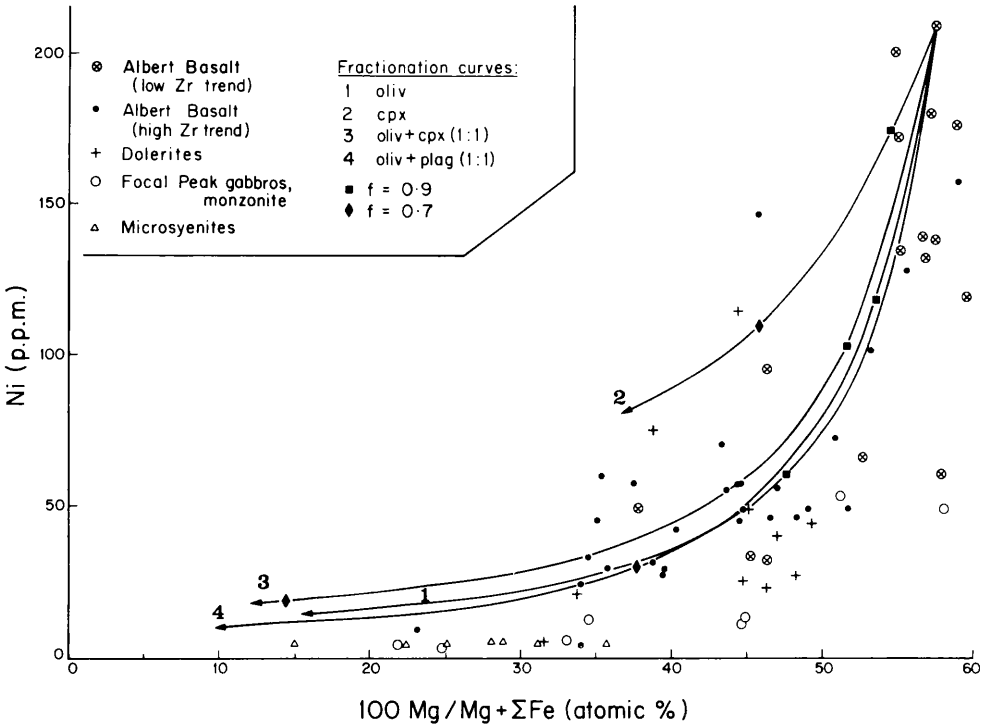


Text fig. 31. Ni versus Mg/Mg + Σ Fe for the intrusive and extrusive mafic to intermediate phases of the Focal Peak Shield Volcano. In this and the succeeding plots, the microsyenites refer to those of Minnages Mountain and Montserrat. Details of the fractionation curves (which are based on Rayleigh fractionation) are given in text; f refers to weight fraction of liquid remaining. Basaltic partition coefficients are used, except with otherwise stated. The high and low Zr trends within the Albert Basalt are based on Text fig. 34.

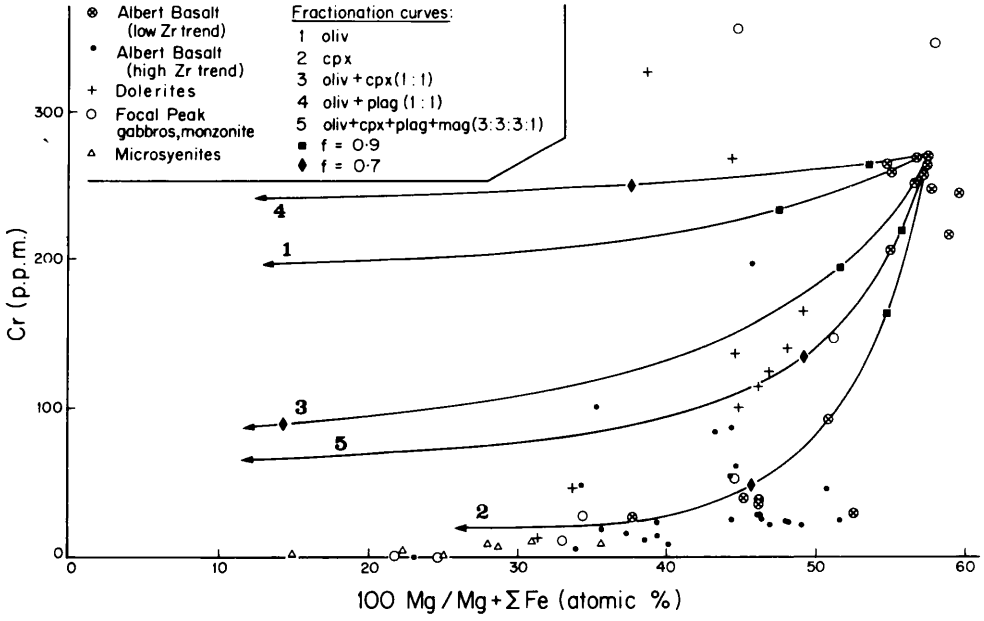


Text fig. 32. Cr versus Mg/Mg + Σ Fe for the intrusive and extrusive mafic to intermediate phases of the Focal Peak Shield Volcano.

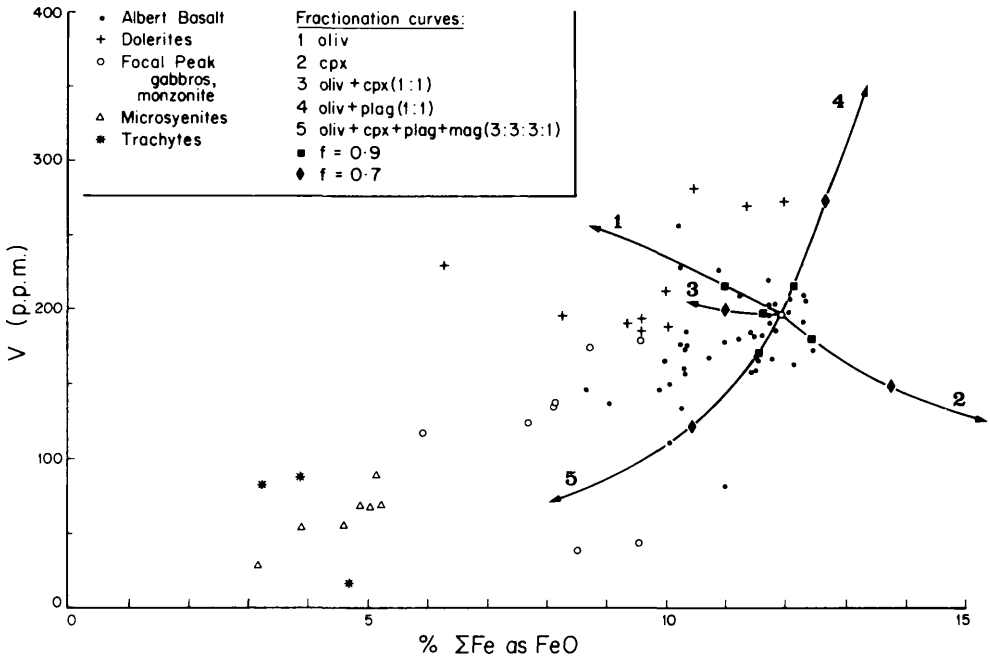


Text fig. 33. V versus FeO for the intrusive and extrusive mafic to intermediate phases of the Focal Peak Shield Volcano.

depletion; to attain this requires a coexisting magnetite phase, which is entirely consistent with the Cr data.

The Zr-Nb relations (Text fig. 34) within the Albert Basalt suggest the possibility of two distinct trends or lineages, both elements correlated, but along differing trends; these two trends cannot be clearly correlated with other geochemical parameters, such as the degree of silica saturation. The exact significance of these differing trends is not known, but the calculated fractionation curves for olivine and augite which are plotted in Text fig. 34 suggest that fractionation could be an explanation. The $K_D$ values used for Zr and Nb for olivine are 0.04 and 0.30, and for augite are 0.75 and 0.20 respectively; these are based on averaged values from the literature, using analyses of natural phenocrysts (see Appendix 1). Thus, the low Zr trend could be readily explained by an assemblage in which augite was a major phase (e.g. up to 50% of assemblage), whereas the high Zr trend is the result of an augite-poor fractionating assemblage. This explanation, however, seems to be effectively negated by the disproportionately high Cr and Ni abundances of most of the low Zr trend samples (Text figs 31, 32), thus suggesting that the low Zr trend, at least, is a primary magmatic characteristic. This does not preclude the high Zr trend as resulting from, or being accentuated by, olivine-dominated fractionation, which is consistent with other trace element data.

Plots for Ba-Rb and Sr-Rb (Text figs 35, 36) in which Rb is used as an incompatible element, show considerable variability of abundances. A very broad correlation is apparent between Rb and Ba in the Albert Basalt, whereas

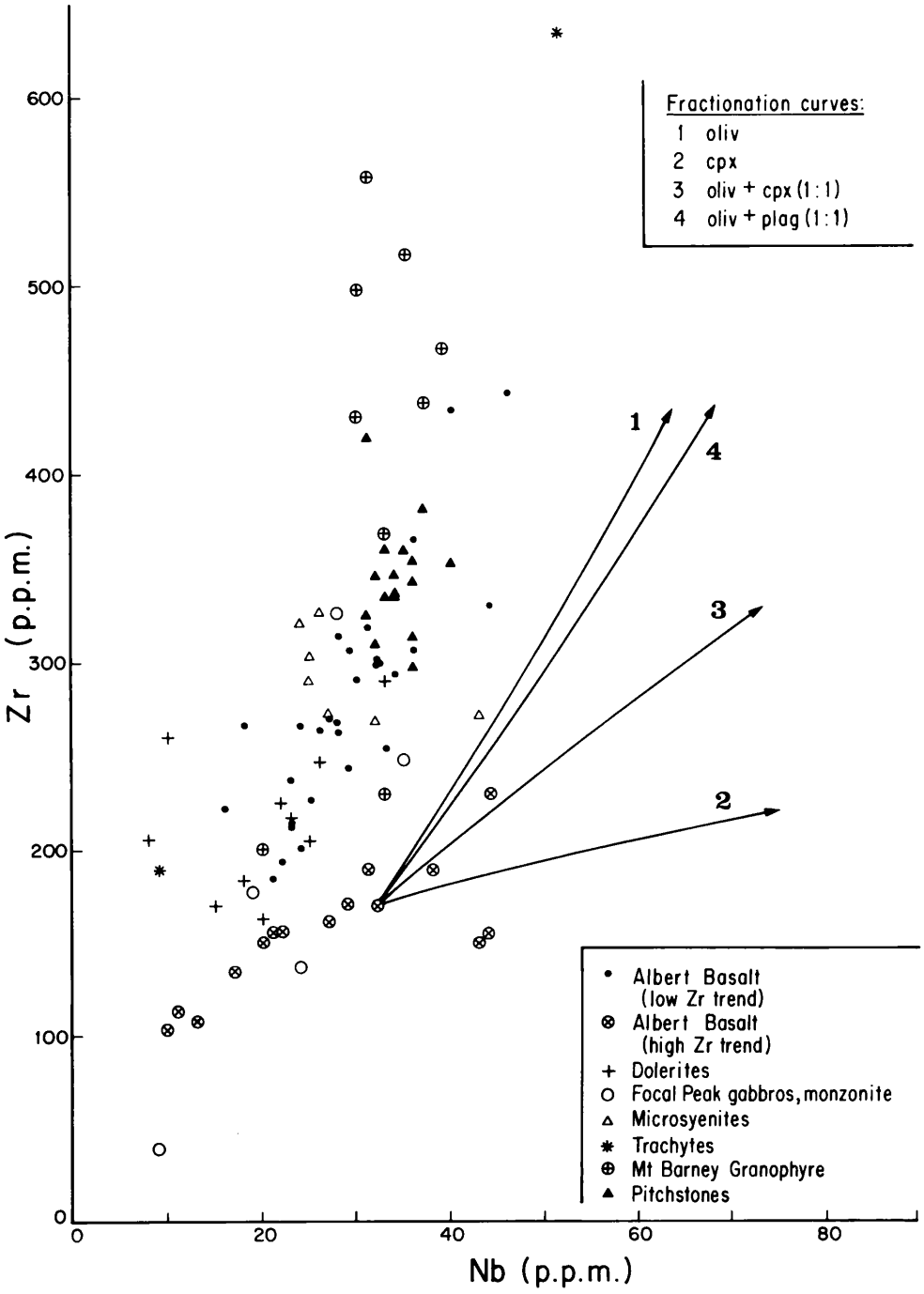


Text fig. 34. Zr versus Nb for all the analysed intrusive and extrusive phases of the Focal Peak Shield Volcano. Note the subdivision of the Albert Basalt into high and low Zr trends.

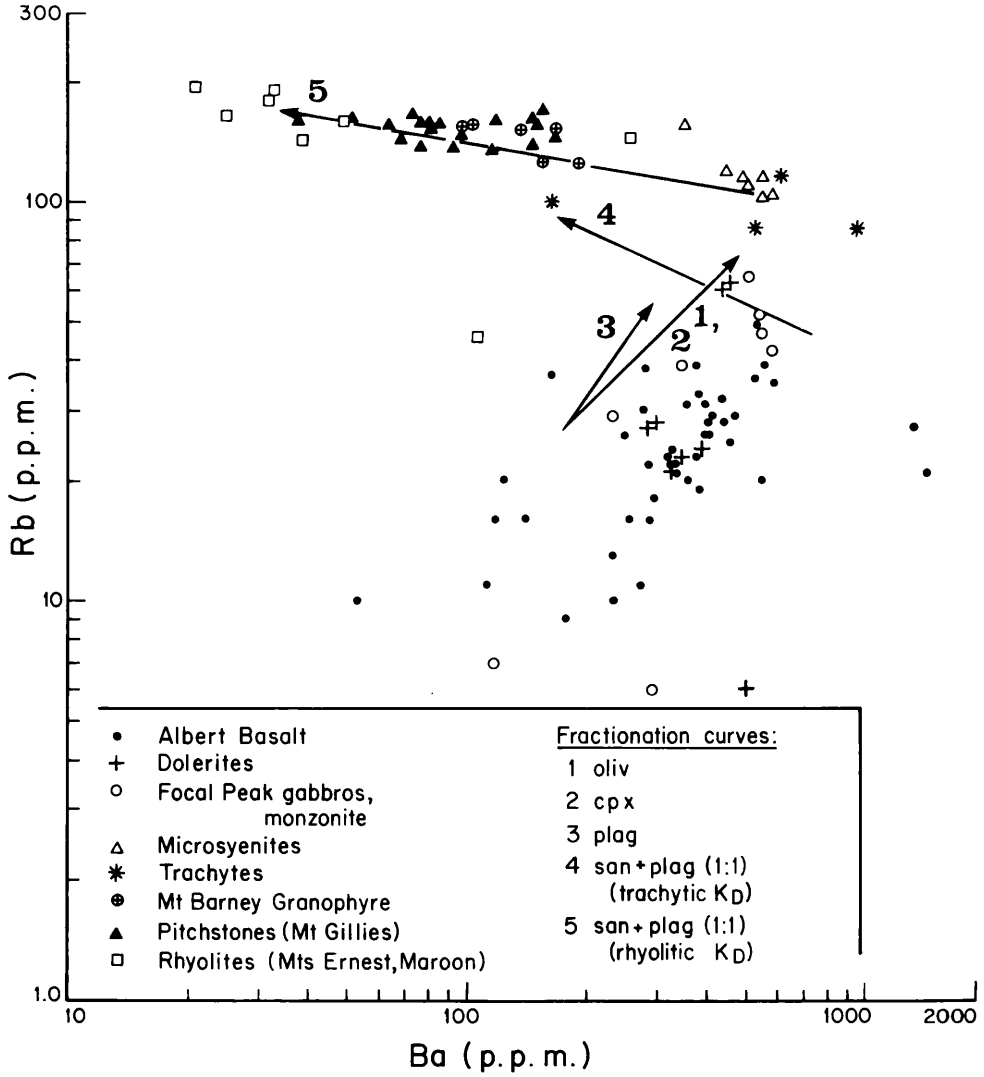


Text fig. 35. Rb versus Ba for all the analysed intrusive and extrusive phases of the Focal Peak Shield Volcano. Curve 4 is based on trachytic partition coefficients ($K_D$), and curve 5 on rhyolitic partition coefficients (Appendix 1); further data given in text and caption to Text fig. 31.

the Sr abundances show little overall change with increasing Rb. Reference again to the calculated fractionation curves for olivine, augite, and plagioclase show that these trace element trends are quite consistent with fractionation of a composite assemblage containing olivine, plagioclase, and augite, in agreement with the Cr and Ni data previously discussed. Magnetite is not precluded by the Rb, Ba, and Sr data, as it has no significant effect on their relative behaviour during fractionation.

In summary, the combined trace and major element data for the Albert Basalt indicate considerable chemical variability within the formation. Much of this variability is shown to be consistent with crystal fractionation involv-

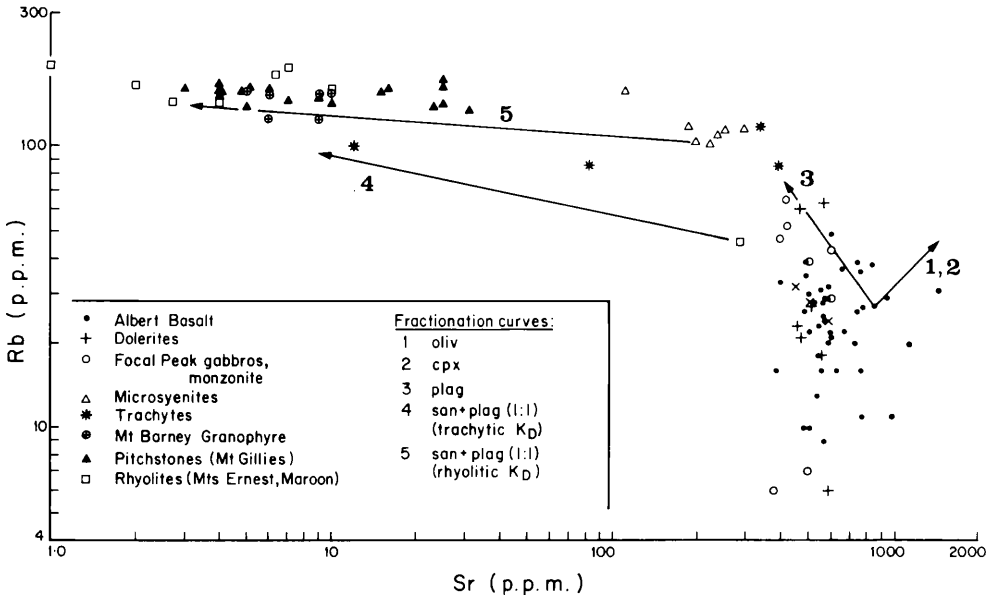


Text fig. 36. Rb versus Sr for all the analysed intrusive and extrusive phases of the Focal Peak Shield Volcano. See caption to Text fig. 35 for further data.

ing the relative, but variable separation of olivine, plagioclase, augite, and magnetite phases prior to eruption. Nevertheless, there is additional chemical variability, such as for $K_2O$ and Zr, which is interpreted to represent variable primary characteristics, together with the operation of lower crustal assimilation (exchange) processes, the latter suggested by some Pb isotopic compositions (Ewart, 1982).

The Focal Peak Intrusives and the Mount Barney Dolerites. The Focal Peak gabbroic and associated monzonitic and syenitic intrusives are essentially bimodal in terms of silica saturation (Fig. 29), two samples being ne-normative, the remainder being Q-normative. The various doleritic intrusives exhibit a somewhat similar bimodal silica saturation, with again most samples Q-normative. Thus, in terms of this parameter, the intrusives are chemically not exactly equivalent to the Albert lavas; in the case of the gabbroic rocks this is at least partly attributable to cumulative processes (e.g. noting the high $Al_2O_3$ of the gabbros). In terms of other chemical characteristics, (Text figs 30 to 36) the various mafic intrusives are similar to the Albert lavas, both in terms of variability and their absolute abundance ranges.

Of particular interest is the chemistry of the microsyenites from Minnages Mountain and Montserrat. These rocks, which are all quartz-bearing (see also Text fig. 37), exhibit strongly depleted Cr, Ni, and V abundances, enrichment of Rb, and the initial stages of Ba and Sr depletion. Reference to Text figs 31 to 33, and the previous discussion dealing with the Albert Basalt, indicate that the Cr, Ni, and V behaviour is well explained by continued crystal

TABLE 5. AVERAGED CHEMICAL AND MINERALOGICAL DATA FOR MAFIC AND INTERMEDIATE INTRUSIVE AND EXTRUSIVE PHASES OF THE FOCAL PEAK SHIELD. AVERAGED BEECHMONT-HOBWEE DATA PRESENTED FOR COMPARISON

| | Albert Basalt | Beechmont-Hobwee Basalt | Mt Barney central complex Dolerites | Ballow Cone Sheets | Focal Peak Mafic Gabbro | Pluton Gabbro | Monzonite | Minnages Mtn Microsyenite | Montserrat Microsyenite | Steamers Trachyte Member[3] | Trachytes 33148 | Trachytes 33057 |
|---|---|---|---|---|---|---|---|---|---|---|---|---|
| $SiO_2$ | 48.47 | 51.13 | 51.69 | 50.32 | 50.40 | 55.14 | 58.02 | 66.53 | 68.10 | 67.63 | 67.16 | 66.90 |
| $TiO_2$ | 2.29 | 2.26 | 2.36 | 2.26 | 1.66 | 2.31 | 1.76 | 1.01 | 0.95 | 0.44 | 0.88 | 0.55 |
| $Al_2O_3$ | 15.86 | 15.54 | 15.62 | 15.14 | 18.52 | 14.85 | 14.34 | 13.65 | 13.56 | 14.03 | 13.94 | 14.36 |
| $Fe_2O_3$ | 4.01 | 3.57 | 3.71 | 2.23 | 2.25 | 3.76 | 4.47 | 2.78 | 2.09 | 2.81 | 2.87 | 0.97 |
| FeO | 7.40 | 7.14 | 6.43 | 7.41 | 5.03 | 5.42 | 4.56 | 2.64 | 2.74 | 1.33 | 2.11 | 2.99 |
| Σ FeO* | 11.01 | 10.35 | 9.77 | 9.42 | 7.06 | 8.80 | 8.58 | 5.14 | 4.62 | 3.86 | 4.69 | 3.86 |
| MnO | 0.15 | 0.14 | 0.15 | 0.14 | 0.11 | 0.11 | 0.13 | 0.07 | 0.07 | 0.09 | 0.04 | 0.08 |
| MgO | 5.68 | 4.97 | 3.94 | 5.36 | 5.29 | 3.82 | 1.78 | 1.35 | 1.15 | 0.25 | 0.26 | 1.58 |
| CaO | 7.37 | 7.49 | 6.84 | 8.03 | 8.69 | 6.68 | 4.45 | 2.43 | 2.02 | 1.25 | 0.94 | 2.14 |
| $Na_2O$ | 3.76 | 3.63 | 3.89 | 3.71 | 3.84 | 4.56 | 4.34 | 3.90 | 3.70 | 3.76 | 5.62 | 3.24 |
| $K_2O$ | 1.45 | 1.32 | 1.38 | 1.49 | 1.03 | 2.03 | 2.76 | 3.71 | 3.59 | 5.34 | 4.42 | 3.56 |
| $P_2O_5$ | 0.72 | 0.55 | 0.59 | 0.52 | 0.32 | 0.62 | 0.66 | 0.25 | 0.26 | 0.06 | 0.24 | 0.12 |
| $\Sigma H_2O$ | 2.54 | 2.29 | 3.28 | 3.25 | 2.87 | 0.96 | 1.65 | 1.45 | 1.37 | 2.62 | 1.10 | 2.07 |
| Total | 99.71 | 100.03 | 99.87 | 99.87 | 99.98 | 100.23 | 98.92 | 99.80 | 99.59 | 99.61 | 99.58 | 98.56 |
| n | 45 | 37 | 6 | 3 | 4 | 4 | 3 | 3 | 8 | 4 | 1 | 1 |
| Trace Elements (p.m.m. – x-ray fluorescence analyses) | | | | | | | | | | | | |
| Rb | 25 | 22 | 35 | 28 | 18 | 29 | 55 | 103 | 119 | 112 | 86 | 117 |
| Sr | 697 | 495 | 502 | 509 | 542 | 490 | 408 | 197 | 216 | 83 | 82 | 338 |
| Ba | 383 | 348 | 358 | 368 | 178 | 413 | 540 | 594 | 491 | 1205 | 961 | 620 |
| Th | 3.5 | 2 | 3 | 3 | 2 | 3 | 6 | 13 | 14 | 11.5 | 8 | 5 |
| Zr | 237 | 211 | 216 | 223 | 108 | 237 | 445 | 327 | 288 | 913 | 635 | 189 |
| Zn | 129 | 108 | 119 | 116 | 87 | 85 | 132 | 161 | 136 | – | 238 | 81 |
| Nb | 28 | 19 | 20 | 25 | 13 | 29 | 35 | 26 | 29 | 28 | 51 | 9 |
| Ce | 56 | 48 | 49 | 44 | 29 | 41 | 78 | 73 | 74 | 93 | 129 | 66 |
| Y | 28 | 27 | 29 | 23 | 11 | 23 | 39 | 38 | 52 | 49 | 65 | 32 |
| V | 175 | 156 | 224 | 198 | 126 | 164 | 69 | 69 | 61 | 10 | 17 | 88 |
| Cr | 95 | 113 | 143 | 117 | 247 | 140 | 10 | 5 | 7 | < 1 | 3 | 30 |
| Ni | 77 | 54 | 36 | 33 | 52 | 11 | 7 | 5 | 6 | – | 7 | 2 |
| Cu | 43 | 33 | 21 | 28 | 33 | 47 | 17 | 15 | 45 | – | 2 | 22 |
| n | 45 | 22 | 6 | 3 | 2 | 3 | 3 | 1 | 6 | 4 | 1 | 1 |
| Modal Analyses (vol %) – Phenocryst/microphenocryst Phases | | | | | | | | | | | | |
| Plagioclase | 1.0 | 7.9 | – | – | 70.8 | 74.8 | – | – | – | 0.9 | – | – |
| Alkali feldspar | – | – | – | – | – | – | – | – | – | 14.2 | 8.9 | – |
| Olivine | 2.3 | 1.4 | – | – | – | – | – | – | – | 1.0 | (?)0.2 | – |
| Clinopyroxene | 0.03 | 0.13 | – | – | 25.5 | 13.9 | – | – | – | 0.7 | 2.2 | – |
| Fe-Ti oxides | 0.05 | 0.01 | – | – | 2.4 | 7.4 | – | – | – | 0.2 | 0.2 | – |
| Matrix | 96.6 | 90.6 | – | – | – | – | – | – | – | 83.0 | 88.5 | – |
| n | 39 | 24 | – | – | 3[1] | 1[2] | – | – | – | 2 | – | – |

[1] Includes 1.1% quartz + 0.1% apatite

Σ FeO* = total Fe as FeO

[2] Includes 3.6% quartz + 0.3% apatite

[3] From Grenfell (1984)

n = Number of samples used in each data set.

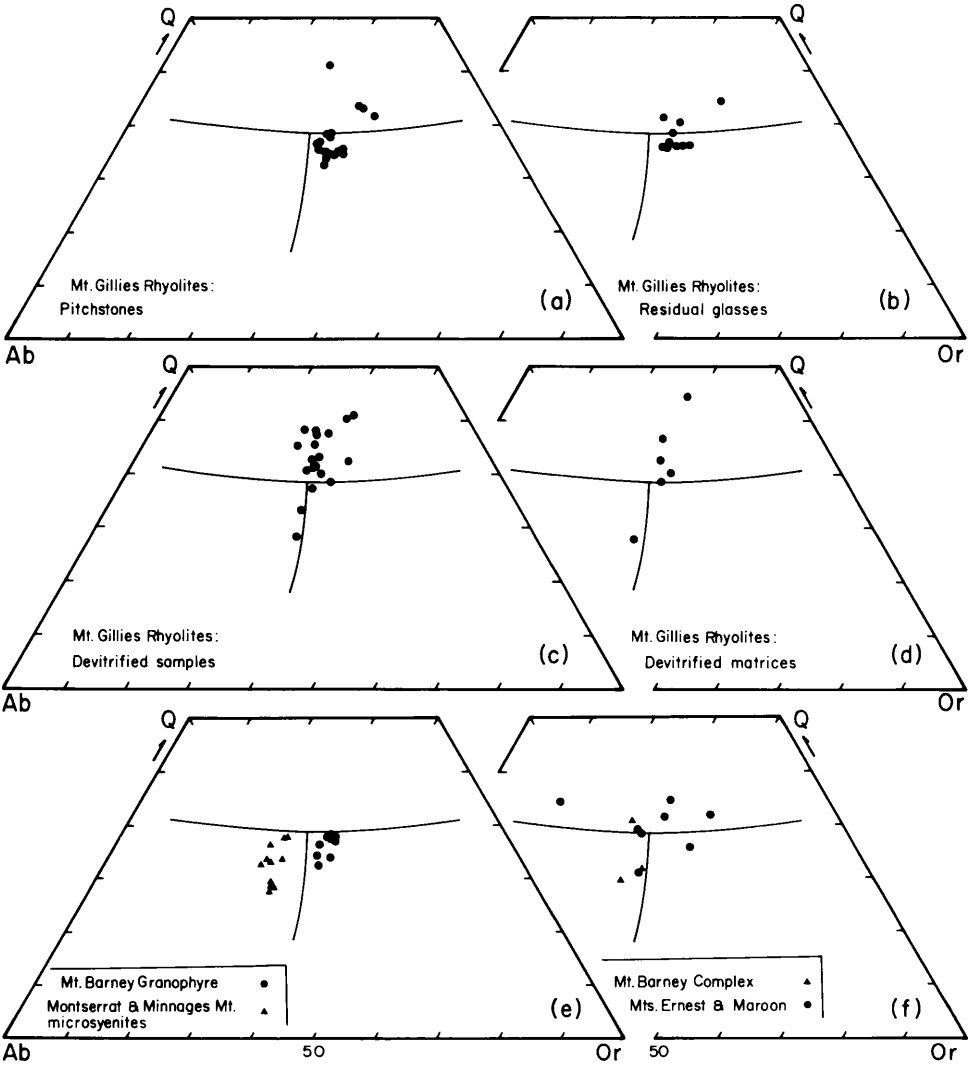


Text fig. 37. Normative (C.I.P.W.) Q, Ab, and Or compositions of the intermediate to acid intrusive and extrusive phases of the Focal Peak Shield Volcano. The separated residual glasses from the pitchstones, and the matrices from the devitrified rhyolites are also plotted, from the lavas of the Mount Gillies Volcanics. The quartz-feldspar boundary curves are from James and Hamilton (1969), based on the composition $[Q\text{-}ab\text{-}Or]_{97}\ An_3$, at 1 kb water pressure.

fractionation, from a mafic parental magma, of olivine, plagioclase, augite, and magnetite. The Sr and Ba behaviour (Text figs 35, 36), however, gives the first indication of the increasing relative importance of feldspar in such fractionation processes. This becomes even more so in the rhyolitic lavas.

In Text figs 37 and 38 comparison can be made between the microsyenite, the Mount Barney Granophyre, and the rhyolite compositions, in terms of the quartz-feldspar, and ternary feldspar systems. The microsyenites are notably more Ab (and An)-enriched compared with the granophyre and the rhyolites, projecting somewhat displaced from the ternary piercing point in the quartz-

feldspar system, and above the two-feldspar boundary curve in the feldspar system. For the syenites these differences are interpreted to be consistent with fractionation from a more mafic parental liquid. Such an origin is considered unlikely for the granophyre and the rhyolites (see Ewart 1982, and subsequent discussion in following sections).

Mount Gillies Rhyolite. As previously noted, these can be considered as two groupings, the pitchstones and the devitrified lithologies. As previously shown, they are mineralogically essentially identical, and can be regarded as comagmatic. In Table 6, a comparison is presented of the averaged whole rock analyses of the two groups (the pitchstone data excluding those analyses clearly showing Na-leaching; see below). Plots, in terms of normative Q-Ab-Or, and An-An-Ab-Or, are presented in Text figs 37a, c and 38 c, e. The rhyolites can be best regarded as potassic, high silica-rhyolites, and are closely similar to rhyolites in other anorogenic regions (see Ewart, 1979).

The plots of the rhyolite data in the quartz-feldspar system indicate some scatter amongst the pitchstones, and an even greater scatter amongst the compositions of the devitrified rhyolites, especially with regard to normative Q. A similar feature is shown by the residual glasses, and devitrified matrices separated from the two rhyolite lithologies (Text figs 37 b, d). In the ternary feldspar plots (Text figs, 38, c to f), the scatter is less pronounced, although some variation of Ab-Or is notable in a few samples. The scatter of data is interpreted to be due to post-eruptive alteration effects. These are of two main types: (a) Selective Na-loss during hydration, which has modified some of the pitchstone compositions, and occurs most frequently in those pitchstones with greater than approximately 3.8% total $H_2O$ (cf. Lipman, 1966). (b) Silicification and devitrification. The averaged data in Table 6 show the higher $SiO_2$ which seems to characterize the devitrified Mount Gillies rhyolites (see also Ross 1985b). $\Sigma$Fe, CaO, $K_2O$, and Zn are the elements which seem to exhibit the most obvious resulting decreases in concentrations. $Fe_2O_3/FeO$ ratios increase during devitrification, as normally found. The silicification process seems to be particularly common in the SE. Queensland region, having been found in devitrified rhyolites dykes, for example, from the Mount Alford centre, and in Triassic rhyolites (unpublished data). The effect is not always found, as shown by Ewart *et al.* (1977) for the Binna Burra rhyolites, the devitrified samples of which, however, were collected from within massive flow units. Apparently the phenomenon has not been described from other volcanic regions, and is presumably uncommon. In southeast Queensland, it is interpreted as a localized weathering feature, involving partial dissolution of feldspar, especially alkali feldspars, and deposition of secondary silica in the matrices of the rhyolites, which are commonly relatively porous after devitrification (see also averaged devitrified matrix composition in Table 6). Minor rhyolitic intrusions and extrusions, and the outer parts of more massive outcrops, are evidently most susceptible to silicification.

Thus, for the purposes of the following descriptions of the primary magmatic behaviour and geochemical characteristics, only the data for the pitchstones are used, excluding Na-leached samples.

Within the quartz-feldspar system (Text fig. 37) the pitchstones project close to the experimentally determined piercing point for the [A-Ab-Or]$_{97}$

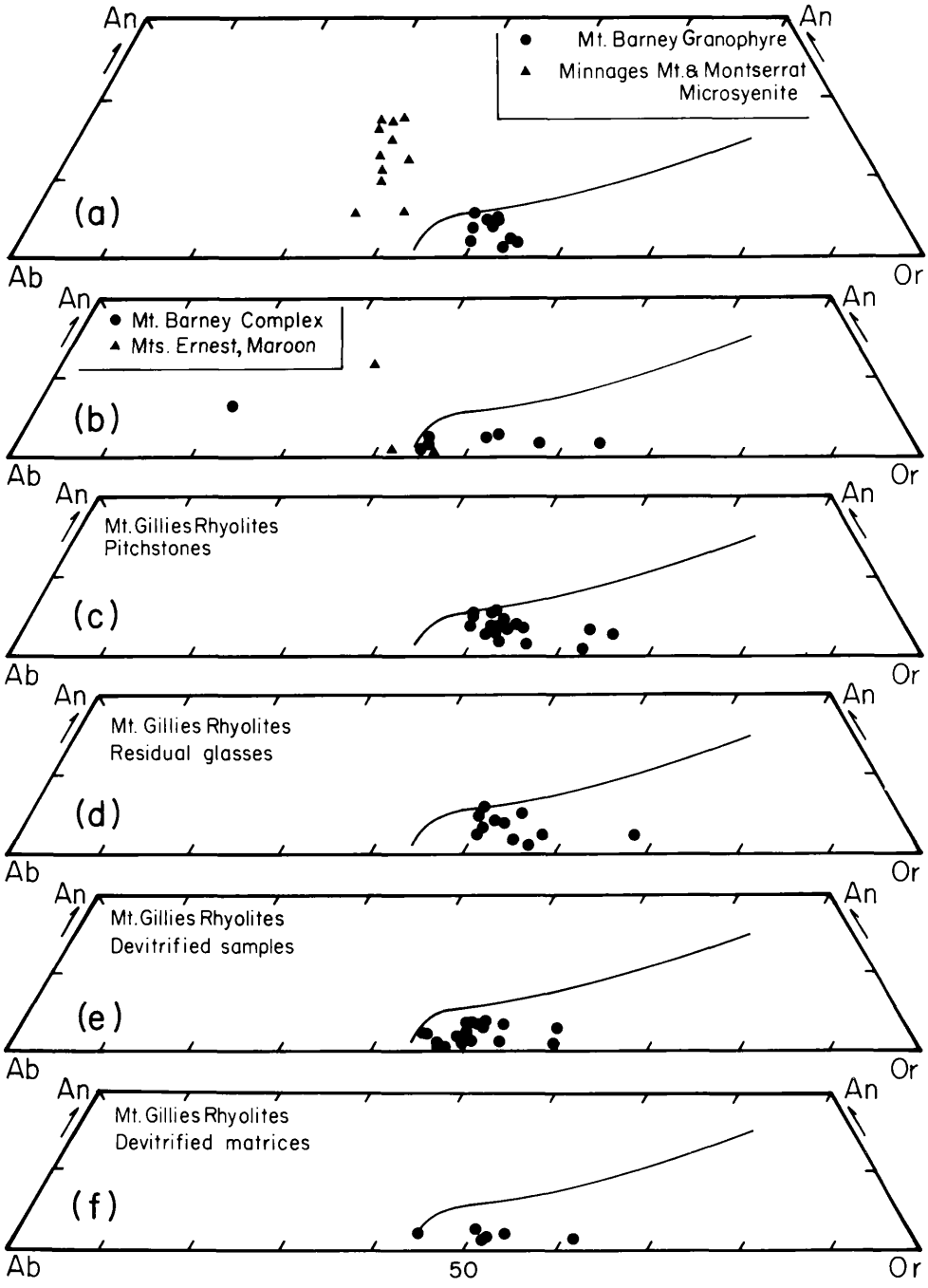


Text fig. 38. Normative (C.I.P.W.) ternary feldspar compositions of intermediate to acid intrusive and extrusive phases of the Focal Peak Shield Volcano. Based on whole rock samples, plus separated residual glasses and devitrified matrices (Mount Gillies Volcanics). The quartz saturated two feldspar boundary curve (1 kb water pressure) is from James and Hamilton (1969).

TABLE 6. AVERAGED CHEMICAL AND MINERALOGICAL DATA FOR THE ACID INTRUSIVE AND EXTRUSIVE PHASES OF THE MOUNT BARNEY CENTRAL COMPLEX. CHEMICAL DATA RECALCULATED TO ANHYDROUS BASIS.

| | Mount Gillies Rhyolites | | | | | | | | |
|---|---|---|---|---|---|---|---|---|---|
| | Pitchstones: Whole rocks [1] | Residual Glasses[1] | Devitrified: Whole Rocks | Devitrified: Matrices | Mt Barney Granophyre | Mt Maroon Rhyolite: Devitrified | Mt Ernest rhyolite Devitrified | Pitchstone Mr Barney central complex (33030) | Binna Burra Rhyolite |
| $SiO_2$ | 75.95(0.68)[2] | 76.57 (0.83) | 79.09(1.96) | 79.10(2.05) | 76.15(1.36) | 78.27 | 77.92 | 74.94 | 76.72 |
| $TiO_2$ | 0.17 (0.05) | 0.14(0.03) | 0.13(0.04) | 0.10(0.02) | 0.18(0.05) | 0.14 | 0.08 | 0.20 | 0.07 |
| $Al_2O_3$ | 12.35(0.34) | 12.38(0.51) | 11.17(1.13) | 11.37(1.88) | 12.33(0.20) | 12.18 | 12.16 | 12.23 | 12.57 |
| $Fe_2O_3$ | 0.73(0.59) | 0.63(0 30) | 0.66(0.50) | 0.69(0.32) | 1.22(0.76) | 0 98 | 0.96 | 0.59 | 0.77 |
| FeO | 1.14(0.25) | 1.01(0.31) | 0.31(0.13) | 0.15(0.17) | 0.53(0.21) | 0.10 | 0.17 | 1.69 | 0.46 |
| Σ FeO* | 1.80 – | 1.58 – | 0.90 – | 0.77 – | 1.63 – | 0.98 | 1.03 | 2.22 | 1.15 |
| MnO | 0.03(0.01) | 0.02(0.01) | 0.01(0.01) | 0.02(0.02) | 0.02(0.02) | 0.01 | 0.01 | 0.03 | 0.01 |
| MgO | 0.10(0.07) | 0.03(0.03) | 0.12(0.16) | 0.06(0.08) | 0.21(0.24) | 0.01 | 0.08 | 0.44 | 0.03 |
| CaO | 0.74(0.18) | 0.60(0.13) | 0.33(0.12) | 0.28(0.09) | 0.51(0.29) | 0.29 | 0.15 | 0.73 | 0.44 |
| $Na_2O$ | 3.32(0.15) | 3 23(0.20) | 3.31(0.58) | 3.28(0.84) | 3.38(0.21) | 3.06 | 3.83 | 4.04 | 3.60 |
| $K_2O$ | 5.45(0.30) | 5.37(0.27) | 4.86(0.46) | 5.02(0.37) | 5.43(0.22) | 4.96 | 4.62 | 5.08 | 5.31 |
| $P_2O_5$ | 0.02(0.02) | 0.01(0.01) | 0.02(0.01) | 0.02(0.01) | 0.02(0.02) | 0.01 | 0.01 | 0.02 | 0.01 |
| $\Sigma H_2O$(original) | (3.42)(0.65) | (3.65)(0.46) | (0.98)(0.50) | (0.54)(0.57) | (0.79) | (1.27) | (0.71) | (4.11) | (2.77) |
| Σ (original) | 99.74 | 99.86 | 99.84 | 99.74 | 100.19 | 100.03 | 100.37 | 100.33 | 99.78 |
| Trace Elements (p.p.m.) – Recalculated to anhydrous basis (X-ray fluorescence analyses) | | | | | | | | | |
| Rb | 159 | 189 | 158 | 118 | 145 | 153 | 195 | 145 | 486 |
| Sr | 12 | 6.7 | 5.9 | 2.0 | 7.6 | 7 | 4 | 26 | 1 |
| Ba | 112 | 61 | 74 | 47 | 144 | 46 | 27 | 154 | 11 |
| Th | 21 | 25 | 21 | 21 | 19 | 25 | 18 | 21 | 45 |
| Zr | 363 | 312 | 304 | 162 | 399 | 352 | 243 | 428 | 141 |
| Zn | 147 | 175 | 82 | 79 | 132 | 186 | 179 | 105 | 152 |
| Nb | 36 | 40 | 33 | 31 | 30 | 47 | 52 | 27 | 60 |
| Ce | 175 | 188 | 136 | 133 | 161 | 80 | 31 | 133 | 62 |
| Y | 74 | 87 | 49 | 49 | 68 | 47 | 40 | 71 | 98 |
| V | 2.5 | 3.2 | 1.0 | 4.0 | 2 | 2 | 1.5 | 3 | 1 |
| Cr | 1.6 | 2.5 | 1.3 | 2.0 | 2 | 1.5 | – | – | < 0.5 |
| Ni | 6.2 | 4.7 | 7.0 | 8.3 | 6 | 6.5 | 7.5 | 5 | 2 |
| Pb | 23 | 28 | 23 | 29 | 27 | 23 | 32 | 21 | 45 |
| Cu | 9 | 8 | 10 | 8 | 11 | 9.5 | 10 | 9 | 11 |
| n | 16 | 8 | 19 | 6 | 9 | 2 | 2 | 1 | 10 |
| Modal analyses (vol%) – Phenocryst/Microphenocryst phases | | | | | | | | | |
| Plagioclase | tr | – | – | – | – | – | – | – | 0.19 |
| Alkali Feldspar | 13.3(3.6) | – | 12.1(4.2) | – | – | 13.8 | 7.1 | 16.1 | 1.2 |
| Quartz | 3.5(2.1) | – | 3.6(2.6) | – | – | 5.9 | 3.2 | – | 0.66 |
| Biotite | – | – | – | – | – | – | – | – | 0.05 |
| Cpx | 0.7(0.5) | – | ) 0.7(0.6) | – | – | ) 0.6 | ) 0.4 | 0.6 | – |
| Olivine | 0.2(0.2) | – | ) | – | – | ) | ) | 0.7 | – |
| Fe-Ti oxides | < 0.1 | – | < 0.1 | – | – | < 0.1 | < 0.1 | 0.3 | 0.08 |
| Matrix | 82.3(3 9) | – | 83.6(5.8) | – | – | 79.7 | 89.3 | 82.3 | 97.8 |
| n | 42 | – | 34 | – | – | 2 | 10 | 1 | 8 |

[1] Excluding samples showing evidence of Na-leaching. [2] Figures in brackets represent one standard deviation.
Σ FeO* = Total Fe as FeO n = Number of samples used in each data set.

$An_3$ composition (James and Hamilton, 1969), but slightly displaced towards the Or component; the An content of this particular experimental composition is considered appropriate for the compositions of the Mount Gillies rhyolites. Within the ternary feldspar system (Text fig. 38), the rhyolites plot on the Or side of the experimentally determined quartz-saturated two-feldspar boundary curve; this seems to be consistent with the very sporadic occurrence of resorbed phenocrystal plagioclase in these rhyolites. It is thus relevant to compare the compositions of the separated residual glasses of these pitchstones, which are plotted in Text fig. 37b; their averaged compositions are presented in Table 6. It is clear that in terms of the normative quartz and feldspar components, the residual glasses are essentially identical to the whole rock compositions, and this implies 'ternary minimum' crystallisation, notwithstanding the small discrepancy between the experimentally determined minima compositions (in the quartz-feldspar and ternary feldspar systems) and the natural compositions. This discrepancy is possibly attributable to the fact that the experimental boundary curves plotted are determined at 1 kb water pressure; the rhyolites are interpreted to have crystallised under near anhydrous conditions (e.g. Ewart, 1981). Ternary minimum crystallisation also supports the interpretation by Ross (1977) and Ewart (1985) that plagioclase was an earlier crystallising phenocrystal phase, but has been subsequently resorbed (see earlier mineralogical descriptions).

With respect to other aspects of the geochemistry of the rhyolites (Table 6), it is evident that they are quite strongly depleted in MnO, MgO, $P_2O_5$, Sr, Ba, V, Cr and Ni, and exhibit relative enrichments in Rb, Ce, Th, and Y, compared to the Albert Basalt (Table 5). The depletion of the elements noted above is not as extreme as that of the Binna Burra rhyolites (Table 6), which are also considerably more enriched in Rb, Th, Pb, and Y. Comparison of Nb and Zr abundances between the Albert Basalt and the rhyolites show, however, that their abundances overlap; this is contrary to the expected situation if the rhyolites were simply derived by extended fractional crystallisation (or convective fractionation) of a basaltic parent. The discontinuities of many trace element parameters, and especially isotopic compositions, between the rhyolitic and mafic magmas of the region are discussed in Ewart (1982, 1985), and Ewart *et al.* (1986), and are interpreted as evidence for separate magma sources for the two groups of magmas. The Mount Gillies rhyolites do show strong evidence, however, for the operation of crystal-liquid fractionation prior to their eruption, in common with the other SE. Queensland rhyolites (Ewart *et al.*, 1985). This is best exemplified by the Rb-Ba and Rb-Sr plots in which the trends of varying depletion of Ba, and especially Sr, are compared between the various rhyolites, granophyre, and microsyenites of the whole Focal Peak Complex. These are modelled in Text figs 35 and 36, by means of a mixed plagioclase + sanidine (1:1 ratio) assemblage (starting from two assumed trachytic parental abundances); the fractionation of feldspar is the only viable way currently known in which to produce such depletion of these elements, and is further supported by the pitchstone whole rock-residual glass data (Table 6). Two sets of calculated feldspar fractionation curves are illustrated in Text Figs 35 and 36, one based on two sets of partition coefficients, one trachytic, and the second rhyolitic (see Appendix 1), the latter being significantly higher

for most elements (e.g. see Mahood and Hildreth, 1983). It is clear that to reproduce the Rb-Ba and Rb-Sr depletion trends most closely, it is necessary that the rhyolitic partition coefficients are operative, which is obviously consistent with the gross chemistry of the rhyolites and granophyres. The more extreme Sr depletion (compared to Ba) is also fully consistent with the relatively high Sr partition coefficients. (Appendix 1).

Rhyolites of Mounts Ernest and Maroon: Averaged and representative analyses of these are presented in Table 6. The rhyolites of Mounts Ernest and Maroon are devitrified, and show evidence for secondary silicification, as previously discussed, which has seriously modified the chemistry of some samples (Text figs 37, 38). In terms of the overall geochemistry, these rhyolites are very similar to the rhyolites of the Mount Gillies Volcanics, those of Mounts Maroon and Ernest showing a somewhat stronger depletion of Ba and Sr.

Mount Barney Granophyre. Perhaps the most geochemically signficant aspect of this large granophyre intrusion is the comparison of its overall major and trace element chemistry with the rhyolites, particularly the Mount Gillies rhyolites. The normative feldspar and quartz-feldspar compositions of the analysed granophyre samples (Text figs 37, 38) have virtually identical ranges to the unaltered pitchstones, and the trace element data plotted in Text figs 34 to 36 again exhibit similar behaviour, although Zr is somewhat higher in some granophyre samples. The most significant comparisons are illustrated by the averaged granophyre and Mount Gillies whole rock pitchstone analyses in Table 6. Both the major and trace elements are remarkably similar, and there can be little doubt that the granophyre and the rhyolites are comagmatic. This is consistent with the mineralogy, previously described.

Trachytes. Analyses of two trachytes are presented in Table 5; as previously noted, such extrusives are relatively rare in the Focal Peak centre. In terms of their overall geochemistry, they are comparable with the microsyenites. As such, their overall geochemical features are consistent with crystal-liquid fractionation, to the same general level of operation as in the microsyenites. Notwithstanding this, the two trachytes themselves do exhibit contrasting trace element abundances, most notably in Zr, Ce, Nb, Y. V, and Zn.

## ACKNOWLEDGEMENTS

The writers wish to thank P.J. Stephenson and M.J. Duggan for helpful comments and constructive criticism, and P.J. Stephenson for some additional information. Financial assistance from A.R.G.C. and University of Queensland Research Grants is acknowledged. J.A. Ross was supported as a Commonwealth Research Fellow.

# APPENDIX 1: BASALTIC, TRACHTIC, AND RHYOLITIC PARTITION COEFFICIENTS USED IN FRACTIONATION CALCULATIONS (1)

## 1. BASALTIC(2) PARTITION COEFFICIENTS

| Element | | | Clinopyroxene | Olivine | Plagioclase | Magnetite |
|---|---|---|---|---|---|---|
| Rb | mean | – | 0.027 (10)(3) | 0.05 (4)(3) | 0.12 (19)(3) | – |
| | range | – | 0.0014-0.08 | 0.0002-0.19 | 0.026-0.35 | |
| Sr | mean | – | 0.096 (11) | 0.047 (6) | 1.6 (13) | – |
| | range | – | 0.037-0.52 | 0.0002-0.12 | 1.04-2.22 | |
| Ba | mean | – | 0.17 (10) | 0.075 (5) | 0.40 (12) | – |
| | range | – | 0.0016-0.47 | 0.0001-0.27 | 0.15-0.77 | |
| Zr | mean | – | 0.75 (4) | 0.04 (1) | 0.03 (1) | 3.2 (1) |
| | range | – | 0.14-1.24 | – | – | – |
| Nb | mean | – | 0.20 (4) | 0.30 (2) | 0.16 (2) | 13.1 (1) |
| | range | – | 0.40-0.38 | 0.15-0.45 | 0.12-0.20 | – |
| Cr | mean | – | 5.8 (5) | 2.4 (7) | 0.02 (2) | 5.0 (1) |
| | range | – | 1.9-13.0 | 1.23-3.07 | 0.02 | – |
| Ni | mean | – | 2.8 (7) | 12.6 (15) | 0.08 (3) | 1.4 (1) |
| | range | – | 0.26-4.4 | 4.5-17.0 | 0.06-0.10 | – |
| V | mean | – | 1.8 (4) | 0.13 (3) | 0.04 (3) | 17.5 (1) |
| | range | – | 0.74-3.8 | 0.03-0.21 | 0.01-0.10 | – |

## 2. TRACHYTIC AND RHYOLITIC COEFFICIENTS

| | | | Trachytes | | Rhyolites | |
|---|---|---|---|---|---|---|
| Element | | | Plagioclase | Sanidine | Plagioclase | Sanidine |
| Rb | mean | – | 0.10 (6) | 0.50 (2) | 0.098 (37) | 0.73 (10) |
| | range | – | 0.05-0.18 | 0.35-0.66 | 0.01-0.34 | 0.29-1.4 |
| Sr | mean | – | 5.6 (8) | 3.0 (8) | 11.2 (41) | 6.2 (12) |
| | range | – | 3.1-8.6 | 1.2-3.9 | 3.0-36.8 | 0.97-17.3 |
| Ba | mean | – | 0.94 (8) | 4.1 (7) | 1.58 (41) | 7.3 (10) |
| | range | – | 0.58-1.4 | 1.2-9.2 | 0.37-6.5 | 1.2-18.1 |

(1) Extracted from a partition coefficient file, prepared by A.R. Duncan and A. Ewart, held in the Department of Geology, University of Queensland. Data from literature, based on analysed phenocryst phases all naturally occurring.

(2) The basalt and trachyte definitions follow Le Maitre (1984). The rhyolite grouping used is non-peralkaline, with $SiO_2$ between 68-74%, and total alkalis $>4\%$.

(3) Figures in brackets refer to number of data sets.

## APPENDIX 2: AGE (*) OF VOLCANIC AND INTRUSIVE ROCKS OF THE TWEED AND FOCAL PEAK VOLCANOES

**(*) Age in Ma corrected to the constants listed by Steiger and Jager (1977)**

| | | | |
|---|---|---|---|
| *Mount Warning and Tweed Volcano intrusives* | | | |
| Mount Warning | biotite in gabbro | 22.9, 23.7 | Ref. 1 |
| Mount Warning | trachyandesite | 23.4 | Ref. 3 |
| Surprise Rock | alkali rhyolite | 23.6 | Ref. 5 |
| Natural Bridge (3 km SSW. of) (Previously recorded as Hillview Rhyolite) | comendite (K-feldspar) | 22.8 | Refs 4,6 |
| *Tweed Volcano Lavas* | | | |
| Natural Bridge (S. of) | Hobwee Basalt (914 m) | 20.5 | Ref. 4 |
| Natural Bridge (S. of) | Hobwee Basalt (824 m) | 20.6 | Ref. 4 |
| Natural Bridge (S. of ) | Binna Burra Rhyolite (651 m) | 21.3 | Ref. 4 |
| Binna Burra | Binna Burra Rhyolite (K-feldspar) | 20.8, 20.9 | Ref. 5 |
| Beechmont | Beechmont Basalt | 21.6 (A) | Ref. 1 |
| Binna Burra | Beechmont Basalt (top) | 21.8 | Ref. 1 |
| Canungra (W. of) | Beechmont Basalt (base) | 22.3 | Ref. 1 |
| Fingal Point | Tholeiitic andesite | 23.2 | Ref. 2 |
| Burleigh Heads | Tholeiitic andesite | 23.5 | Ref. 2 |
| *Intrusives associated with the Focal Peak Volcano* | | | |
| Mount Gillies | K-feldspar in rhyolite | 23.2, 23.3 | Ref. 1 |
| Mount Barney | granophyre | 24.0 | Ref. 1 |
| Campbells Folly | K-feldspar in rhyolite | 25.5 | Ref. 5 |
| Mount Lindesay | Mount Gillies Volcanics (K-feldspar in rhyolite) | 24.8 | Ref. 5 |
| Natural Bridge (3 km SSW. of) | Albert Basalt (330 m)† | 22.8 | Refs 4,6 |
| Natural Bridge (3 km SSW. of) | Albert Basalt (312 m)† | 23.0, 23.1 | Refs 4,6 |

Ref. 1: Webb *et al.* 1967; Ref. 2: McDougall and Wilkinson, 1967; Ref. 3: Ewart *et al.* 1971; Ref. 4: Wellman and McDougall, 1974; Ref. 5: Ewart, 1982; Ref. 6: Wellman, 1975 and Ph.D. thesis (unpubl.).
A = slightly altered (2 ages from more strongly altered specimens have been omitted).
† See Notes.

Notes
1. Surprise Rock intrusive should be younger (from field relations).
2. Burleigh Heads rock is remote from major lava area, and might be associated with a separate centre of eruption, so too may the 'basalt' of Fingal Point, which shows chemical similarities to the Albert Basalt.
3. Basalts, 3 km SSW. of Natural Bridge were referred to the Albert Basalt (refs 5,6) because they were lower than a comendite thought to belong to the Hillview Rhyolite. Recent mapping by Wilmott (1983) has shown that these basalts are stratigraphically higher than the Hillview Rhyolite (= Mount Gillies Volcanics), and should be in the Beechmont Basalt.

## REFERENCES


BRUCE, I. 1978. The petrology of the Cedar Creek Area, Mount Warning, northeast New South Wales. B.Sc. (Hons) thesis, Univ. Qd (unpubl.).

BRYAN, W.H. 1941. Spherulites and allied structures, Part I. *Proc. R. Soc. Qd* **52**: 41-53.

BRYAN, W.H. 1954. Spherulites and allied structures, Part II. The spherulites of Binna Burra. *Proc. R. Soc. Qd* **65**: 51-70.

BRYAN, W.H. & JONES, O.A. 1946. The geological history of Queensland – a stratigraphical outline. *Pap. Dep. Geol. Univ. Qd* **2**(12): 1-103.

CROOK, K.A.W. & McGARITY, J.W. 1956. The volcanic stratigraphy of the Minyon Falls district, N.S.W. *J. Proc. R. Soc. N.S.W.* **89**: 212–218.

DUGGAN, M.B. 1975. Mineralogy and petrology of the southern portion of the Tweed Shield Volcano, northeastern New South Wales. Ph.D. thesis, Univ. New England (unpubl.).

DUGGAN, M.B. & MASON, D.R. 1978. Stratigraphy of the Lamington Volcanics in far northeastern New South Wales. *J. geol. Soc. Aust.* **25**: 65-73.

EWART, A. 1979. A review of the mineralogy and chemistry of Tertiary – Recent dacitic, latitic, rhyolitic and related salic volcanic rocks. *In* BARKER, F. (Ed.): Trondhjemites, dacites and related rocks, Ch. 2, 13-121. Developments in petrology, 6.

EWART, A. 1981. The mineralogy and chemistry of the anorogenic Tertiary silicic volcanics of S.E. Queensland and N.E. New South Wales, Australia. *J. geophy. Res.* **86** (B 11): 10242-10256.

EWART, A. 1982. Petrogenesis of the Tertiary anorogenic volcanic series of southern Queensland, Australia, in the light of trace element geochemistry and O, Sr and Pb isotopes. *J. Petrology* **23**: 344-382.

EWART, A. 1985. Aspects of the mineralogy and chemistry of the intermediate-silicic Cainozoic volcanic rocks of eastern Australia. Part 2. Mineralogy and Petrogenesis. *Aust. J. Earth Sci.* (in press). **32**(4): 383-413.

EWART, A., BAXTER, K. & ROSS, J.A. 1980. The petrology and petrogenesis of the Tertiary anorogenic mafic lavas of southern and central Queensland, Australia – possible implications for crustal thickening. *Contr. Miner. Petrol.* **75**: 129-152.

EWART, A., CHAPPELL, B.W. & LE MAITRE, R.W. 1985. Aspects of the mineralogy and chemistry of the intermediate-silicic Cainozoic volcanic rocks of eastern Australia. Part 1. Introduction and geochemistry. *Aust. J. Earth Sci.* **32**(4):359–382.

EWART, A., & GRENFELL, A. 1985. Cainozoic volcanic centres in southeastern Queensland, with special reference to the Main Range, Bunya Mountains, and the volcanic centres of the northern Brisbane coastal region. *Pap. Dep. Geol. Univ. Qd* **11** (3): 1-57.

EWART, A., OVERSBY, V.M. & MATEEN, A. 1977. Petrology and isotope geochemistry of Tertiary lavas from the northern flank of the Tweed volcano, southern Queensland. *J. Petrology* **18**: 73-113.

EWART, A., PATERSON, H.L., SMART, P.G., & STEVENS, N.C. 1971. Binna Burra – Mount Warning. *In* PLAYFORD, G. (Ed.) Geological excursions handbook, ANZAAS 43rd Congress, Brisbane, Section 3 – Geology and Geol. Soc. Aust. Inc. Qd Div., Brisbane.

EXON, N. 1972. Notes on the Lamington Volcanics of the McPherson Ranges, Queensland – New South Wales border. *Rec. Bur. Miner. Resour. Geol. Geophys. Aust.*, 1972/17.

GOULD, W. 1970. The petrology of the Mt. Nullum igneous complex, east of Mt. Warning, north-east New South Wales. B.Sc. (Hons) thesis, Univ. Qd (unpubl).

GREEN, D.C. 1964. The volcanic rocks of Mt. Tamborine, south-east Queensland. M.Sc. thesis, Univ. Qd (unpubl.).

GREEN, D.C. 1968. Further evidence for a continuum of basaltic compositions from south-east Queensland. *J. geol. Soc. Aust.* **15**: 159.

GREEN, D.C. 1970. Transitional basalts from the eastern Australia Tertiary province. *Bull. volcanol.* **33**: 930-941.

HILL, D. 1951. Geology *In* MACK, G. (Ed.): ANZAAS Handbook of Queensland, Aust. N.Z. Assoc. Advmt Sci., Brisbane.

JAMES, R.S. & HAMILTON, D.L. 1969. Phase relations in the system $NaAlSi_3O_8$ – $KAlSi_3O_8$ – $CaAl_2Si_2O_8$ – $SiO_2$ at 1 kilobar water vapour pressure. *Contr. Miner. Petrol.* **21**: 111-141.

LE MAITRE, R.W. 1984. A proposal by the IUGS subcommission on the systematics of igneous rocks for a chemical classification of volcanic rocks based on the total alkali silica (TAS) diagram. *Aust. J. Earth Sci.* **31** (2): 243-255.

LIPMAN, P.W. 1966. Water pressures during differentiation and crystallization of some ash-flow magmas from southern Nevada. *Am. J. Sci.***264**: 810-826.

McDOUGALL, I. & WILKINSON, J.F.G. 1967. Potassium-argon dates on some Cainozoic volcanic rocks from northeastern New South Wales. *J. geol. Soc. Aust.* **14**: 225-233.

McELROY, C.T. 1962. The geology of the Clarence – Moreton Basin. *Mem. geol. Surv. N.S.W.* Geology, 9.

McTAGGART, N.R. 1962. The sequence of Tertiary volcanic and sedimentary rocks of the Mount Warning Volcanic Shield. *J. Proc. R. Soc. N.S.W.***95** (1961): 135-144.

MAHOOD, G. & HILDRETH, W. 1983. Large partition coefficients for trace elements in high-silica rhyolites. *Geochem. Cosmochem. Acta*, **47**: 11-30.

PATERSON, H.L. 1970. The geology and petrology of the Korrumbyn Creek area of the Mount Warning Igneous Complex of north-eastern New South Wales. B.Sc. (Hons) thesis, Univ. Qd (unpubl.).

RICHARDS, H.C. 1916. The volcanic rocks of south-eastern Queensland. *Proc. R. Soc. Qd* **27**: 105-204.

ROSS, J.A. 1974. The Focal Peak Shield Volcano, southeast Queensland – evidence from its eastern flank. *Proc. R. Soc. Qd* **85**: 111-117.

ROSS, J.A. 1977. The Tertiary Focal Peak Shield Volcano, south-east Queensland – a geological study of its eastern flank. Ph.D. thesis, Univ. Qd (unpubl.).

ROSS, J.A. 1985a. Tuff – lava from southeast Queensland, Australia. *Current Sci.* **54**(6) 272-274.

ROSS, J.A. 1985b. Secondary silicification of rhyolites from the Focal Peak Shield Volcano, Australia. *Current Sci.* **54**(22): 1168-1171.

SMART, P.G. 1970. The petrology of the summit region of the Mount Warning Central Complex of north-eastern N.S.W. B.Sc. (Hons) thesis, Univ. Qd (unpubl.).

SMITH, R.L. & BAILEY, R.A. 1968. Resurgent cauldrons. *In* COATES, R.R., HAY, R.L. & ANDERSON, C.A. (Eds): Studies in volcanology. *Geol. Soc. Am. Mem.* **116**: 613-622.

SOLOMON, P.J. 1959. The Mount Warning Shield Volcano. M.Sc. thesis, Univ. Qd (unpubl.).

SOLOMON, P.J. 1964. The Mount Warning Shield Volcano. A general geological and geomorphological study of the dissected shield. *Pap. Dep. Geol. Univ. Qd* **5**(10): 1-12.

STEIGER, R.H. & JAGER, E. 1977. Subcommission on geochronology: convention on the use of decay constants in geo- and cosmochronology. *Earth planet. Sci. Lett.* **36**: 359-362.

STEPHENSON, P.J. 1954. An introduction to the northern geology of the Mt. Barney central complex. B.Sc. (Hons) thesis, Univ. Qd (unpubl.).

STEPHENSON, P.J. 1956. The geology and petrology of the Mt. Barney Central Complex, Queensland. Ph.D. thesis, Univ. London (unpubl.).

STEPHENSON, P.J. 1959. The Mt. Barney Central Complex, S.E. Queensland. *Geol. Mag.* **94** (2): 125-136.

STEVENS, N.C.1970. Miocene lava flows and eruptive centres near Brisbane, Australia. *Bull. volcanol.* **34** (2): 353-371.

STEVENS, N.C. 1976. Geology and landforms *in* Monroe, R. & Stevens, N.C. (Eds), The Border Ranges. R. Soc. Qd, Brisbane.

STEVENS, N.C. 1984. Queensland field geology guide. Geol. Soc. Aust. Qd Div., Brisbane.

STORMER, J.C., Jr. 1983. The effects of recalculation on estimates of temperature and oxygen fugacity from analyses of multicomponent iron-titanium oxides. *Am. Mineral* **68**: 586-594.

TWEEDALE, G. 1950. Geology of the Binna Burra volcanics. B.Sc. (Hons) thesis, Univ. Qd (unpubl.).

UTTLEY, P.J. 1972. The geology of the Lamington Volcanics of the McPherson Ranges, Queensland – New South Wales border. B.Sc. (Hons) thesis, Univ. Qd (unpubl.).

WALKOM, A.B. 1916. *Fenestella* and *Polypora (?)* in southeastern Queensland. *Proc. R. Soc. Qd* **28**:101-103.

WATT, D.W. 1971. Geology of Springbrook, southeast Queensland. B.Sc. (Hons) thesis, Univ. Qd (unpubl.).

WEBB, A.W., STEVENS, N.C. & McDOUGALL, I. 1967. Isotopic age determinations on Tertiary volcanic rocks and intrusives of southeastern Queensland. *Proc. R. Soc. Qd* **79**: 79-92.

WELLMAN, P. 1975. Palaeomagnetism of two mid-Tertiary basaltic volcanics in Queensland Australia. *Proc. R. Soc. Qd* **86**(24): 147-153.

WELLMAN, P. & McDOUGALL, I. 1974. Potassium – Argon ages on the Cainozoic volcanic rocks of New South Wales. *J. geol. Soc. Aust.* **21**: 247-272.

WILKINSON, J.F.G. 1968. The magmatic affinities of some volcanic rocks from the Tweed Shield Volcano, S.E. Queensland – N.E. New South Wales. *Geol. Mag.* **105**: 275-288.

WILKINSON, J.F.G. & BINNS, R.A. 1969. Hawaiite of high pressure origin from north-eastern New South Wales. *Nature* **22**: 553-555.

WILMOTT, W.F. 1983. Slope stability and its contstraints on closer settlement in the Canungra-Beechmont-Numinbah area, southeast Queensland. Geol. Surv. Qd Rec. 1983/64.

*A. Ewart, N.C. Stevens, J.A Ross*
*Dept. of Geology & Mineralogy*
*University of Queensland*
*St. Lucia*
*Brisbane*
*Queensland, 4067*

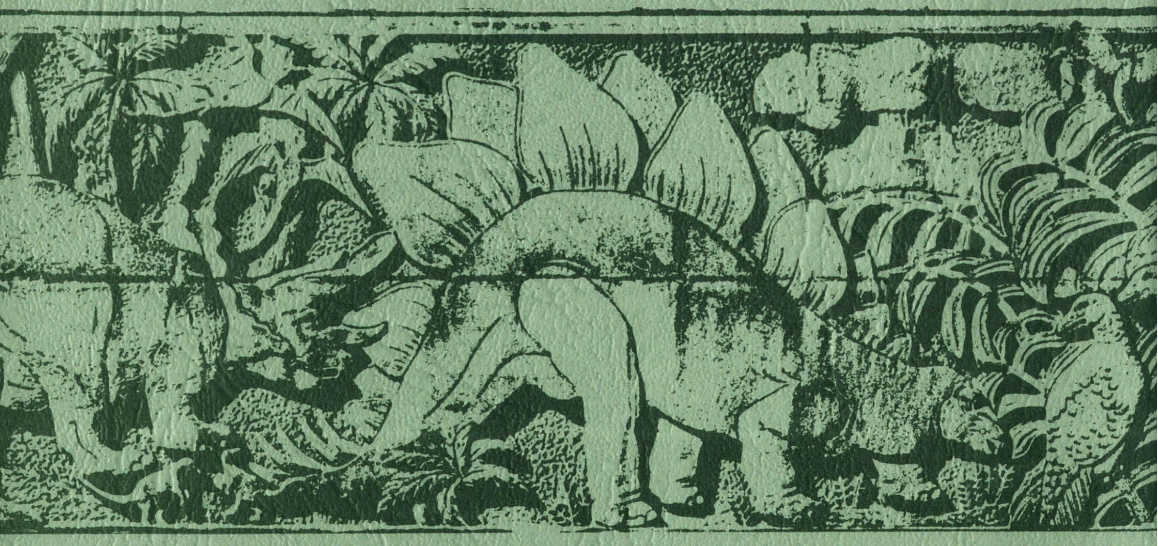

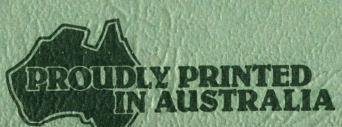
PROUDLY PRINTED
IN AUSTRALIA